

VERIFICATION OF ALLOWABLE STRESSES IN ASME SECTION III,
SUBSECTION NH FOR GRADE 91 STEEL

PART 1: BASE METAL

R. W. Swindeman
Cromtech Inc
Oak Ridge, TN 37830-7856

M. J. Swindeman
University of Dayton Research Institute
Dayton, OH 45469-0110

B. W. Roberts
BW Roberts Consultants
Chattanooga, TN 37416

B. E. Thurgood
Bpva Engineering
San Diego, CA 92131

D. L. Marriott
Stress Engineering Services
Mason, OH 45040

September, 2007

ABSTRACT

The database for the creep-rupture of 9Cr-1Mo-V (Grade 91) steel was collected and reviewed to determine if it met the needs for recommending time-dependent strength values, S_t , for coverage in ASME Section III Subsection NH (ASME III-NH) to 650°C (1200°F) and 600,000 hours. The accumulated database included over 300 tests for 1% total strain, nearly 400 tests for tertiary creep, and nearly 1700 tests to rupture. Procedures for analyzing creep and rupture data for ASME III-NH were reviewed and compared to the procedures used to develop the current allowable stress values for Gr 91 for ASME II-D. The criteria in ASME III-NH for estimating S_t included the average strength for 1% total strain for times to 600,000 hours, 80% of the minimum strength for tertiary creep for times to 600,000 hours, and 67% of the minimum rupture strength values for times to 600,000 hours. Time-temperature-stress parametric formulations were selected to correlate the data and make predictions of the long-time strength. It was found that the stress corresponding to 1% total strain and the initiation of tertiary creep were not the controlling criteria over the temperature-time range of concern. It was found that small adjustments to the current values in III-NH could be introduced but that the existing values were conservative and could be retained. The existing database was found to be adequate to extend the coverage to 600,000 hours for temperatures below 650°C (1200°F).

INTRODUCTION

A three-year collaborative effort has been established between the Department of Energy (DOE) and the American Society of Mechanical Engineers (ASME) to address technical issues related to codes and standards applicable to the Generation IV Nuclear Energy Systems Program [1]. A number of tasks have been identified that are managed through the ASME Standards Technology, LLC (ASME ST-LLC) and involve significant industry, university, and independent consultant activities. One of the tasks is the *Verification of Allowable Stresses in ASME Section III, Subsection NH With Emphasis an Alloy 800H and Grade 91 Steel*. The subtask on 9Cr-1Mo-V (Gr 91) steel involves both the verification of the current allowable stresses and the assessment of the data needed, if any, to extend the ASME Section III coverage of Gr 91 steel to 600,000 hours at 650°C (1200°F). To this end a review and re-analysis is provided here that identifies data sources and analytical procedures that have been used in code-related work on Gr 91.

IDENTIFICATION OF MATERIALS

Grade 91 steel is one of several ferritic/martensitic and ferritic/bainitic steel of interest for the Generation IV pressure vessel. ASME III-NH identifies the permitted SA specifications and associated product forms for Gr 91 in Table I-14.1 (a). Included are forgings (SA-182), seamless tubing (SA-213), seamless pipe (SA-335), and plate products (SA-387). Specifications for similar products produced in Asia and Europe have similar chemistry requirements and are considered to be equivalent to the SA specifications. Thus, data produced on Gr 91 have been assembled into a single database without regard to country of origin.

Table 1. Chemical specifications for Grade 91 (wt %)

| Element | SA-182* | SA-213* | SA-387* | EN 10216-2 |
|---------|------------|------------|------------|------------|
| C | 0.08-0.12 | 0.08-0.12 | 0.08-0.12 | .08-0.12 |
| Mn | 0.30-0.60 | 0.30-0.60 | 0.30-0.60 | 0.30-0.60 |
| P | 0.020max | 0.020max | 0.020max | 0.020max |
| S | 0.010max | 0.010max | 0.010max | 0.010max |
| Si | 0.20-0.50 | 0.20-0.50 | 0.20-0.50 | 0.20-0.50 |
| Ni | 0.40max | 0.40max | 0.40max | 0.40max |
| Cr | 8.0-9.50 | 8.0-9.50 | 8.0-9.50 | 8.0-9.5 |
| Mo | 0.85-1.05 | 0.85-1.05 | 0.85-1.05 | 0.85-1.05 |
| Cb | 0.06-0.10 | 0.06-0.10 | 0.06-0.10 | 0.06-0.10 |
| N | 0.03-0.070 | 0.03-0.070 | 0.03-0.070 | 0.03-0.07 |
| Al | 0.04max | 0.04max | 0.02max | 0.04max |
| V | 0.18-0.25 | 0.18-0.25 | 0.18-0.25 | 0.18-0.25 |
| Ti | | | 0.01max | |
| Zr | | | 0.01max | |

*Note: 2007 ASME Section II Part A for SA specifications

AVAILABLE SOURCES FOR CREEP-RUPTURE DATA

A development program on 9Cr-1Mo-V steel was undertaken by Combustion Engineering in 1975. The property goals for the material were outlined by Patriarca, et al. in 1976 [2], and a screening program was undertaken to reach these goals by optimizing carbide formers, identifying the best levels for nitrogen and nickel, minimizing δ -ferrite content, and optimizing the “consolidation practice” on impact properties. Twenty-six experimental heats and one commercial heat were examined, and a report on these by Combustion Engineering in 1976 was the first to provide a significant listing of tensile and creep-rupture tests on both experimental and commercial lots of Gr 91 [3]. Here, Bodine, et al. provided data for time to 1% creep, tertiary creep, and rupture life for three lots to approximately 6000 hours and temperatures to 650°C (1200°F) and Roberts produced a preliminary estimate of stress intensities S_m and S_t to 300,000 hours. From 1975 to the mid-1990s, the U.S. Department of Energy supported further mechanical testing of Gr 91, and the Oak Ridge National Laboratory (ORNL) assumed the management of the technology program. In parallel, intensive investigations were undertaken in Europe and Asia to qualify the material for usage in power-generating applications as a replacement for austenitic stainless steels in the temperature range from 550 to 650°C (1020 to 1200°F). In November of 1981, an expanded data package was prepared by ORNL to meet the ASTM specification requirements and to qualify the material for insertion into power boilers on a trial basis. A data package for plate, bar, and tube products was submitted for ASME Section I and Section VIII, Division 1 acceptance in June of 1982. At that time there were seven commercial heats, two of which were re-melts, and fifteen lots of plate, bar, and tubing. The creep-rupture database included over 80 rupture tests extending to as long as 20,000 hours. In November of 1984, the data package was prepared for submission to ASME Section III with estimated stress intensities for Code Case N-47. Data for hot-extruded pipe and forgings were added along with data for commercial tubing produced in Japan. The expanded database included about 180 tests on fourteen heats and many lots. No data produced in Europe or Asia were included in the submission to ASME Section III. Material representations for the estimation of stress intensities for a draft CC for N-47 were produced by Sikka and Booker [4, 5]. Data were received from the Japan Atomic Power Co. for inclusion into the database [6].

In 1992, the allowable stresses in ASME II-D were challenged by the Europeans. A collection of stress-rupture data from U.S., European, and Asian sources was undertaken by the Metal Properties Council (MPC) [7, 8], and a re-analysis of the data produced some changes in the allowable stresses in ASME Section II-D that were applicable for Section I and Section VII, Division I construction [9]. These allowable stresses were based on the criteria in ASME Section II, Appendix 1. In response, some changes were made to draft CC for N-47, although the criteria for setting stress intensities differed from Section II-D and the MPC database upon which the stresses were based was not provided. One notable item was that the stress lines in ASME II-D Table 1A for Gr 91 products \geq 75-mm (3-in.) listed lower values than thinner products in the temperature range of 550 to 600°C (1020 to 1100°F). Except for Table I-14.2 (S_o values), the draft CC for N-47 was not changed to reflect the product thickness distinction. The database

available for use in the evaluation of stress intensities for N-47 was expanded in 1993 by the addition of the German stress-rupture database [7] and the Japanese database [8]. However, no data for time to 1% creep or time to tertiary creep was accumulated. In 1995, the European developed a database, incorporating the U.S and Japanese data as well as their own and set values for the average rupture strength that have not changed to this day [10]. More recently, additional data provided by the Japan Atomic Power Company [11], the National Institute for Materials Science (NIMS) [12, 13], the Japan Nuclear Development Institute [14], and Europe [14] have become available.

GENERAL TRENDS IN THE CREEP BEHAVIOR OF Gr 91 STEEL

A typical creep curve that forms the basis for the rules in Subsection NH is sketched in Figure 1 [15]. This curve is separated into three stages of creep labeled: primary creep stage, secondary creep stage, and tertiary creep stage. The “components” of the total strain are assigned the identities illustrated in the figure: elastic-plastic strain, primary creep strain, and secondary creep strain. The intercept strain shown in Figure 1 implies an exhaustion or limit to the primary creep component. The difference between this intercept strain and the elastic-plastic strain, identified as the primary creep strain in Figure 1, is often called the “transient strain limit.” It should be noticed that the creep curve intercepts 1% total strain before transient creep is exhausted and the time to 1% strain ($t_{1\%}$) may be short relative to the rupture life (t_R). An important term not included in Figure 1 is the minimum creep rate (mcr). The product of the mcr and time has the same definition as the secondary creep component in the Figure 1. This product is sometimes called the Monkman-Grant strain [16]. Another important term that is included in Figure 1 but not in reference 15 is the 0.2% offset tertiary creep strain and time. The strain and time (t_3) for tertiary creep are obtained from the creep curve at a point that is 0.2% above the extension of the secondary creep line [17]. Clearly tertiary creep starts before the 0.2% offset limit is reached. A significant tertiary creep stage is shown in the Figure 1. However, the presence of necking and cracking beyond 5% strain complicates the interpretation of a tertiary creep component.

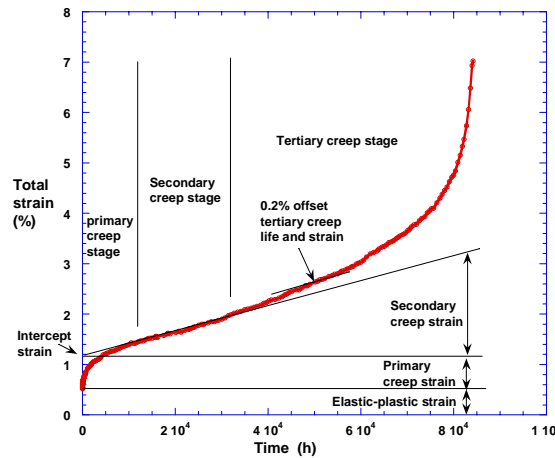


Figure 1. Definitions for components of creep used in ASME Section III Subsection NH

CHARACTERISTICS OF THE CREEP DATABASE FOR ALLOY Gr 91

The database assembled for the verification of allowable stresses in ASME III-NH provides information bearing on the three criteria in ASME III-NH that relate to time-dependent stress limits: time to 1% to strain ($t_{1\%}$); time to initiate tertiary creep (t_3); and time to rupture (t_R). With respect to the time to $t_{1\%}$, the bulk of the data were extracted from the US database with additional data from the NIMS report [13]. The data in the US database were entered as the time to 1% creep strain rather than time to 1% total strain. The NIMS database reported both time to 1% creep strain and time to 1% total strain. The ratio of these two times was found to be proportional to the applied stress. This ratio was used to convert the times in the US database to times to 1% total strain. The distribution of data is shown in Fig. 2. Altogether, a total of 312 values for $t_{1\%}$ creep were available. These were distributed from 450 to 780°C (840 to 1435°F) with times to 25,000 hours. Most data fell between 500 and 650°C (930 and 1200°F) at times below 5,000 hours.

A substantial database for $t_{1\%}$ exists within the European database [15]. These were distributed more-or-less evenly at 550, 600, and 650°C (1020, 1110, and 1200°F) with a few short time data at 700°C (1292°F). The European data were not included in the database used to validate the ASME III-NH stress intensity values.

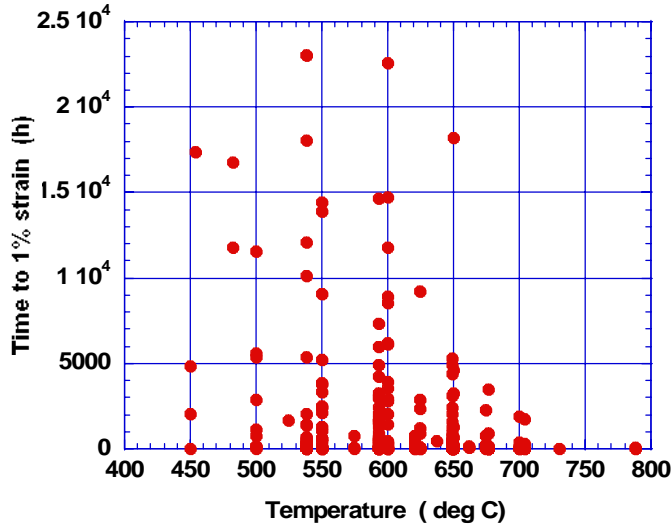


Fig. 2. Distribution of time to 1% strain ($t_{1\%}$) data with temperature

With respect to the time to t_3 , the bulk of the data were extracted from the US database and the Japanese institutions [6, 12, 13]. The distribution of data is shown in Fig. 3. Altogether, a total of 398 values for t_3 creep were available. These were distributed from 450 to 780°C (840 to 1435°F) with times to 60,000 hours. Most data fell between 500 and 650°C (930 and 1200°F) at times less than 20,000 hours.

The database for rupture was large and included US, European, and Asian contributions. The distribution of data is shown in Fig. 4. Over 1700 rupture data existed in the temperature of 450 to 780°C (840 to 1735°F) with most data between 450 and 700°C (840 and 1292°F). Products included tubes, pipes, plates, forging, and a billet. Product thicknesses ranged from 6 to 550 mm (1/4 to 21 in.).

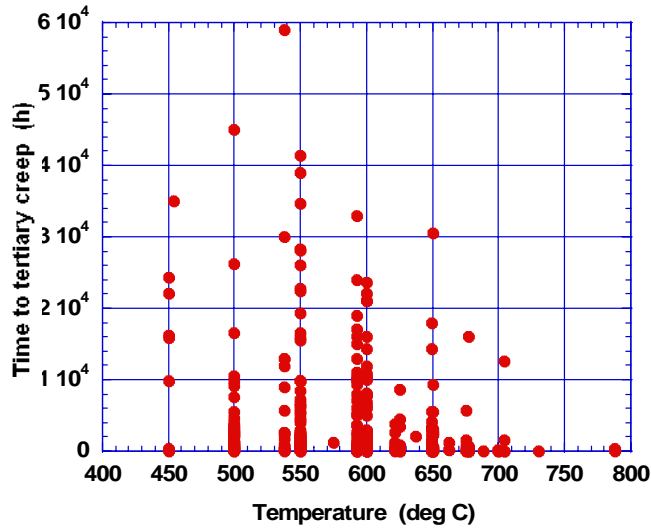


Fig. 3. The distribution of the time to t_3 data with temperature

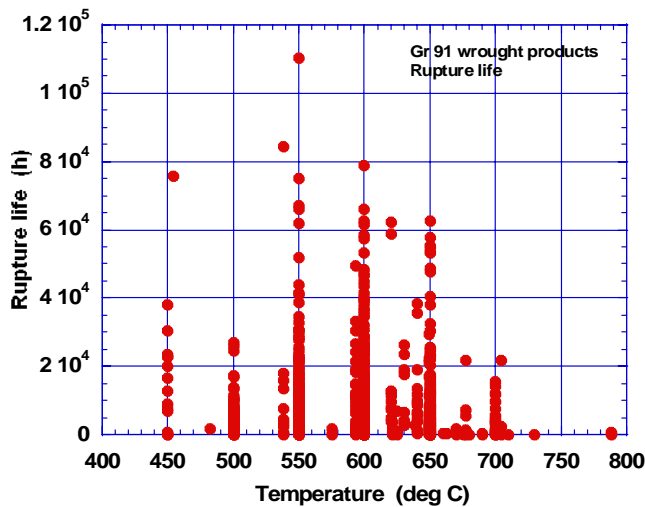


Fig. 4. The distribution of the time rupture data with temperature

DATA ANALYSIS PROCEDURES

Criteria for Setting S_t Values

The criteria for setting allowable stresses for ASME Section I and Section II (identified in Appendix 1 in Section II-D) differ from the criteria for setting allowable stress intensities for ASME Section III Subsection NH (identified in paragraph NH-3221). (a) Appendix 1 has a creep rate criterion which is 100% of the stress to produce a creep rate if 0.01%/1000h, while paragraph NH-3221 has a total (elastic, plastic, primary plus secondary creep) strain criterion which is 100% of the average stress to produce 1% total strain in a specific time, say 100,000 hours; (b) Appendix 1 has a rupture strength criterion of F_{avg} times the average stress to produce rupture in 100,000 hours, while paragraph NH-3221 calls for 67% of the minimum stress to produce rupture in a specific time, say 100,000 hours; (c) Appendix 1 has a second rupture strength criterion of 80% of the minimum stress to produce rupture in 100,000 hours, while NH-3221 calls for 80% of the minimum stress to cause initiation of tertiary creep in a specific time, say 100,000 hours. The factor F_{ave} used in Appendix 1 has the value 0.67 or less and depends on the slope of the stress-rupture curve around 100,000 hours [18]. Criteria (a) and (c) for III-NH require knowledge of the creep strain-time behavior.

Procedures for Estimating the Average Strength for 1% Strain and the Minimum Strength for the Onset of Tertiary Creep

There are no specific guidelines for estimating criteria (a) and (c) for ASME III-NH. Ideally, the development of material models for plasticity and creep as a function of time, temperature, and stress for times to the limit set for III-NH could be used to determine the stress to produce 1% total strain and the “initiation” of tertiary creep. Knowledge of how the curves vary from lot-to-lot could be used to determine the minimum strength values. Attempts have been made to develop such models for producing the isochronous stress-strain curves in III-NH [19-21], but often the available data were judged to be insufficient to cover the range of products needed to fully develop the two criteria based on creep. The direct correlation of $t_{1\%}$ and t_3 permitted the use of a larger database for comparison of the criterion based on rupture strength. For this work on Gr 91, data analysis procedures for all three criteria were similar.

Selection of Analysis Methods:

Several methods of analysis were selected. These were based time-temperature parameters. In the first method, the Larson-Miller parameter (LMP) was selected in combination with a stress function $f(S)$ that was a four-term (“third-order”) polynomial in log stress. Thus, for the 1% total strain:

$$LMP = T_K (C + \log t_{1\%}). \quad (1)$$

Where C was the Larson-Miller parametric constant and T_K was in Kelvins. The stress function was equated to the LMP:

$$LMP = f(S) = a_0 + a_1 \log S + a_2 (\log S)^2 + a_3 (\log S)^3 \quad (2)$$

where a_i was a series of four constants. Using a least squares fitting method in which $\log t_{1\%}$ was the dependent variable and T and $\log S$ were independent variables, the optimum values for C and a_i were determined. In this approach, all lots were processed together which produced a “global” or “single batch” analysis and one value for C that applied to all lots. Using the “best fit” values for $f(S)$ and C , the $\log t_{1\%}$ values calculated along with the residual, r_i , for each datum:

$$r_i = \log(t_{\text{observed}}/t_{\text{calculated}}) \quad (3)$$

The standard error of estimate (SEE) was obtained from the analysis in the customary way:

$$SEE = [\sum(\log t_{\text{observed}} - \log t_{\text{calculated}})^2/(N_d - D_f)]^{1/2} \quad (4)$$

Where N_d was the number of data and D_f was the degrees of freedom.

A second analysis was undertaken that was essentially a Larson Miller parametric approach but employed a “lot-centered” procedure developed by Sjodahl that calculated a lot constant (C_{lot}) for each lot along with the Larson Miller constant, C , which represented the average lot constant (C_{ave}) for the lots [4, 23]. Only the average lot constant was used in estimating life, although the variation in the C_{lot} values was of interest in comparing lots.

The third method investigated was based on the Orr-Sherby-Dorn (OSD) parameter. Whereas the Larson-Miller parameter assumed that the activation energy for the process was stress dependent, the OSD parameter assumed that the activation energy for the process was not dependent on stress. Here:

$$t_{1\%} = A \exp(Q/RT_k) S^n \exp(\beta S) \quad (5)$$

where A , Q/R , n , and β are materials constants calculated by least squares regression analysis. R is the gas constant. The OSD parametric constant was written such that $t_{1\%}$ was expressed in the \log_{10} form:

$$OSD = Q/2.30258RT_K - \log t_{1\%} \quad (6)$$

The stress function $f(S)$ shown in equation (5) was written in \log_{10} form:

$$f(S) = D + n \log S + \beta' S \quad (7)$$

Where D was $\ln A / 2.30258$, and β' was $\beta / 2.30258$. Lot centering was not used in the fit of the OSD parameter.

The procedures for t_3 and t_R were the same as those used for $t_{1\%}$.

The underlying assumption in the regression analyses was that the residuals were normally distributed about zero. Also, it was expected that residuals would be more-or-less uniformly distributed with time, temperature, and stress. These aspects of the parametric fits were examined graphically.

The minimum t_3 and minimum t_R for each temperature were based on a reduction in log life of 1.65 multiples of the standard error of estimate (SEE) produced by the model. The estimation of the minimum stress required that the appropriate root of the polynomial in $\log S$ be found.

RESULTS

Time to 1% total strain, $t_{1\%}$:

The fit of the Larson Miller parameter to the 1% total strain data is shown in Figure 5 (left). Data exhibited considerable scatter about the mean trend $f(S)$ which curved downward with the increasing value of the LMP parameter. The optimum value of C for the global fit was 36.69157 which was one point lower than the C_{ave} value (37.67024) found for the lot-centered analysis. The distribution of residuals about the mean for the global analysis is shown in the histogram in Figure 6 (left). The SEE was 0.432 log cycle in time for the global analysis and 0.440 log cycle for the lot-centered analysis. The stress functions, $f(S)$, for the two fits were similar, so the parametric curve for the lot-centered analysis closely resembled the curve shown in Figure 5 (left). The lot constants ranged from 36.865 for the strongest lot to 38.141 for the weakest lot. Both the weakest and strongest were tube products.

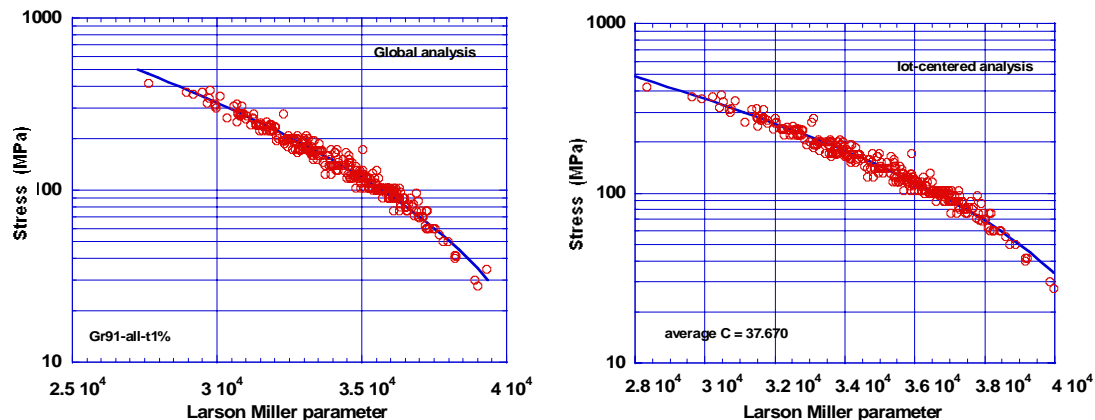


Figure 5. Fit of the Larson Miller parameter to the time to 1% total strain for 17 lots (left) Global; (right) Lot-centered

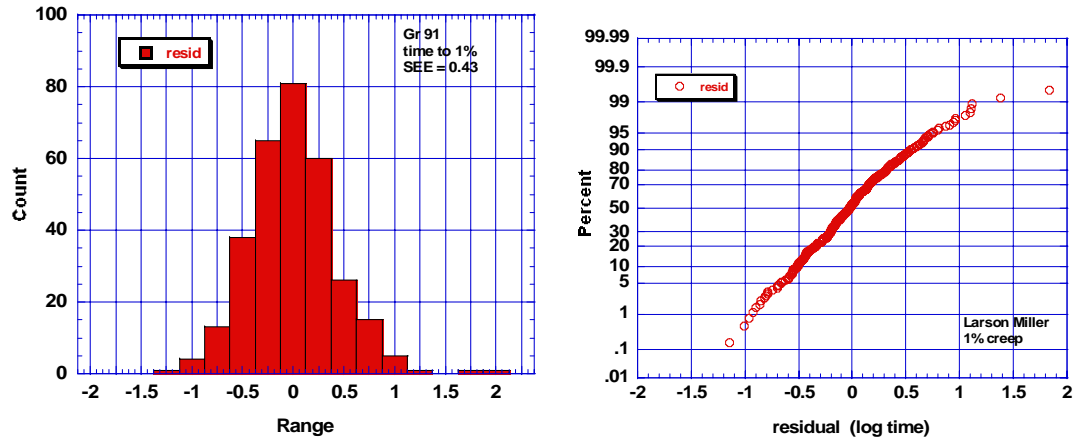


Figure 6. Histogram of residuals (left) and frequency graph for residuals (right).

The global and lot-centered Larson Miller approaches produced very similar curves for stress versus $t_{1\%}$, and one such set of curves is shown in Figure 7 for temperatures from 450 to 650°C (842 to 1202°F). These curves were close to those developed by Caminada, et al. from the European database [14].

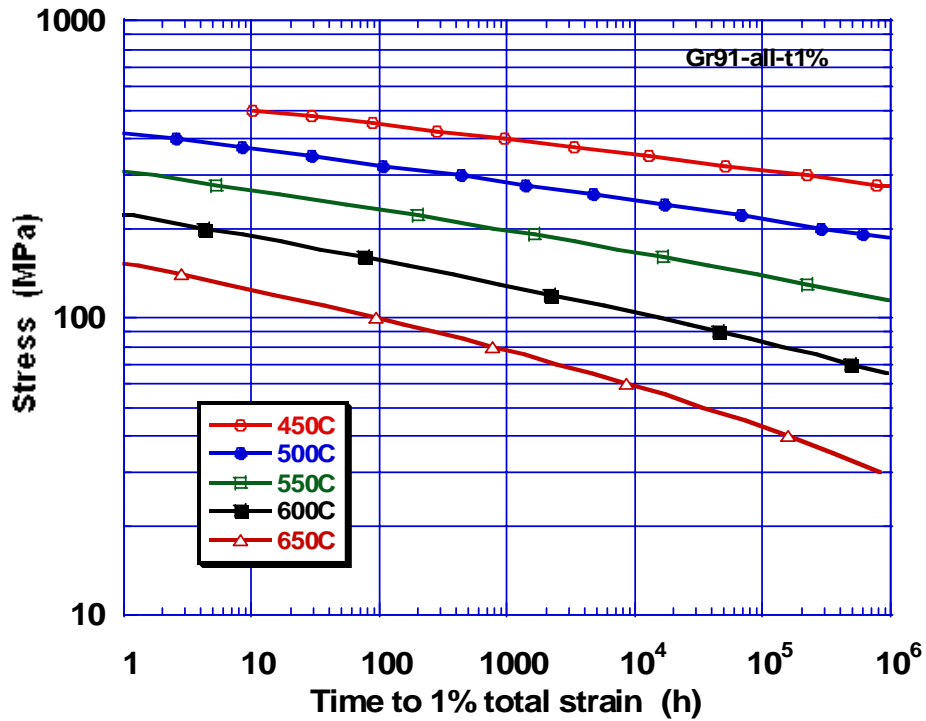


Fig. 7. Stress versus $t_{1\%}$ based on the Larson Miller parameter

The fit of the OSD parameter to the $t_{1\%}$ data is shown in Figure 8. The general character of the curve was similar to the Larson Miller curves. The SEE for the OSD parameter was slightly greater (0.449 log time) than the Larson Miller fit but the OSD parameter contained one less parametric constant. The stress versus $t_{1\%}$ curves were very similar except at 650°C (1202°F), where the OSD predicted lower long-time strength.

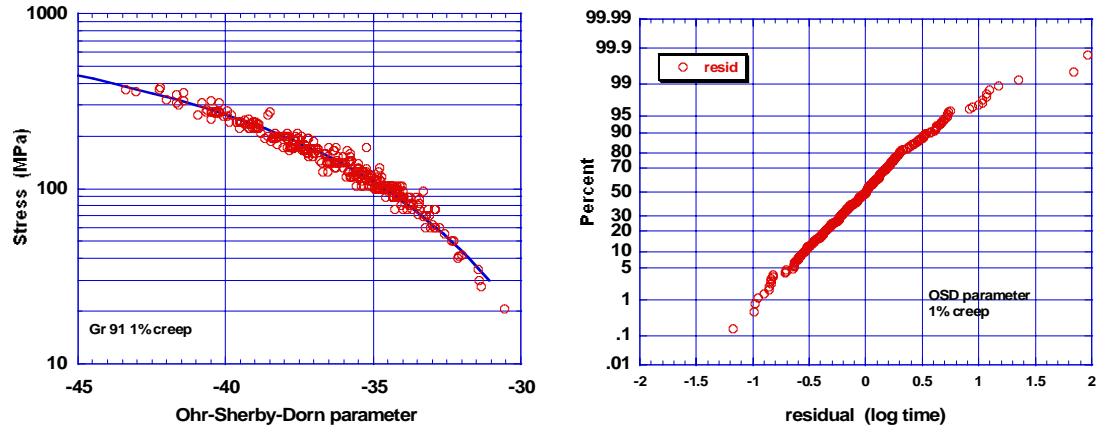


Fig. 8. The fit of data to the OSD parameter (left) and residual frequency graph (right).

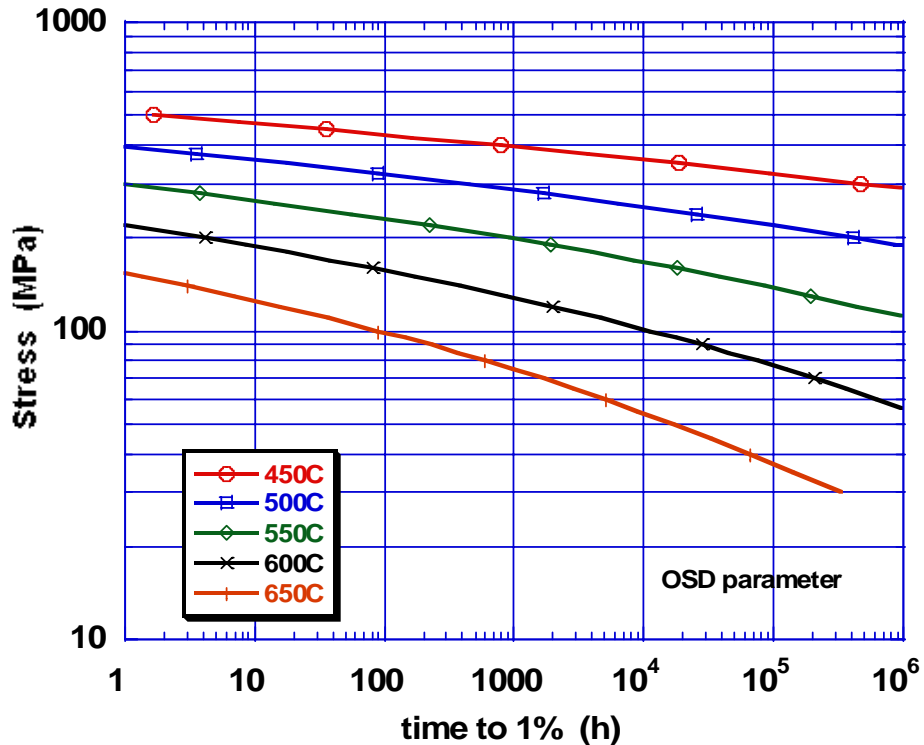


Fig. 9. Stress versus $t_{1\%}$ based on the Orr-Sherby-Dorn parameter

Time to the initiation of tertiary creep, t_3 :

The database for t_3 included 392 data for 27 lots. The Larson Miller parameter fits produced parametric constants of 30.4198 and 34.8888 for the global and lot-centered fits, respectively. The stress versus parameter curves are shown in Figure 10. The SEE values were 0.381 and 0.419 in log time for the global and lot-centered fits, respectively.

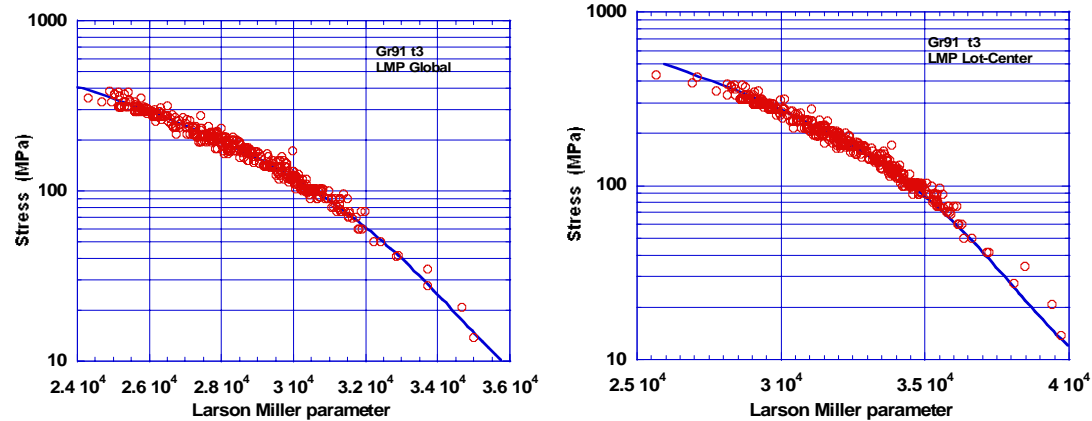


Fig. 10. Fit of the Larson Miller parameter to the time to tertiary, t_3 , for 27 lots (left) Global; (right) Lot-centered.

Plot of the histogram for the lot constants and frequency distribution of the residuals for the lot-centered analysis are shown in Figure 11. The histogram shows how the lot constants for three of the product forms were distributed. The 10 tube products averaged 34.907 with a standard deviation of 0.275, the 12 plate products averaged 34.788 with a standard deviation of 0.315, and 5 thick-section products averaged 35.163 with a standard deviation of 0.465. The frequency distribution curve indicated a small deviation from a normal distribution of residuals, as suggested in the plot shown in Figure 11 (right).

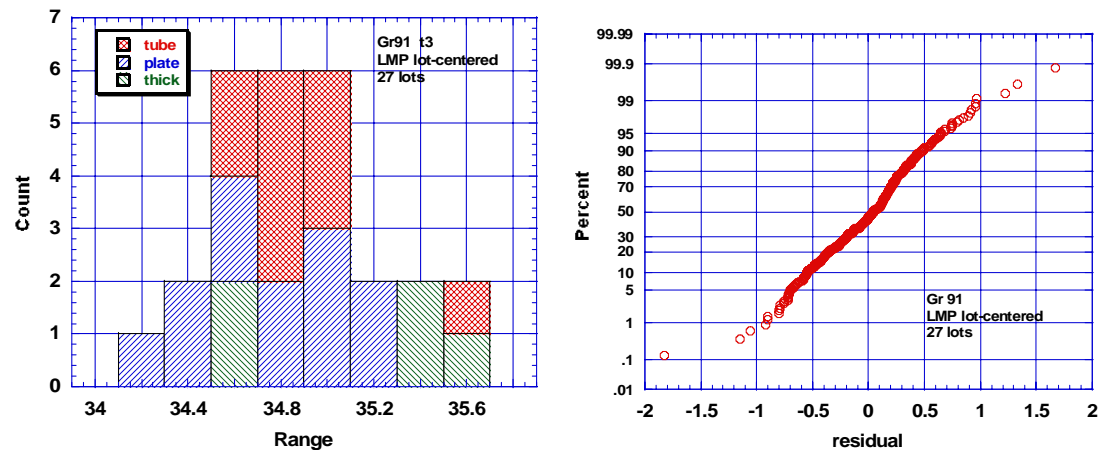


Fig. 11. Distribution of Larson Miller parameter lot constants for tertiary creep with product form (left) and percentage distribution of residuals for all lots (right).

Figure 12 shows isothermal curves for the average stress to the initiate tertiary creep produced by the Larson Miller lot-centered model. These curves were similar to curves produced by the global fit. For long times, the global fit produced a lower SEE and slightly lower stresses than the lot-centered fit, but the difference was not judged to be significant.

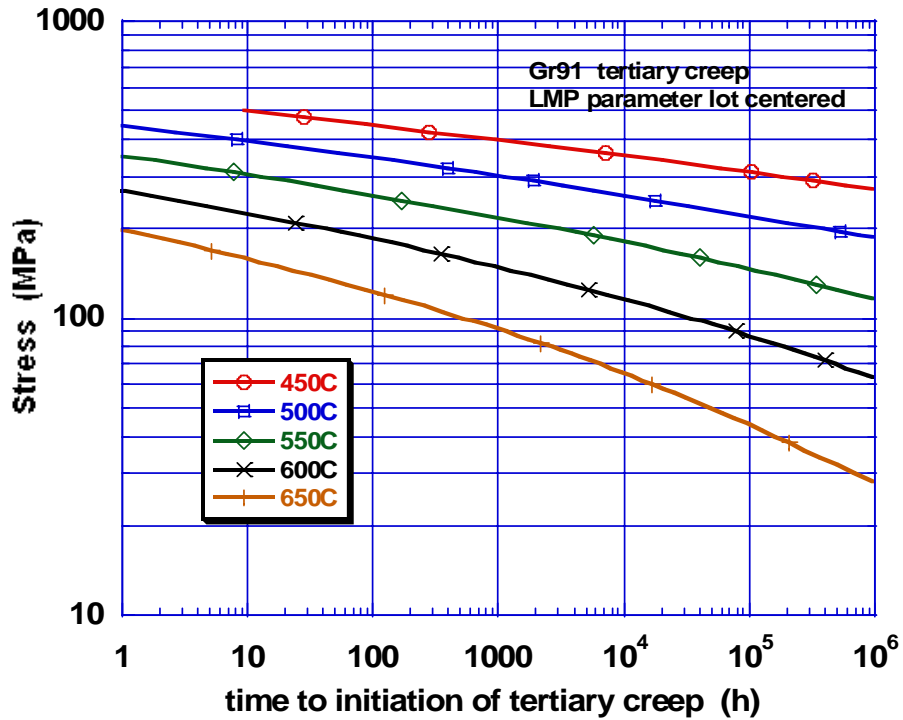


Fig. 12. Stress versus the time to the initiation of tertiary creep for several temperatures based on the Larson Miller lot-centered model.

A plot for the stress versus OSD parameter for t_3 data is shown in Figure 13 (left) and the frequency distribution of the residuals is shown in Figure 13 (right). The stress function approached a stress exponent of -2.7 as stress diminished. The OSD parameter captured the trend of the very low stress data better than the Larson Miller parameter. The SEE, however, was higher than that for the LMP and the percentage versus residual curve plotted in Figure 13 (right) departed somewhat a normal trend at the tails. A family of curves for average stress to initiate tertiary creep as a function of time is plotted in Figure 4. Comparison of these curves with those in Figure 12 indicated that the OSD parameter produced similar stresses for short times and low temperatures but lower stresses for long times at high temperatures.

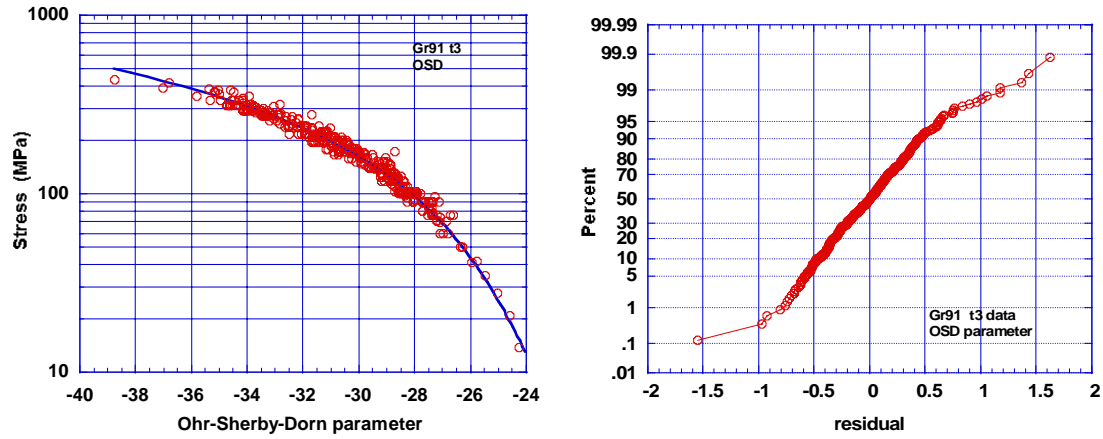


Fig. 13. Fit of the Orr-Sherby-Dorn parameter to the time to tertiary creep

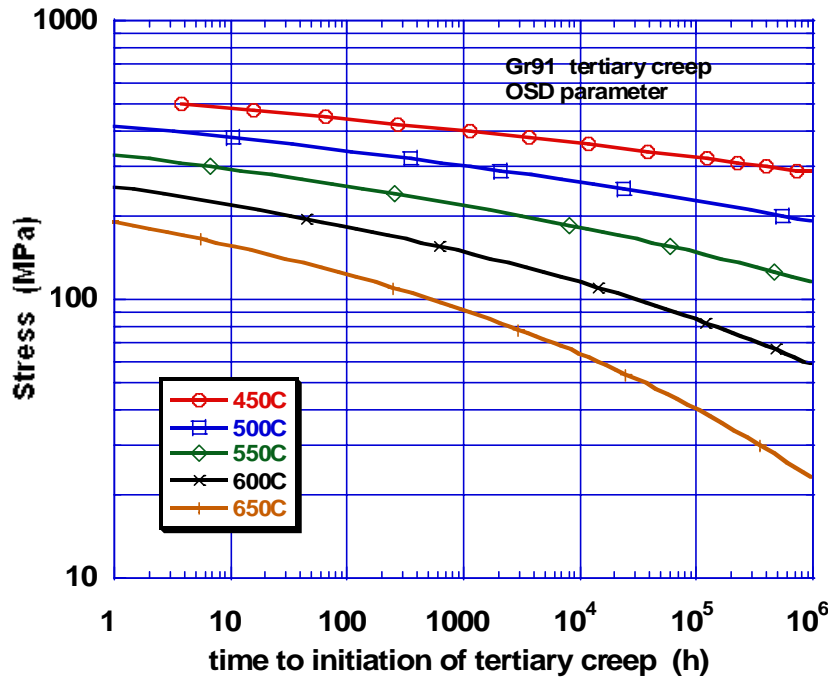


Fig. 14. Average stress to produce the initiation of tertiary creep versus time for several temperatures based on the Orr-Sherby-Dorn parametric model.

As an alternative to developing a time-temperature-stress model directly from the t_3 data, the utilization of the correlation between tertiary creep life, t_3 , and rupture life, t_R , was examined. This correlation, attributed to Leyda and Rowe [17], works very well for Gr 91, as may be seen in Figure 15 (left). To a first approximation, the ratio t_3/t_R was found to be 0.629 with a standard deviation of 0.089, as shown in Figure 15 (right). A least squares fit to the data in Figure 15 (left) found: $t_3 = 82.232 + 0.62271 t_R$.

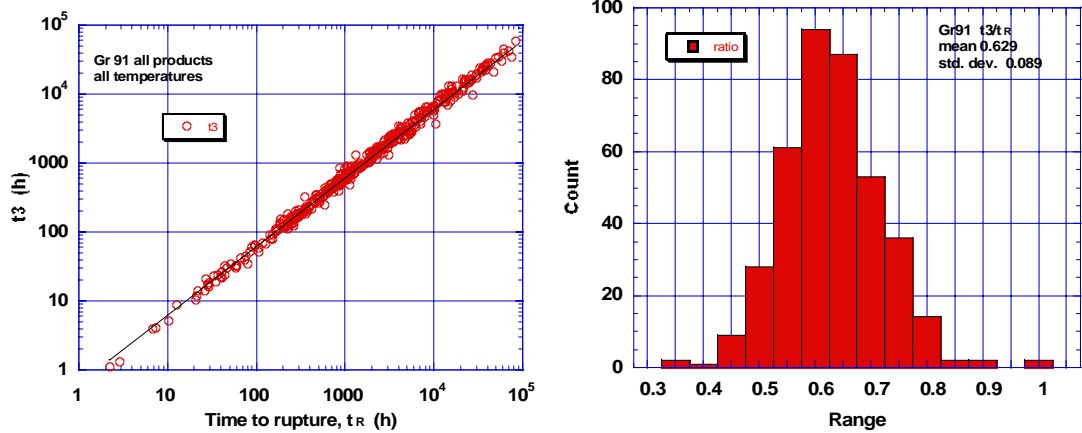


Fig. 15. The Leyda-Rowe correlation between t_3 and t_R (left) and histogram of the t_3/t_R ratio values for 312 data (right).

Stress-rupture, t_R :

As outlined in earlier section on available sources for creep-rupture data, the correlation of stress-rupture data to predict the long-time strength of Gr 91 steel has been an on-going activity on an international level for decades. The undertakings have been largely in support for the use of Gr 91 steel in ASME BPV Codes Section I and VIII, ASME Piping Codes B31.1 and B31.3, and corresponding overseas construction codes. The objective has been to estimate accurately the allowable stresses at the upper limit of the use temperature for Gr 91 steel. Many parametric procedures have been developed and compared but there remains no consensus as to which is best. Techniques to “improve” the accuracy of long time estimations include “censoring” data by not using data for times less than 3000 hours [24], region splitting by not using data produced at stresses above a fraction of the hot yield strength [25], and adding more parametric constants to the time-temperature-stress models [26]. However, it should be recognized that the criteria for setting S_t in III-NH are conservative relative to the criteria in ASME II-D Table 1-100, so the onus to produce accurate estimates from the same database is not as demanding.

Data corresponding to rupture lives less than 100 hours were not used in the analyses. This left nearly 1600 data covering temperatures from 450 to 780°C (840 to 1435°F). The Larson Miller global fit to these data is shown in Figure 16 (left) and lot-centered fit is shown in Figure 16 (right). One fit appeared to be as good as the other, although there was a four point difference in the optimized parametric constant: ~26 for the global fit and ~30 for the lot centered fit. The SEE values were similar: 0.333 in log time for the global fit and 0.345 in log time for the lot-centered fit. The distribution of residuals for the two fits was similar, and information is shown in Figure 17 for the lot centered model. The plots show how the residuals were distributed about zero. The distributions with temperature and stress are shown in Figure 18. These distributions show no strong bias

(Figures 18a and 18b). When plotted against the observed rupture lives, the residuals tended to move from a negative bias to a positive bias with increasing life (Figure 18c). Also, the US data tended to exhibit greater lives than the combined database (Figure 18d), while the long-time tests in the database tended to have shorter lives than predicted (Figure 18d). A few long-time test in the US data base were discontinued at times that placed them longer than predicted.

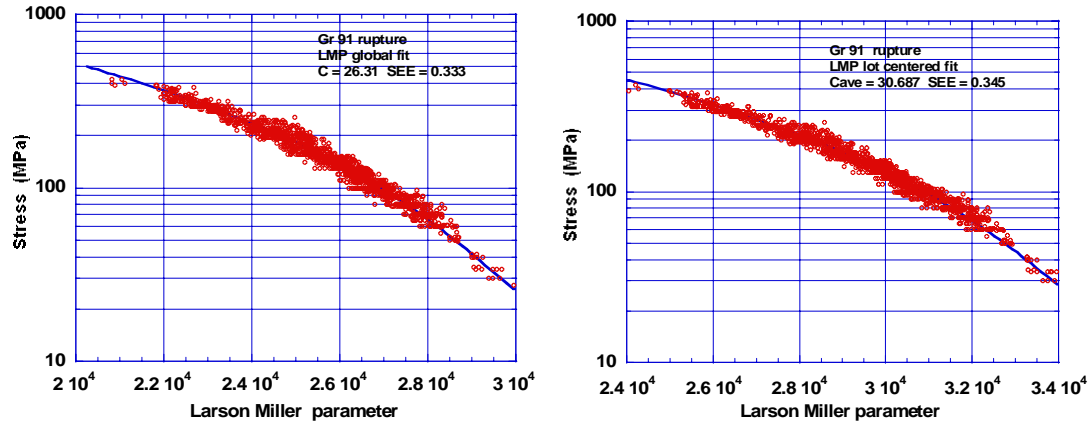


Fig. 16. Fit of the Larson Miller parameter to rupture data: (left) global fit; (right) lot-centered fit.

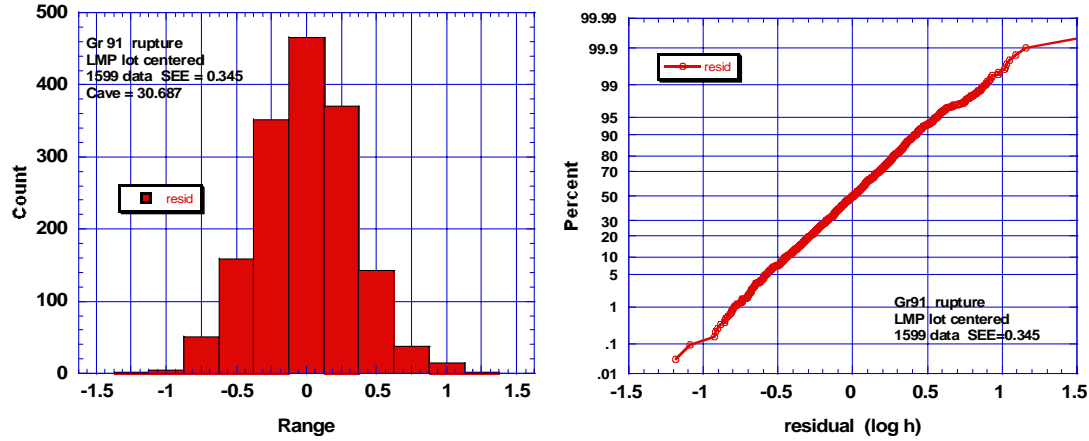


Fig. 17. The distribution of residuals for the fit of the Larson Miller parameter lot-centered procedure to rupture data: count versus range histogram (left); percent versus range graph (right)

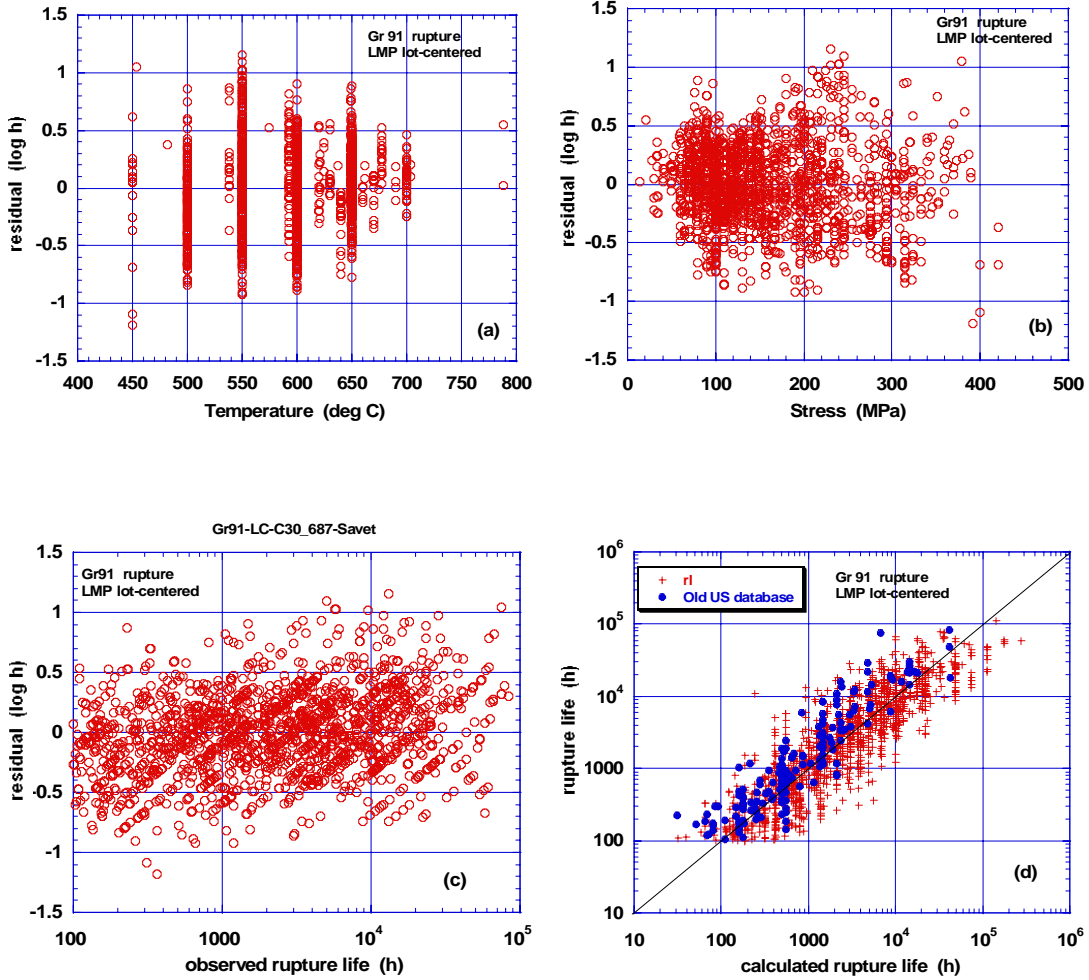


Fig. 18. Plots showing the characteristics of the fit of the Larson Miller lot-center model to rupture data: (a) residuals versus temperature; (b) residuals versus stress; (c) residuals versus observed rupture life; and (d) rupture life versus calculated rupture life.

An evaluation of the lot constants produced interesting results. These are shown in Table 2 below and in Figure 19. Since the log of the life for the LMP is given by $f(S)/T_k - C$, the lower C_{lot} values produced longer predicted lives for the same $f(S)$ and T_k . As indicated in Table 2, the US data manifested the lowest C_{lot} values and correspondingly the longest lives, as indicated in Figure 18d. The plates manifested the lowest C_{lot} values within the products and the forgings the highest. As observed by Prager [9], the thicker products often had lower ultimate strength (UTS) and high C_{lot} values. This trend is shown in Figure 19. The decrease in C_{lot} with increasing UTS appeared to be the trend, more-or-less for all products, as indicated in Figure 19 (left). The dependence of C_{lot} on thickness was less obvious as shown in Figure 19 (right). Products that were 75 mm (3/4 in.) or thicker consistently manifested higher C_{lot} values. ASME II-D lists lower stress values for these products at some temperatures.

Table 2. Average lot constants for different products

| Item | Number | Lot Constant | Std. Deviation |
|----------------|--------|--------------|----------------|
| all | 104 | 30.687 | 0.273 |
| US | 11 | 30.457 | 0.125 |
| others | 93 | 30.714 | 0.272 |
| | | | |
| tubes | 48 | 30.682 | 0.241 |
| plates | 34 | 30.606 | 0.301 |
| pipes | 13 | 30.824 | 0.176 |
| forgings | 9 | 30.936 | 0.261 |
| | | | |
| thick products | 19 | 30.872 | 0.227 |

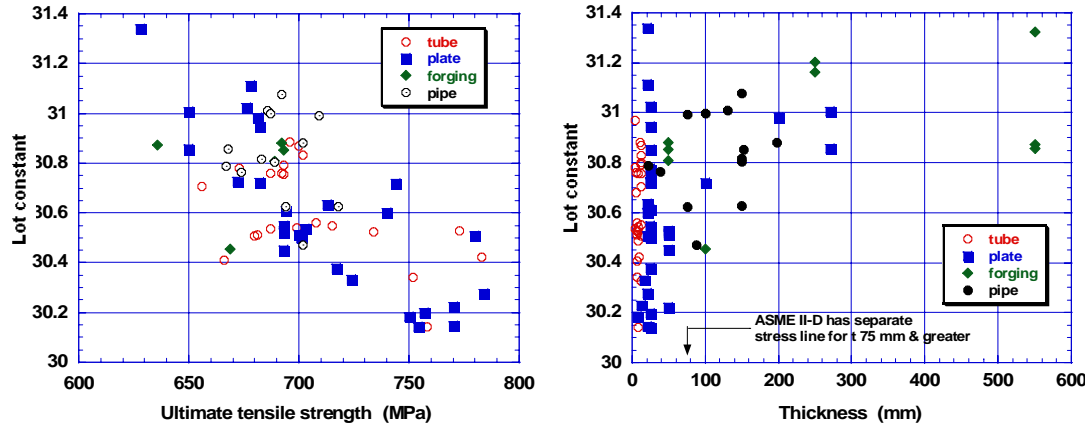


Fig. 19. Correlation of the Larson Miller parameter lot constants with ultimate tensile strength (left) and product thickness (right).

Finally, the average stress versus time-to-rupture curves are plotted in Figure 20 for values obtained from the Larson Miller lot-centered correlation. Temperatures cover 450 to 650°C (840 to 1200°F) and times cover 1 to 10^6 hours.

The form of the stress function, $f(S)$, used in conjunction with the OSD parametric model, was the same as used by Sikka, Cowgill, and Roberts in their early work on Gr 91 [4]. The exception was that a global procedure rather than a lot-centered procedure was introduced. The fit of the data to the parameter is shown in Figure 21. The SEE for the fit of the OSD parameter to the data was about the same as for the Larson Miller parameter with the SEE being 0.337 log cycle in time. The parametric constant was low (25681K) compared to the value found reported by Sikka, Cowgill, and Roberts (31876K), but the stress exponent that dominates the very long-time behavior was about the same, about -2.54 for this fit and -2.49 for the Sikka, Cowgill, and Roberts fit [3]. The average stress to produce rupture, calculated from the OSD parameter, is shown in

Figure 22. Comparing these curves to the LMP isothermal curves in Figure 20 revealed that the OSD parameter predicted significantly lower stresses at high temperatures and long times.

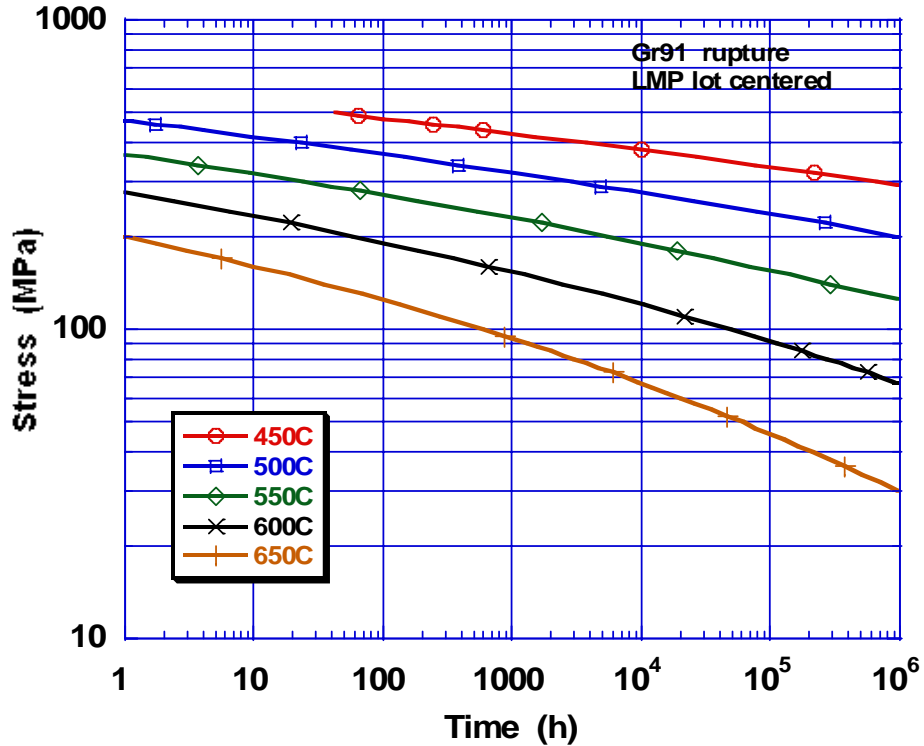


Fig. 20. Average stress versus time to rupture base on the Larson Miller lot-centered model

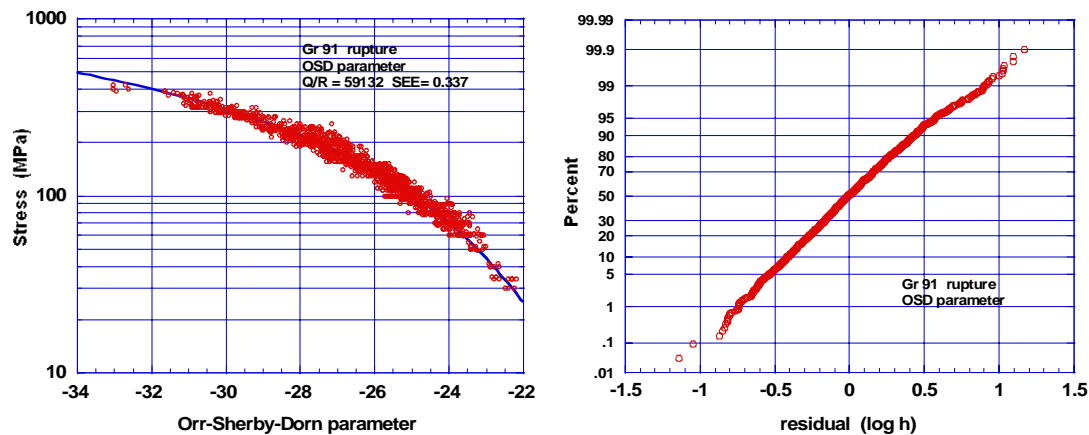


Fig. 21. Fit of the Orr-Sherby-Dorn parameter to rupture data

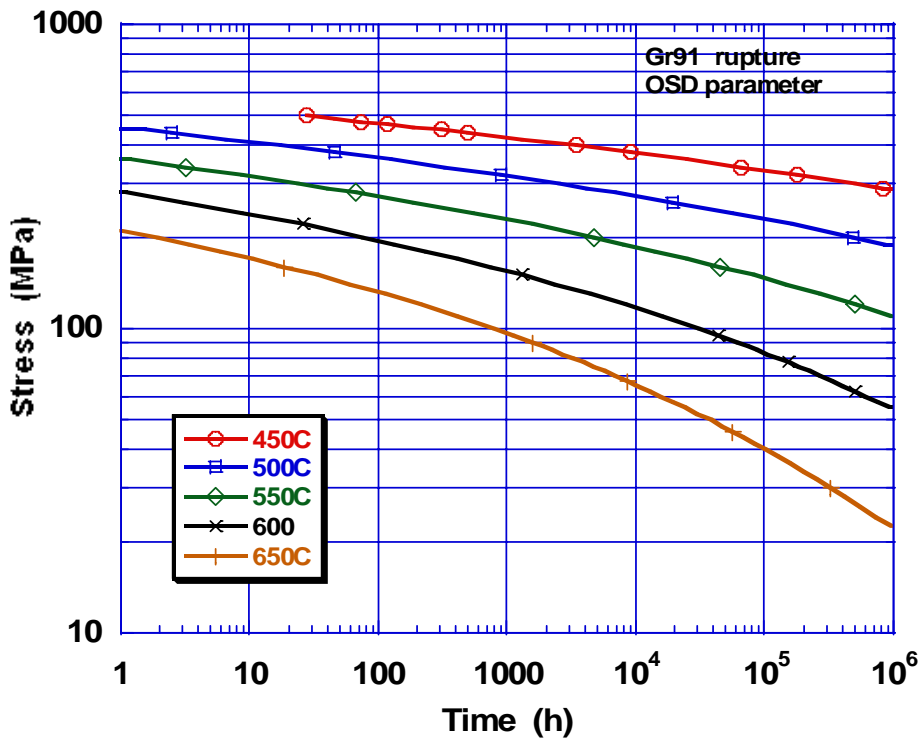


Fig. 22. Average stress versus time to rupture based on the Orr-Sherby-Dorn model

The average strength at 100,000 hours estimated from the LMP and OSD parameters are compared to other estimates in Table 3. These include the current values on which ASME II-D stresses are based. At 550°C (1020°F) and below, stress allowables are controlled by time-independent properties so rupture strengths in this temperatures range are often not reported. At 550°C (1020°F) and above, the rupture strength controls the allowables. The table shows that the original work of Sikka, Cowgill, and Roberts produced stresses that were high and reflected the higher strength of the original US lots. Subsequent analyses on the new larger database produced lower stresses, especially at 600 and 625°C (595 and 1155°F). Of all of the more recent analyses, the OSD global parametric analysis performed in this work produced the lowest stresses. The LM lot-centered parametric analysis, on the other hand, produced stresses that were more-or-less in the mid-range of the predicted values of the other parametric procedures. For this reason it was judged to be a reasonable model on which to evaluate the validity of the current S_t values in ASME III-NH.

Table 3. Comparison of the strength for 100,000 hours estimate by different methods

| Temp (deg C) | Sikka, et al. | | This Work | | ASME II-D | | ASME II-D | | Kimura | | Kimura | | Cipolla | | Cipolla | | ECCC | |
|--------------------------------------|---------------|--------|-----------|---------------------------------|-----------|--------|-------------|------|--------|------|--------|--------|---------|------|---------|--|------|--|
| | 1984 | OSD LC | LMP LC | OSD G | <75 mm | ≥75 mm | pipe, plate | RS | RS | tube | MRM-MC | MRM-MC | ECCC | 2005 | 1995 | | | |
| 450 | | | | 335 | 332 | | | | | | | | | | | | | |
| 475 | | | | 283 | 278 | | | | | | | | | | | | | |
| 500 | | | | 236 | 229 | | | | | | | | | | | | 258 | |
| 525 | | 208 | | 193 | 185 | | | | | | | | | | | | 210* | |
| 550 | | 167 | | 155 | 146 | | | | | 153 | 160 | 150 | 160 | 166 | | | | |
| 575 | | 131 | | 121 | 112 | 132 | 120 | 121 | 123 | 116 | 123 | 116 | 123 | 127* | | | | |
| 600 | 98.6 | | 91 | 83 | 97 | 91.9 | 94.2 | 92.5 | 85 | 85 | 93 | 93 | 94 | | | | | |
| 625 | 71.8 | | 66 | 59 | 67.9 | 68.2 | 71.1 | 66.4 | 62 | 62 | 67 | 67 | 69* | | | | | |
| 650 | 49.8 | | 46 | 40 | 43.1 | 43.1 | 51.3 | 44.3 | 44 | 44 | 48 | 48 | 49 | | | | | |
| | | | | | | | | | | | | | | | | | | |
| ODS LC= Orr-Sherby-Dorn lot-centered | | | | MRM= Mendelson-Roberts-Manson | | | | | | | | | | | | | | |
| LMP LC= Larson Miller lot-centered | | | | MC= minimum commitment | | | | | | | | | | | | | | |
| OSD G= Orr-Sherby-Dorn global | | | | ECCC= ECCC recommendations 1999 | | | | | | | | | | | | | | |
| RS= region splitting | | | | 210*= interpolated value | | | | | | | | | | | | | | |

EVALUATION OF THE CRITERIA CONTROLLING S_t

The various correlations developed in the previous section were used to plot strength versus time curves according to the criteria specified in NH-3221 for the selection of S_t . The first two plots in Figure 23 show the average stress for 1% strain against time as determined by either the Larson-Miller (left) or Orr-Sherby-Dorn (right) parameter. For most of the range of temperature and time the two parameters produce similar results, but at the longer times and higher temperatures the OSD parameter produced slightly lower stress values. The second set of plots compares the tertiary creep criterion, namely 80% of the minimum stress for the initiation of tertiary creep. Again, the two parameters produced similar stresses for most conditions, while at the long time and low temperatures the OSD parameter produced lower stresses. For all conditions, the tertiary creep criterion produced lower stresses than the 1% creep criterion. The third pair of plots compares the stress-rupture criterion for the two parameters. Again, the OSD parameter produced lower stresses for longer times at the higher temperatures. For all times and temperatures, the stress-rupture criterion produced equivalent or lower stresses than the 1% creep or tertiary creep criterion.

As mentioned in the previous section, the Larson Miller lot-centered parametric model was chosen for estimating the S_t values on a “trial basis.” A plot of the recommended S_t values against time (“load duration” in ASME III-NH) is shown in Figure 24. The low-temperature, short-time values are not included in the plot. The current S_t values are included in the figure for comparison purposes. As may be seen, the new values are slightly higher for most conditions of stress and temperature. The selection of the OSD parameter would reduce the values by approximately 10% and drop the “new” S_t values to below those currently in ASME III-NH. This is a conservative option. It appears that the current values are conservative and close enough to the re-calculated values to be retained as they currently exist. The new model could serve to justify an extension of the values to 600,000 hours.

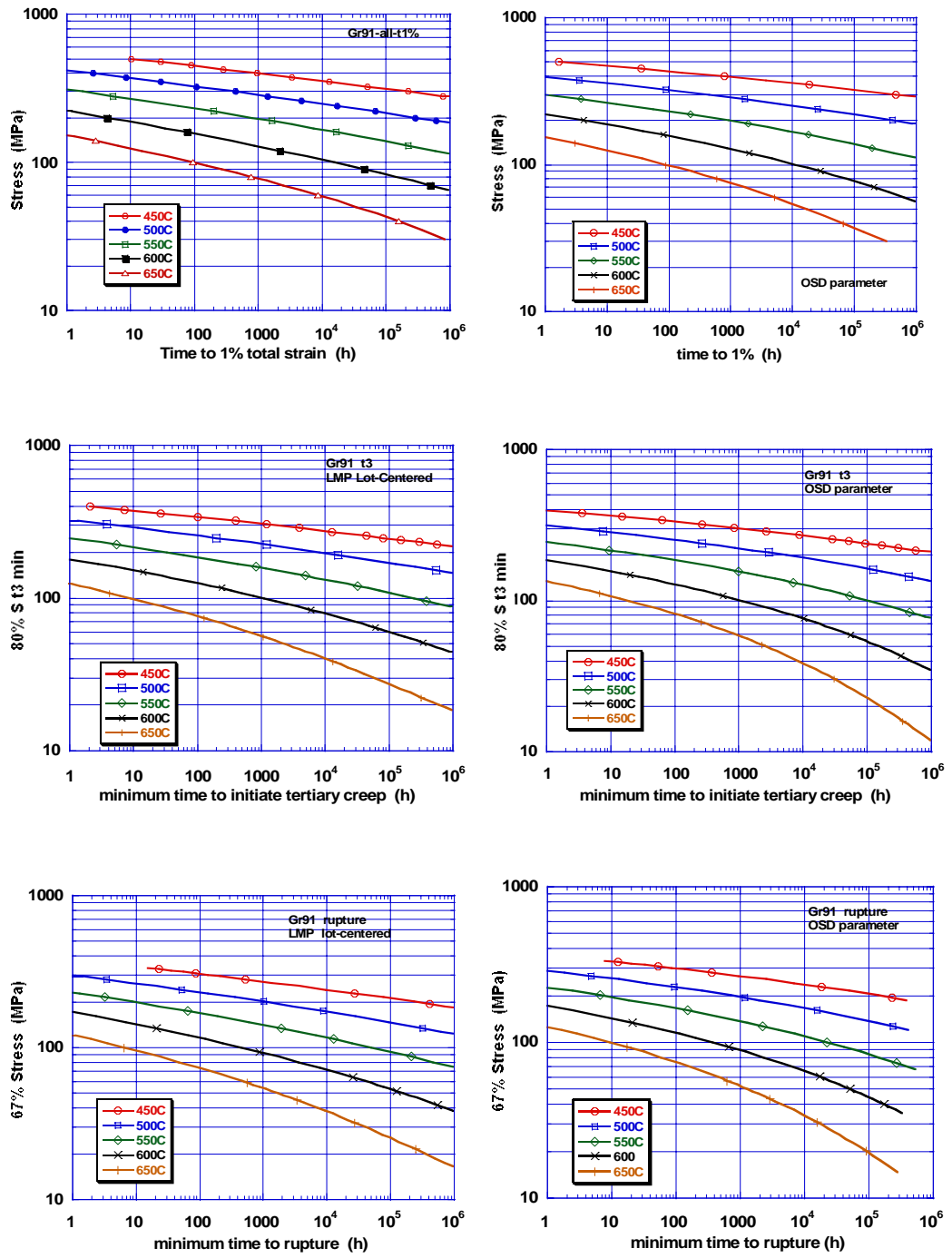


Fig. 23. Stress versus time curves plotted according to ASME III-NH time-dependent criteria.

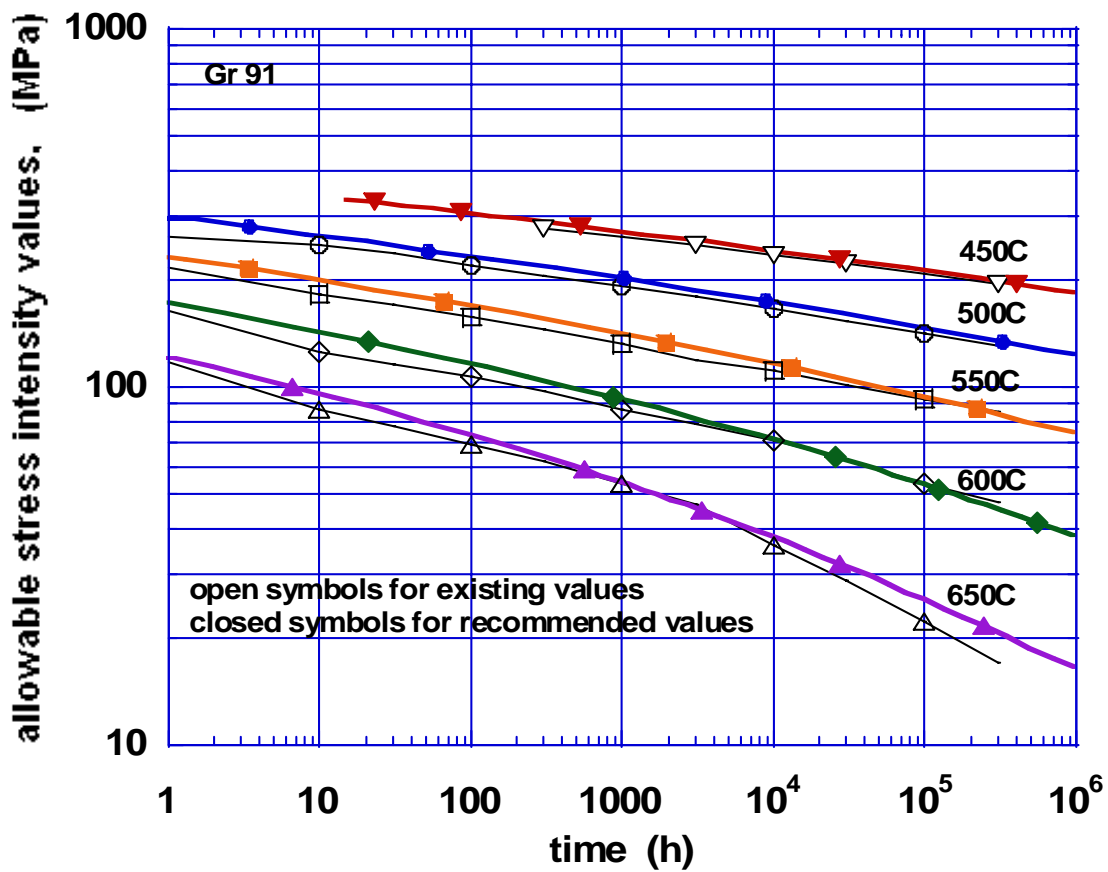


Fig. 24. Comparison of current S_t values with values based on the Larson Miller parameter and new database.

SUMMARY AND RECOMMENDATIONS

The sources for high-temperature creep-rupture data for alloy Gr 91 were reviewed and the development of S_t values was traced for ASME Section III, Subsection-NH.

A database for time to 1% strain, time to the initiation of tertiary creep, and rupture life was collected and characterized. Data for times equal to and greater than 100 h were correlated over the temperature range from 450 to 780°C (840 to 1435°F) by means of the Larson Miller and Orr-Sherby-Dorn time-temperature parameters.

Applying the Criteria set forth in ASME III-NH, it was found that the rupture strength controlled the allowable stress intensity values for all temperatures and times.

The S_t values estimated from the expanded database were found to be slightly greater than the values currently listed in ASME III-NH for some combinations of temperature and time. The new recommended values were based on the Larson Miller lot-centered parametric procedure. Since the current values in III-NH are conservative relative to these “recommended values” there does not appear to be a strong justification for replacing current values.

ACKNOWLEDGEMENTS

This work was supported by ASME ST-LLC and managed by J. Ramirez. Technical oversight was provided by R. I. Jetter and C. Hoffmann. Part of the review undertaking was supported by UT-Battelle LLC under Subcontract 4000045435. The authors acknowledge the support and encouragement of W. R. Corwin and W. Ren of the Oak Ridge National Laboratory.

REFERENCES

1. T. E. McGreevy and R. I. Jetter, “DOE-ASME Generation IV Materials Tasks,” *Proceedings of PVP2006-ICPVT-11*, July 23-27, Vancouver, BC, Canada, 2006.
2. P. Patriarca, S. D. Harkness, J. M. Duke, and L. R. Cooper, “U. S. Advanced Materials Development Program for Steam Generators,” *Nuclear Technology*, Vol. 28, March 1976, 516-536.
3. G. C. Bodine, Jr., B. Chakravarti, C. M. Owens, B. W. Roberts, D. M. Vandergriff, and C. T. Ward, *A Program for the Development of Advanced Ferritic Alloys for LMFBR Structural Applications*, TR-MCD-015, Combustion Engineering, Inc., Windsor CT (September 1977)
4. V. K. Sikka, M. G. Cowgill, and B. W. Roberts, “Creep Properties of Modified 9Cr-1Mo Steel,” pp. 413-423 in *Proceedings of Topical Conference on Ferritic Alloys for Use in Nuclear Energy Technologies*, ASM International, Materials Park, OH, 1985.
5. M. K. Booker, “Creep Equation for Modified 9Cr-1Mo Steel,” submission to the *Nuclear Systems Materials Handbook*, Oak Ridge National Laboratory, Oak Ridge, TN, 1990.
6. M. Ueta, The Japan Atomic Power Co. Ltd., “Material Data Sheets of Mod. 9Cr-1Mo Steel,” letter to C. R. Brinkman, Oak Ridge National Laboratory, Oak Ridge, TN, January 10, 1992.

7. K. Harmann, Mannesmann Industries, Dusseldorf, Germany, "P91/T91 creep rupture strength", letter to R. W. Swindeman, Oak Ridge National Laboratory, Oak Ridge, TN, September 14, 1992.
8. F. Masuyama, Mitsubishi Heavy Industries, Ltd., "Heat Treatment for 9Cr-1Mo-V Grades," letter to B. L. Roberts, Tennessee Valley Authority, January 19, 1993.
9. M. Prager, "Stress Rupture Properties of T/P 91 with Lower Tensile Strength," Metals Properties, New York, NY, (September 19, 1994).
10. *ECCC Data Sheet for Steel X10CrMoVNb9-1*, 1995
11. *Material Test Data of 2.25Cr-1Mo Steel and Mod. 9Cr-1Mo Steel*, JNC TN9450 2003-004, O-arai Engineering Center, Japan Nuclear Development Institute, Naka-gun, Ibaraki-Ken, Japan (June 2003)
12. *Data Sheets on the Elevated-Temperature Properties of 9Cr-1Mo-V-Nb Steel Tubes for Boilers and Heat Exchangers (ASME SA-213/SA-213M Grade T91 and 9Cr-1Mo-V-Nb Steel Plates for Boilers and Pressure Vessels (ASME SA-387/SA-387M Grade 91)*. NRIM Data Sheet No. 43, National Institute for Materials Science, Sengen, Tsukuba-shi, Ibaraki, Japan (1996)
13. *NIMS CREEP DATA SHEET ATLAS OF CREEP DEFORMATION PROPERTY*, No. D-1, National Institute for Materials Science, Sengen, Tsukuba-shi, Ibaraki, Japan (31 March 2007)
14. S. Camineda, G. Cumino, L. Cipolla, A. Di Gianfrancesco, "Long Term Creep Behavior and Microstructural Evolution of ASTM Grade 91 Steel," pp. 1071-1085 in *Proceedings from the Fourth International Conference on Advances in Materials Technology for Fossil Power Plants*, ASM International, Materials Park, OH, 2005.
15. R. I. Jetter, "Subsection NH- Class 1 Components in Elevated Temperature Service," *Companion Guide to the ASME Boiler & Pressure Vessel Code*, K. R. Rao, ed., American Society of Mechanical Engineers, New York, NY, 2002, pp. 369-404.
16. F. C. Monkman and N. J. Grant, " An Empirical Relationship between Rupture Life and Minimum Creep Rate in Creep-Rupture Tests," *Proceedings of the American Society for Testing and Materials*, 1956, Vol. 56, 593-605.
17. W. E. Leyda and J. P. Rowe, *A Study of the Time for Departure from Secondary Creep for Eighteen Steels*, ASM Technical Report No. P 9-6.1, American Society for Metals, Metals Park, OH, 1969.

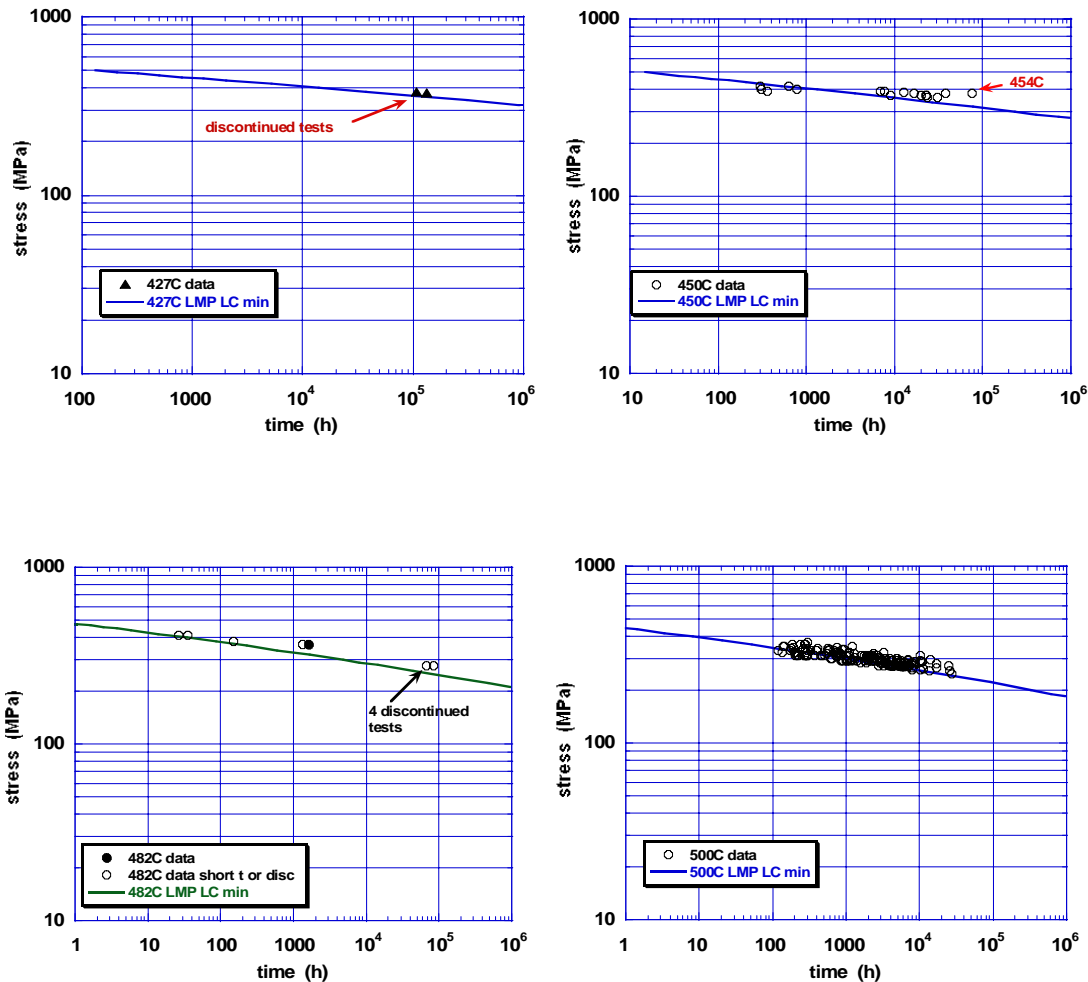
18. M. Prager, "Proposed Implementation of Criteria for Assignment of Allowable Stresses High in the Creep Range, pp 273-293 in *Structural Integrity, NDE, Risk and Material Performance for Petroleum, Process and Power*, PVP-Vol. 336, American Society of Mechanical Engineering, New York, NY 1996.
20. J. C. Moosbrugger, "Development and Confirmation of Improved Inelastic Deformation Model, pp. 75-103 in *JAPC-USDOE Joint Study on Structural Design Methods and Data for Modified 9Cr-1Mo Steel Annual Report for Period April 1, 1990-March 31, 1991*, ORNL/9Cr/91-1, Oak Ridge National Laboratory, Oak Ridge TN, 1991.
21. D. I. G. Jones, R. M. French, and R. L. Bagley, "Renewal Inelasticity Theory With a Damage Function," pp. 303-310 in *Heat Resistant Materials II*, ASM International, Materials Park, OH, 1995.
- 22 R. W. Swindeman, "Construction of Isochronous Stress-Strain Curves for 9Cr-1Mo-V Steel, pp. 95-100 in *Advances in Life Prediction Methodology*, PVP-Vol. 391, American Society of Mechanical Engineers, New York, NY, 1999.
23. L. H. Sjodhal, A Comprehensive Method of Rupture Data Analysis With Simplified Models, pp. 501-516 in *Characterization of Materials for Service at Elevated Temperatures*, MPC-7, American Society of Mechanical Engineers, New York NY, 1978.
24. S. Holmstrom and P. Auerkari, "Effect of Short-term Data on Predicted Creep Rupture Life- Pivoting Effect and Optimized Censoring," pp.441-451 in *Creep & Fracture in High Temperature Components- Design & Life Assessments*, DEStech Publications, Inc., Lancaster, PA, 2005.
25. K. Kimura, K. Sawada, K. Kubo, H. Kushima, "Influence of Stress on Degradation and Life Prediction of High Strength Ferritic Steels," pp. 11-18 in *Experience with Creep-Strength Enhanced Ferritic Steels and New and Emerging Computation Methods*, PVP-Vol. 476, American Society of Mechanical Engineers, NY, 2005.
26. S. R. Holdsworth, "The ECCC Approach to Creep Data Assessment," paper presented at the *Eighth International Conference on Creep and Fatigue at Elevated Temperatures*, July 22-26, 2007, American Society of Mechanical Engineers, San Antonio, Texas.
27. W. Bendick, J. Gabrel, and B. Vandenberghe, "Assessment of Creep Rupture Strength for New Martensitic 9%Cr Steels," paper presented at the *Eighth International Conference on Creep and Fatigue at Elevated Temperatures*, July 22-26, 2007, San Antonio, Texas.

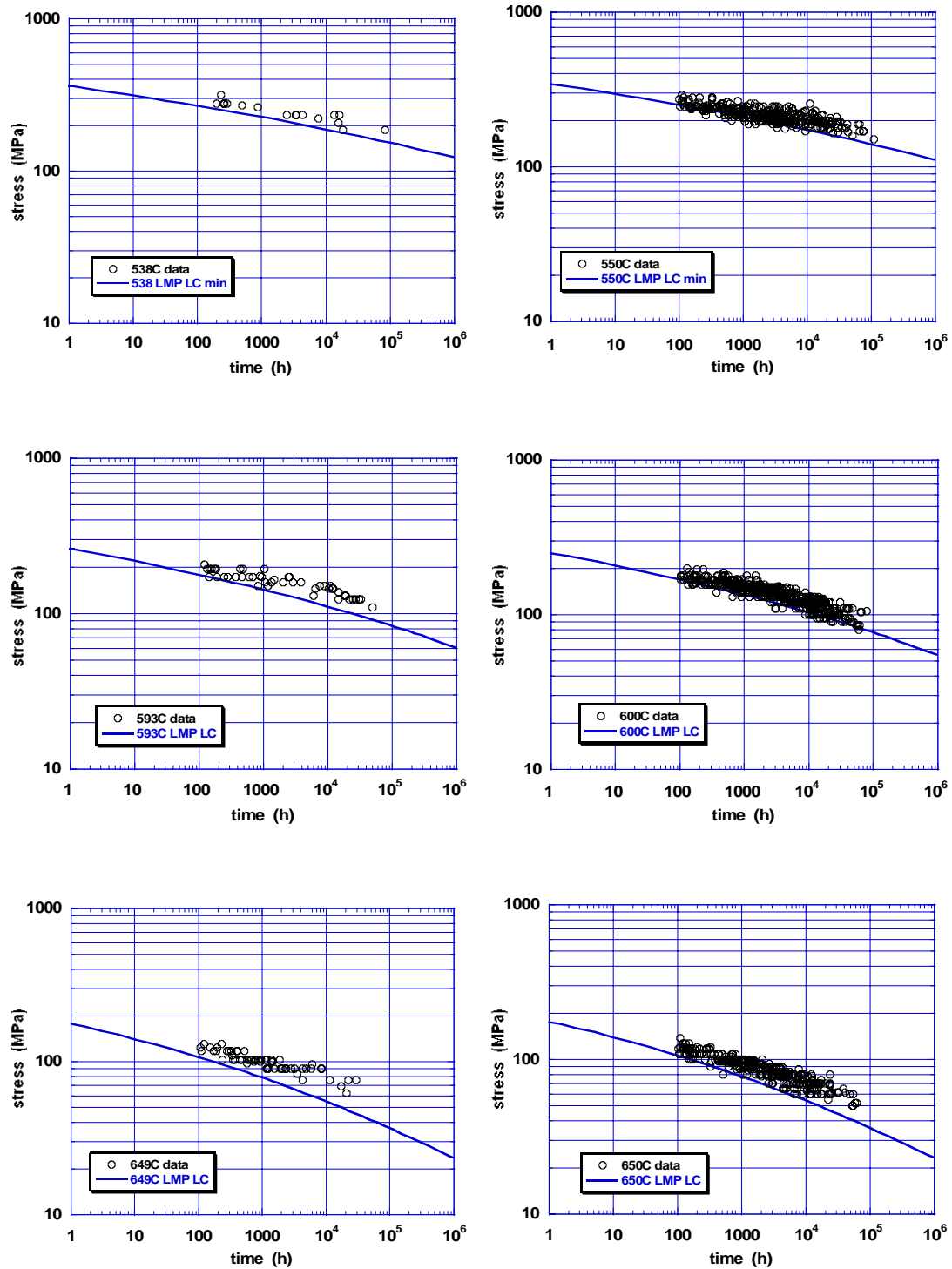
APPENDIX 1

VALUES FOR THE PARAMETRIC CONSTANTS

APPENDIX 2

COMPARISON OF DATA TO MINIMUM STRESS-TO-RUPTURE CURVES BASED ON THE LARSON MILLER LOT-CENTERED PROCEDURE





VERIFICATION OF ALLOWABLE STRESSES IN ASME SECTION III,
SUBSECTION NH FOR GRADE 91 STEEL

PART 2: STRESS FACTORS FOR WELDMENTS

R. W. Swindeman
Cromtech Inc
Oak Ridge, TN 37830-7856

M. J. Swindeman
University of Dayton Research Institute
Dayton, OH 45469-0110

B. W. Roberts
BW Roberts Consultants
Chattanooga, TN 37416

B. E. Thurgood
Bpva Engineering
San Diego, CA 92131

D. L. Marriott
Stress Engineering Services
Mason, OH 45040

November, 2007

ABSTRACT

A creep-rupture database that was used to develop stress rupture factors (SRFs) in ASME Section III Subsection NH (ASME III-NH) for weldments of 9Cr-1Mo-V (Gr 91) steel was re-assembled. The intent was to review the original work, supplement the database with newer data, and validate the applicability of the SRFs to longer time service to meet the needs for the Generation IV nuclear reactor materials program. After a review of the augmented database, approximately 85 of 200 data on weld metal and weldments were selected for the re-evaluation of SRFs. Data were processed using a lot-centered Larson Miller parametric analysis similar to the model used to correlate stress-rupture data for base metal. It was found that the weldments did not follow the same stress dependency in stress-rupture as base metal. As a result, the SRF values depended on both time and temperature. Some SRF values were estimated, but the long-time, low-stress SRF values were found to be lower than those values which formed a basis for the SRFs in 2007 ASME III-NH. Moreover, the lack of long-time data above 540°C (1000°F) made the database unsuitable for the estimation of SRFs for application to all the S_t values covered in ASME III-NH. The coverage needed for the Generation IV nuclear pressure vessels, however, was expected to be for temperatures below 540°C (1000°F). A review of European and Asian work on Gr 91 weldments provided helpful information in this respect. Although significant differences in behavior were reported from one research effort to another, special notice was taken of recent work in Japan to develop weld strength reduction factors (WSRFs) for use in the fossil and petrochemical industries. Here, the WSRFs were based on stress-rupture models applicable to welded components for long-time service to at least 600°C (1110°F). Further testing of Gr 91 weldments for long times and low stresses was recommended

INTRODUCTION

A three-year collaborative effort has been established between the Department of Energy (DOE) and the American Society of Mechanical Engineers (ASME) to address technical issues related to codes and standards applicable to the Generation IV Nuclear Energy Systems Program [1]. A number of tasks have been identified that are managed through the ASME Standards Technology, LLC (ASME ST-LLC) and involve significant industry, university, and independent consultant activities. One of the tasks is the *Verification of Allowable Stresses in ASME Section III, Subsection NH With Emphasis on Alloy 800H and Grade 91 Steel*. A subtask on 9Cr-1Mo-V (Gr 91) steel involved both the verification of the current allowable stresses and the assessment of the data needed to extend the ASME Section III, Subsection NH (ASME III-NH) coverage of Gr 91 steel to 600,000 hours at 650°C (1200°F). A report on this subtask has been produced [2]. A second subtask on Gr 91, reported here, undertook the review and re-evaluation of weld metal and weldment data to make a judgment as to the adequacy of the stress factors for weldments currently listed in ASME III-NH.

IDENTIFICATION OF FILLER METALS FOR Gr 91

Gr 91 steel is one of several ferritic/martensitic and ferritic/bainitic steel of interest for the Generation IV pressure vessel. ASME III-NH identifies the permitted SA specifications and associated product forms for Gr 91 in Table I-14.1 (a). Included are forgings (SA-182), seamless tubing (SA-213), seamless pipe (SA-335), and plate products (SA-387). Specifications for similar products produced in Asia and Europe have similar chemistry requirements and are considered to be equivalent to the SA specifications. The permissible weld materials for Gr 91 listed in ASME III-NH are SFA 5.5 Class E90XX-B9, which applies to shielded metal arc (SMA) welding, SFA5.23 Class EB9, which applies to submerged arc (SA) welding, and SFA5.28 Class ER90S-B9, which applies to gas shielded (GTA or GMA) welding. The chemistries for these deposited filler metals are provided in Table 1 where they may be compared to the specification for the Gr 91 wrought plate product. Of significance are the higher levels of Mn and Ni that are permitted in the filler metals. These elements suppress the martensite start and finish temperatures as well as the A_{c1} critical temperature that limits the upper post weld heat treating (PWHT) temperature. Some specifications for filler metals limit the Mn plus Ni content to 1.5%. The increased Ni in the filler metal is desired for improved toughness. A PWHT temperature of 745°C (1375°F) is recommended in SFA-5.23 and 760°C (1400°F) in SFA-5.28. However, each construction code provides rules for PWHT, and in ASME III-NH, paragraph NH-3357 requires that the PWHT conform to NB-4620. The P number for Gr 91 is 5B (Group 2) and Table NB-4622.1-1 in ASME III-NB requires a PWHT in the temperature range of 730 to 775°C (1350 to 1425°F) for times that depend on the thickness of the product.

Table 1. Chemistries for Grade 91 steel and filler metals

| Element | SA-387 | SFA5.5 E9015-B9 Shielded Metal Arc | SFA5.23 EB9 Submerged Arc | SFA5.28 ER90S-B9 Gas Shielded Arc |
|---------|------------|---------------------------------------|------------------------------|--------------------------------------|
| C | 0.08-0.12 | 0.08-0.13 | 0.07-0.13 | 0.07-0.13 |
| Mn | 0.30-0.60 | 1.2max | 1.25max | 1.2max |
| P | 0.020max | 0.01max | 0.010max | 0.010max |
| S | 0.010max | 0.01max | 0.010max | 0.01max |
| Si | 0.20-0.50 | 0.30max | 0.3max | 0.05-0.30 |
| Ni | 0.40max | 0.8max | 1.00max | 0.8max |
| Cr | 8.0-9.50 | 8.0-10.50 | 8.0-10.00 | 8.0-10.50 |
| Mo | 0.85-1.05 | 0.85-1.20 | 0.80-1.10 | 0.85-1.2 |
| Cb | 0.06-0.10 | 0.02-0.07 | 0.02-0.10 | 0.02-0.10 |
| N | 0.03-0.070 | | 0.03-0.070 | 0.03-0.07 |
| Al | 0.02max | 0.02-0.10 | 0.04max | 0.02max |
| V | 0.18-0.25 | 0.15-0.30 | 0.15-0.25 | 0.15-0.30 |
| Ti | 0.01max | | | |
| Zr | 0.01max | | | |
| Cu | | 0.25max | <0.1 | <0.1 |

Note: 2007 ASME Section II Part A for SA-387 specification

Note: sum of Mn and Ni shall be less than or equal to 1.5%

BACKGROUND AND SOURCES FOR WELDMENT CREEP-RUPTURE DATA

A developmental program on 9Cr-1Mo-V steel was undertaken by Combustion Engineering, Inc in 1975 to meet the property goals identified by Patriarca, et al. in 1976 [2]. A screening program was undertaken to reach these goals [3] that included weld filler metal development. The emphasis was on the Shielded Metal Arc (SMA) process, and batches were produced with 127 different compositions. The SMA wires with the best impact properties were selected for production of larger batches of wire to be used for both the SMA and Gas Tungsten Arc (GTA) welding processes. Creep-rupture testing at 538, 593, and 649°C (100, 1100, and 1200°F) was undertaken on two filler metals that were judged to be the best based on toughness. Of these, one proved to be superior in stress-rupture to the reference base metal and the other inferior. The chemistry of the undiluted weld pad for the best wire was 0.064% C; 0.64% Mn; 0.01% P; 0.011% S; 0.20% Si; 0.02% Ni; 9.15% Cr; 1.03% Mo; 0.04% Cb; 0.053% N, 0.001% Al; 0.16% V; and 0.03% Cu. Work on the poorly performing weld filler metal was discontinued.

From 1975 to the mid-1990s, the U.S. Department of Energy (DOE) supported further mechanical testing of weldments in Gr 91, and the Oak Ridge National Laboratory (ORNL) assumed the management of the technology program. By 1982, when data packages were prepared for submission to ASME Section I and Section VIII for code approval, the available creep-rupture data were from weldments fabricated using both standard 9Cr-1Mo filler and matching 9Cr-1Mo-V filler. Except for the developmental work of Bodine, et al., all welds were produced by the gas tungsten arc (GTA) process.

Further development by Sikka and coworkers produced weldments by the submerged arc (SA) and shielded metal arc (SMA) processes [4-7]. The filler metal most often used was the standard 9Cr-1Mo (Gr 9) steel. By 1987 it became clear that weldments in Gr 91 were significantly weaker than the base metal with the relative weakness increasing with increasing temperature [8, 9]. Various welding procedures and post weld heat treatments were examined but the lower strength associated with a weakness in the fine-grained region of the heat affected zone (HAZ) persisted [10]. These observations were confirmed by intensive investigations of weldment performance undertaken in Europe and Asia to qualify the material and components for usage in power-generating applications for the temperature range from 550 to 650°C (1020 to 1200°F) [11, 12, 13].

The DOE-sponsored programs produced virtually all of the information that led to the development of stress rupture factors for Gr 91 weldments similar to those in ASME III-NH Table 1-14.10 for other materials, and these factors were based on the ratio of the average strength of the weldment (for the ferritics) to the base metal [10]. In the subsequent revisions of ASME III Code Case N-47 that led to ASME III-NH, the material specifications for the Gr 91 filler metals that were addressed by the original code case submission were altered from SFA 5.4 (E505) to those mentioned earlier in this report, namely SFA-5.28 ER 90S-B9, SFA-5.5 E90XX, and SFA-E.23 EB9. Since the HAZ in the base metal was thought to control the stress factor for weldments, the filler metal was not of primary concern and the stress rupture factors were not changed. The stress ruptures factors for Gr 91 were found to be relatively time independent but decreased with increasing temperatures. Since 1990, procedures and estimates of weld strength reduction factors were developed in Europe and Asia and several papers relating to their development have been published. These will be discussed later in the report.

CHARACTERISTICS OF THE CREEP-RUPTURE DATABASE FOR ALLOY Gr 91 WELD METAL AND WELDMENTS

The database re-assembled for the evaluation of stress factors for Gr 91 weldments in ASME III-NH was focused on the stress-rupture behavior. Although some data on creep behavior and ductility were included, they will not be discussed or evaluated in this report. There were a number of significant factors that could be discussed and evaluated with respect to the stress-rupture for weldments. These included:

- base metal composition and product thickness,
- filler metal composition and flux or coating, if used,
- welding process and process variables,
- weld configuration and number of passes,
- preheat temperature, interpass temperature, and hold/drop preheat prior to PWHT,
- post weld heat treat temperature and time,
- test specimen location (all-weld or cross weld) and size,
- failure location (weld, fusion line, HAZ, base metal away from weld).

An effort was made to assemble or reference as much of the weldment information as practical. In Appendix 1, for example, there is a listing of information on approximately 75 weldments. Products included plates, tubes, and pipes of Gr 91 with thicknesses in the range of 9 to 200 mm (3/8 to 8 in.). Filler metals included both standard 9Cr-1Mo steel

and 9C-1Mo-V steel deposited by SMA, GTA, SA, and flux core arc (FCA) welding processes. Not all 75 welded products were tested in creep. Some were used for toughness testing, bend testing, aging studies, tensile tests, fatigue tests, crack growth studies, and the like. Some weldments were tested in the as-welded condition, but most were post weld heat treated (PWHT) in the temperature range of 705 to 785°C (1300 to 1450°F). Emphasis was placed on PWHT at 730 and 760°C (1350 and 1400°F) with times being one hour or longer for products or 25-mm (1-in.) or more thickness. Some weldments were re-normalized and tempered (NT).

Samples were extracted from the weldments in several locations and orientations, and the listing of weldments in Appendix 1 provides information on these topics. For example, “TW” indicates that samples were taken in the cross weld orientation with at least one HAZ in the test section while “all W” indicates that samples were taken from the weld metal and contained no base metal HAZ. A column is supplied that lists a drawing number “DWG XX” that is a sketch of the weldment showing the specimen locations. The sketches are provided in Appendix 2. The cross-weld specimens were typically uniform gage with 32- or 57-mm (1 ¼ or 2 ¼-in.) reduced sections and 6.3-mm (1/4-in.) diameters. These specimens had either one or two weld fusion lines and associated HAZs. About half of the weldments were made with standard 9Cr-1Mo steel filler metal.

A search for the original records of the welding process details and deposit chemistries for the weldments listed in Appendix 1 was unsuccessful in many cases since many were more than 25 years old. Not including the developmental work performed by Bodine, et al., [3] only 18 weld deposit chemistries were found. These chemistries were provided in Appendix 3.

Stress-rupture data for weld and weldment specimens are listed in Appendix 4. There are approximately 200 entries representing about 40 welds and weldments. The table includes temperature, stress, rupture life, elongation, reduction of area, and some information on failure location. The failure location information was obtained by inspecting more than 150 specimens recovered from archival storage. Typically, failures identified as “shear” were in the fine-grained HAZ of the base metal. When the weld HAZ was more normal to the specimen axis, necking was sometimes observed.

The distribution of testing times with filler metals, weld process, PWHT temperature, and test temperatures are shown in Figures 1 through 4. About the same number of tests was performed on weldments from standard Gr 9 and Gr 91 filler metals, but the testing times for the standard filler metal were longer. Several of the longer times represent discontinued creep-rupture tests, so most of the data pertain to times less than 10,000 hours. The longer time tests were mostly from the GTA weldment, although a few of the SA weld exceeded 10,000 hours. Most of the testing was performed at 538 and 593°C (1000 and 1100°F). There were no data below 538°C (1000°F). Finally, the number of tests on material with the 732C (1350F) PWHT was about the same as for the 760°C (1400°F) PWHT.

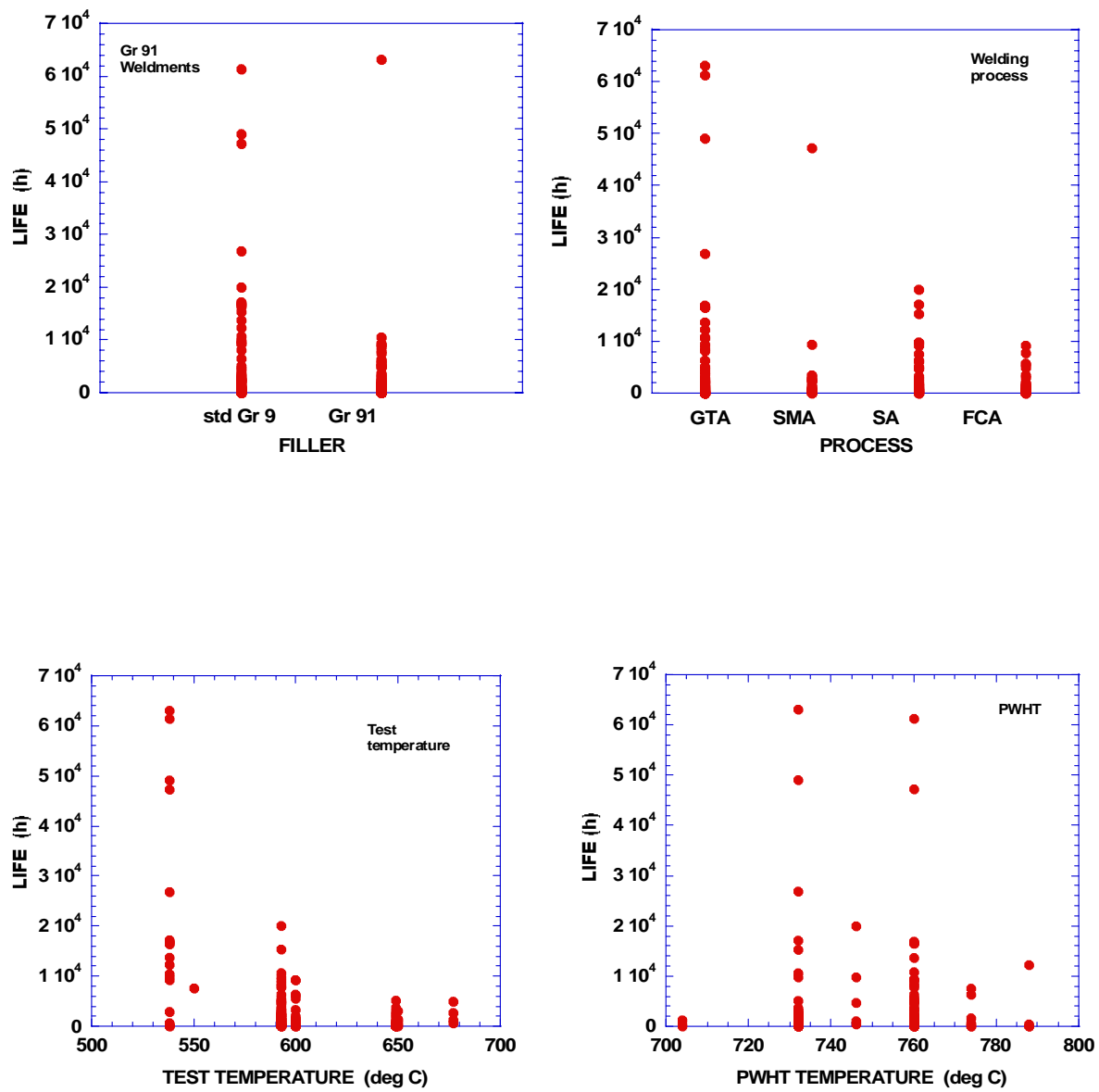


Fig. 1. The distribution of the rupture data with filler metal, weld process, test temperature, and PWHT temperature

DATA EVALUATION

Criterion for Setting the Weldment Stress Rupture Factor Values

The criterion for setting the stress rupture factor (SRF) for Gr 91 weldments in ASME III-NH was the ratio of the average strength of the weldment to the average strength of the base metal. This criterion differs from the weld strength reduction factor (WSRF) which has been used to represent the ratio of the minimum weldment strength to the allowable design stress for the base metal. Typically, ruptures in Gr 91 weldments occurred in the fine-grained HAZ of the base metal at lower stresses and long times.

Evaluation Methods:

The weldment stress rupture factors currently in 2007 ASME III-NH were based on an evaluation of approximately 60 stress-rupture test data from GTA, SMA, and SA weldments produced with both standard 9Cr-1Mo and 9Cr-1Mo-V steel filler metals [10]. These data were included in Appendix 4 and for tests at 538, 593, and 649°C (1000, 1100, and 1200°F) and times in the range of 17 to 17,200 h. Brinkman, et al. used a model developed for Gr 91 base metal and assumed the same temperature and stress dependency for weldments [10]. Thus:

$$\log t_r = C_h - 0.0231 S - 2.385 \log S + 31080/T, \quad (1)$$

where t_r is rupture life (h), S is stress (MPa), T is temperature (K), and C_h is the average “lot constant” obtained from a lot-center regression analysis. For base metal, C_h was -23.737 and for weldments C_h was -24.257. Solving the equation for S using the lot constants for base metal and weldments produced SRFs near 1.0 at high stresses and between 0.5 and 0.6 at very low stresses. These values were proposed in ASME III Code Case N-47, and the SRFs corresponding to 100,000 h were incorporated in ASME III-NH..

In the re-evaluation reported here, a modified database was correlated on the basis of equation (1). Mostly, the same data were used but rupture lives less than 100 h were deleted and some new data for SA weldments and FCA weldments were included. The database was expanded to approximately 85 points. A plot of the weldment rupture data against the “Orr-Sherby-Dorn” parameter ($\log t_r - 31080/T$) from equation (1) is shown in Fig 2. Here, $f(S)$ is the stress function from equation (1) using the lot constant for weldments [10]. The model was judged to be a reasonable fit but lacked data for stresses above 240 MPa and below 40 MPa. Also, the model tended to estimate higher strengths than observed in the 70 to 100 MPa stress range. One very short life datum at 593°C (1100°F) and 89 MPa appeared to be due to a weld metal failure at a defect. The isothermal data trend may be seen in Fig. 3 which shows the stress-rupture data and estimated stress-rupture curves for several temperature. It is clear from Fig. 3 that the estimation of the long-time rupture strengths for weldments would require significant extrapolation at all temperatures above 538°C (1000°F).

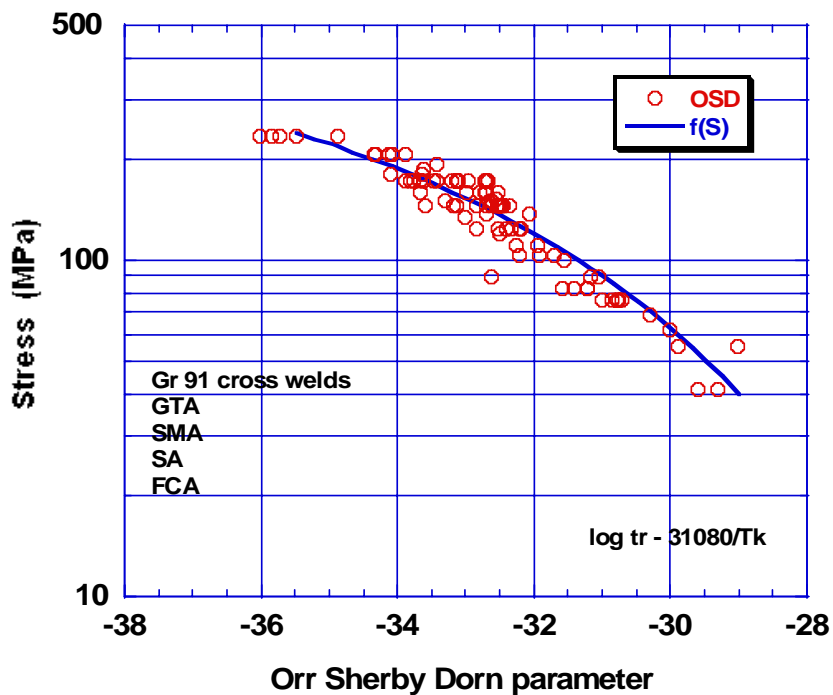


Fig. 2. Correlation of Gr 91 cross weld rupture data with the ASME III-NH model

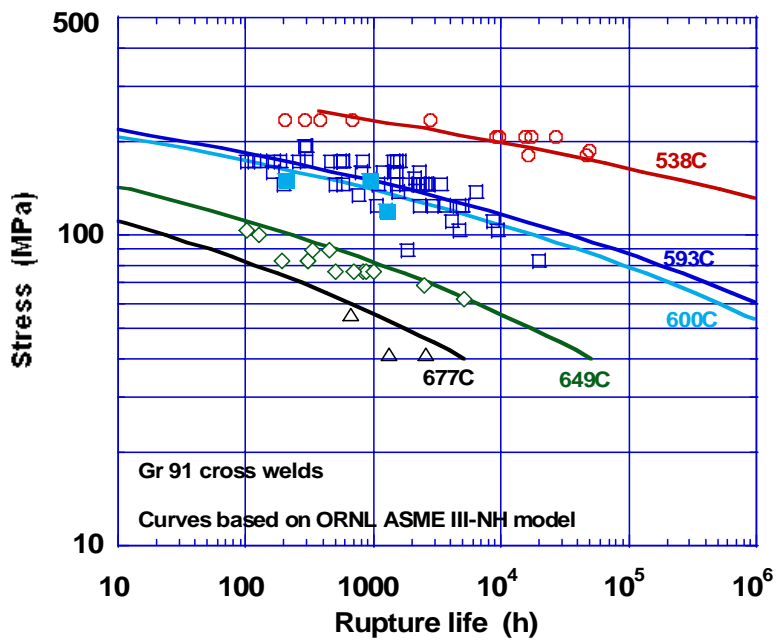


Fig. 3. Gr 91 cross weld rupture data and calculated isothermal curves based on OSD

An alternative evaluation consistent with ASME Section II procedures was performed in which a model based on the Larson-Miller parameter (LMP) was used. Here, the LMP was selected in combination with a stress function $f(S)$ that was a four-term (“third-order”) polynomial in log stress. This model was similar to the model developed for the base metal in Part 1. Thus:

$$LMP = T_K (C + \log t_r). \quad (2)$$

Where C was the average Larson-Miller parametric constant and T_K was in Kelvins.

The stress function was equated to the LMP:

$$LMP = f(S) = a_0 + a_1 \log S + a_2 (\log S)^2 + a_3 (\log S)^3 \quad (3)$$

where a_i was a series of four constants. Using a least squares fitting method in which $\log t_r$ was the dependent variable and T and $\log S$ were independent variables, the optimum values for C and a_i were determined. In this approach, lots were processed by the lot-centering procedure, described elsewhere [10, 14], and an average value for C that applied to all lots was found. Using the “best fit” values for $f(S)$ and C , the $\log t_r$ values calculated along with the residual, r_i , for each datum:

$$r_i = \log (t_{\text{observed}}/t_{\text{calculated}}) \quad (4)$$

The standard error of estimate (SEE) was obtained from the analysis in the customary way:

$$SEE = \left[\sum (\log t_{\text{observed}} - \log t_{\text{calculated}})^2 / (N_d - D_f) \right]^{1/2} \quad (5)$$

Where N_d was the number of data and D_f was the degrees of freedom. The “best fit” values for the parameters were as follows:

$$\begin{aligned} C &= 26.983991 \\ a_0 &= 92750.65583 \\ a_1 &= -92469.32172 \\ a_2 &= 45383.25970 \\ a_3 &= -7807.12738 \end{aligned}$$

The standard error of estimate (SEE) for this model was near 0.385 in log time. The fit of $f(S)$ to the data is shown in Fig. 4. Compared to the stress function proposed for the ASME III-NH evaluation, the fit was better for stress in the range of 70 to 100 MPa but an inflection in the polynomial $f(S)$ turned the curve toward the right at lower stresses. Extrapolation below 40 MPa was not possible. A comparison of data with the calculated isothermal curves is shown in Fig. 5.

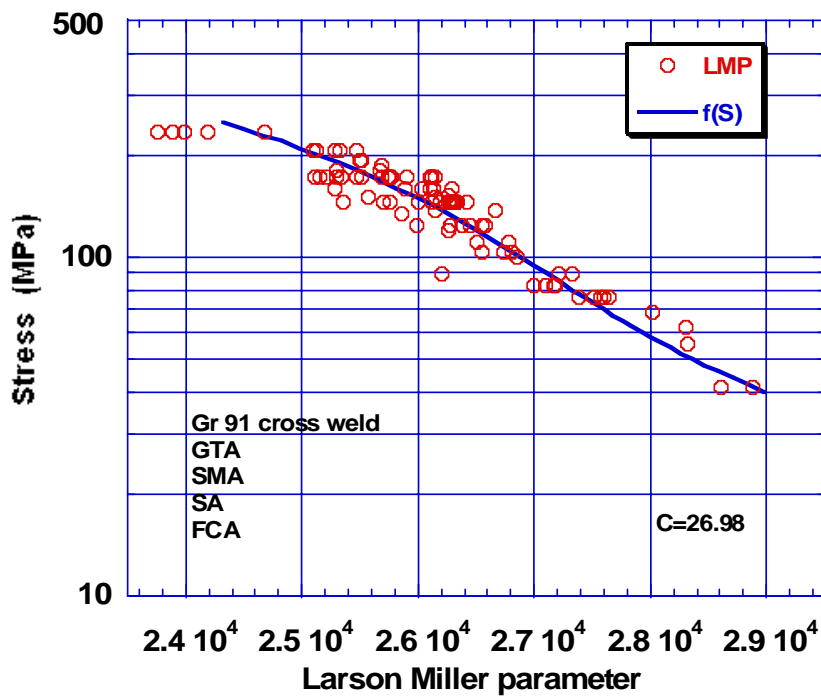


Fig. 4. Correlation of Gr-91 cross weld rupture data with the Larson Miller model

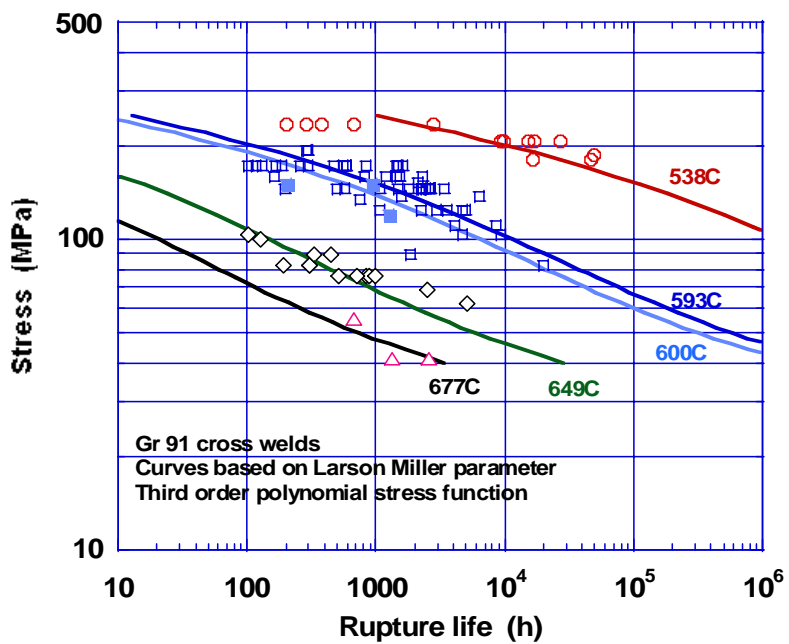


Fig. 5. Gr 91 cross weld rupture data and calculated isothermal curves based on LMP

The average lot constant and the stress function determined for the cross welds with the LMP model described above differed significantly from the base metal model described in Part 1. The average lot constant for the many lots of base metal was near 30.69 while the weldments averaged 26.97. The slope of the stress-rupture curve around 600°C and 10^5 h was -8 for the base metal and $-5 \frac{1}{2}$ for the weldments. However, the inflection in $f(S)$ for the weldments at lower stresses was not established on the basis and any observed isothermal data trend. Most of the lots of weldments contained only one to three data and the trend of life with stress could not be established for such lots. The LMP values for lots with four or more data were adjusted for their specific lot constants and stress was re-plotted against $f(S)$ and the lot LMPs. This construction is shown in Fig. 6. Inspection on the trends revealed the $f(S)$ was a reasonable representation of the data in the stress range of 70 to 220 MPa. These lots were not represented by data at stresses below 70 MPa.

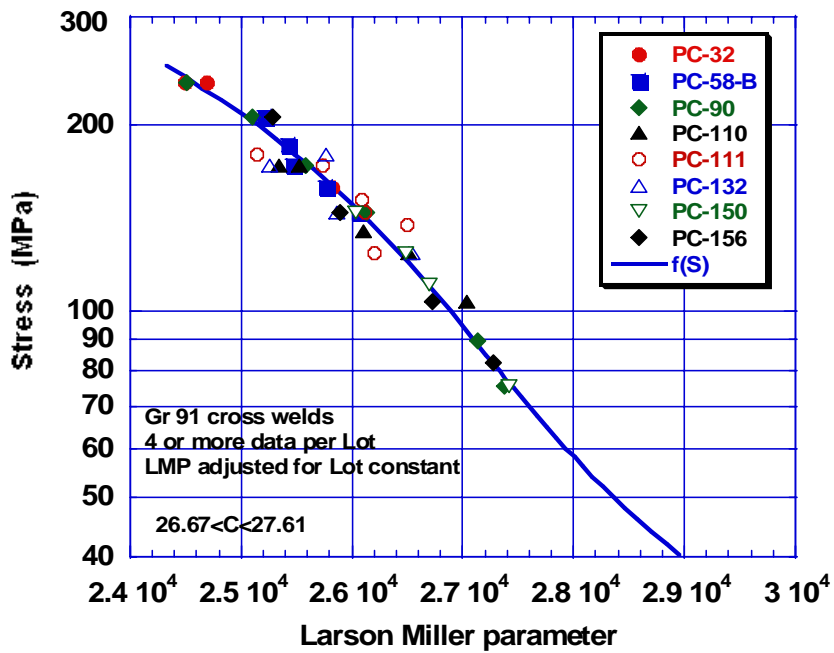


Fig. 6. Stress versus the Larson Miller parameter adjusted for lot constant differences

Estimation of Stress Rupture Factors

The lot-centered LMP stress-rupture model described in Part 1 was used for base metal and the lot-centered LMP stress-rupture model described above was used for weldments. Ratios for selected temperatures and times are provided in Table 2. Because of the lack of suitable data, SRFs are not entered for the shorter times at low temperatures and the longer times at high temperatures. For example, values for 300,000 and 600,000 hours are not provided. At 10^5 h, the SRF values differ significantly from the SRFs in ASME III-NH Table I-14.10 E-1. These values are also shown in Table 2.

Table 2. Estimated stress rupture factors for Gr 91 weldments

| Temperature (deg C) | 10 h | 100 h | 1,000 h | 10,000 h | 100,000 h | ASME III-NH (2007) |
|------------------------|------|-------|---------|----------|-----------|-----------------------|
| 425 | | | | | | 1.00 |
| 450 | | | | | | 0.95 |
| 475 | | | | | | 0.93 |
| 500 | | | | | | 0.92 |
| 525 | | | | 0.97 | 0.92 | 0.91 |
| 550 | | | 1.00 | 0.94 | 0.84 | 0.89 |
| 575 | | 1.00 | 0.97 | 0.80 | 0.73 | 0.87 |
| 600 | 1.00 | 1.00 | 0.91 | 0.77 | 0.66 | 0.84 |
| 625 | 1.00 | 0.95 | 0.81 | 0.68 | 0.66** | 0.80 |
| 650 | 1.00 | 0.86 | 0.72 | 0.68** | | 0.76 |

**** Note: very few data to support these values**

Comparison of the Stress Rupture Factors with other assessments

Since the publication of the estimates SRFs for Gr 91 in the 1980s, there have been many assessments of Gr 91 and its weldments. Early work in Japan revealed low rupture strengths in the fine-grained region of the HAZ. Significant differences between base metal and weldments were observed by Sakaguchi for times to beyond 1000 h at 550, 600, and 650°C (1020, 1110, and 1200°F) with rupture strength ratios as low as 0.60 [15]. A recommendation was made by Sakaguchi to lower the tempering temperature of the base metal to below 700°C (1290°F) but increase the PWHT at 760°C (1400°F). This procedure improved the relative strength of the weldment. About the same time, Toyoda et al. performed stress-rupture tests on weldments with PWHT at 750°C (1380°F) and observed very little reduction in strength for times to 10,000 h [16]. The SRF at 600°C (1100°F) exceeded 0.9 and at 650°C (1200°F) it exceeded 0.85. Similar results were obtained by Taguchi, et al. [17]. They provided stress-rupture curves to 10,000 h for welded joints in plates, forgings, and tubes. At 500 and 550°C (1020 and 1020°F) the weldment strengths were close to base metal strengths while at 650°C (1200°F) the SRF was near 0.87.

Studies were undertaken of the all-weld metal properties and the re-normalized and tempered properties of weld metal and weldments [3, 18, 19, 20, 21]. These studies generally showed improved strength relative to the PWHT weldments, so SRFs below 1.0 were not an issue for “overmatched” filler metals and normalized and tempered weldments..

Middleton et al. performed extensive evaluations of data from laboratory weldment tests, HAZ simulated material tests, and field in-service ruptures to establish the conditions that

produced Type IV cracking in Gr 91 weldments [22]. They defined the temperature-life regions for parent metal failures and for Type IV HAZ failures and made estimates of a weld strength reduction factor (which is 1-SRF). Corresponding values for the long time SRFs at temperatures in the 550 to 600°C (1020 to 1110°F) range were 0.8 to 0.6. Masuyama and Askins published their test results of butt welds in tubes welded to headers and found significant early failures in Gr 91 weldments at 655°C (1210°F) due to Type IV cracking [23]. The SRFs were not provided but appeared to be low. Tanoue et al. evaluated damage in thick-section Gr 91 weldments tested at 650°C (1200°F) [24]. They observed Type IV cracking and failure of the HAZ after 6000 h at 58.8 MPa. Based on the average strength of base metal determined in Part 1 of this report, the SRF from the work of Tanoue et al. would be around 0.81. This value is closer to the ASME III-NH SRF for 650°C (1200°F) than the estimates based on the new model presented here.

Nokada and coworkers examined stress-rupture behavior of welded P91 piping and elbows at 650°C (1200°F) [24, 25]. They tested full-thickness specimens extracted from the piping and elbows in addition to the pressurized pipes and elbows. Results showed similar failure modes and similar stress-rupture behavior in extracted sample and full section components when stress was based on the maximum principal stress. Although no SRFs were provided, it was clear that test data based on full-section, cross weld samples were a reliable indication of pressurized welded piping behavior.

Masuyama and Komai published results on continued testing in Japan of thick-section weldments and butt-welded tubes of Gr 91 [26]. They compared thick-section cross weld specimen data to base metal and included some results on pressurized vessels. One comparison was on the basis of the Larson Miller parameter in which they used a parametric constant of 36 for both the base metal and weldments. The stress functions were found to differ and the trends suggested that the SRFs decreased with increasing temperature and time. Interpolation of the LMP curves for 10⁵ h at 500°C (930°F) indicated an SRF around 0.91 or 0.92. At the other extreme, it was possible to estimate the SRF for 10⁴ h at 650°C (1200°F) to be around 0.77. These SRF values were consistent with values in ASME III-NH. In a later paper, Masuyama re-plotted the LMP curves using a parametric constant of 20 [27]. In this interpretation, the SRF at 650°C (1200°F) decreased to near 0.64. Comparison of the LMP curves for the two parametric constants, however, showed that the higher value for the parametric constant (C=36) was a better choice.

Cohn and Coleman reviewed work on the cross weld testing of Gr 91 and considered the effect of the PWHT temperature [28]. They found better strength when the PWHT was at 649°C (1200°F) rather than 704 or 760°C (1300 to 1400°F). They estimated some SRFs and observed that they decreased with decreasing stress and increasing time. They mentioned SRF values of 0.76 at 621°C (1150°F) and 0.8 at 607°C (1125°F). Most testing involved relatively short times, so decreases in the SRFs below the estimates provided by Cohn and Coleman were judged to be likely for longer times.

Brett and co-workers examined service failures in Gr 91 components and found that materials with high aluminum and low nitrogen were susceptible to premature rupture [29, 30, 31]. The HAZ of weldments in such lots exhibited low rupture strength relative to average strength material. Again, the relative strength decreased with increasing time and increasing temperature. The SRF values at 1000 h were around 0.75 for both 600 and 650°C (1110 and 1200°F). They suggested that SRFs could decrease to a “floor value” near 0.60.

Schubert, Klenk, and Maile studied weldment behavior in several Cr-Mo-V steels for times to beyond 20,000 h [32]. They found that at high stresses and short time failures occurred in the base metals away from the welds. With decreasing stresses and increasing time, HAZ ruptures were encountered, the stress-rupture curves for weldment data diverged from the base metal curves, and life asymptotically approached stress-rupture curves representing 100% simulated HAZ materials. For the class of steels that includes Gr 91, they suggested the SRF should be around 0.95 at 550°C (1020°F) and 0.65 at 600°C (1110°F) for 100,000 h. The value at 550°C (1020°F) is higher than that in ASME III-NH while the value at 650°C (1200°F) is much lower.

The SRFs in ASME III-NH formed the basis for the weld joint strength reduction factors (WSRFs) adopted for use with ASME B31.3 piping rules. The rationale for the WSRF values was provided by Becht [33] who recognized that the criteria for setting stress intensities in ASME III-NH differed from the criteria for setting allowable stresses for B31.1 Table A-1. For temperatures of 566°C (1050°F) and above, the WSRFs for Gr 91 were essentially identical to the SRFs in ASME III-NH.

Tabuchi and Takahashi provided a very comprehensive evaluation of WSRFs for Gr 91 based on a collection of 370 welded joint data [34]. Joining processes included SA, SMA, GTA, and metal active gas (MAG) welds and testing times extended to well beyond 20,000 h at 550°C (1020°F). They used the Larson Miller parameter in combination with a second order polynomial log-stress function to represent the base metal and weldment data. Comparisons with the model used by Brinkman [equation (1)] to develop the SRFs for ASME III-NH revealed a very similar fit and prediction of stresses. Tabuchi and Takahashi also examined subsets of data that included (a) only tests that failed in the HAZ of the base metal and (b) only tests on thicker products that had specimen locations, groove angles, and HAZs typical of components. The recommended model for weldments was as follows:

$$\text{Log } t_r = [34154 + 3494 (\log S) - 2574 (\log S)^2]/Tk - 31.4, \quad (6)$$

where the SEE was 0.267 log cycle in life. This model was based on 141 data from specimens that qualified, with respect to HAZ width and groove angle, as typical of a structural component. The WSRFs recommended Tabuchi and Takahashi were based on 80% of the minimum strength of the weldment for 100,000 h life divided by the allowable stress for the base metal for that same life. The minimum strength corresponded to the stress for a rupture curve that was displaced to shorter times by 1.65 multiples of the SEE of the model [equation (5)]. This criterion for estimating the WSRF

was different than the criterion used by Brinkman for estimating the SRFs for ASME III-NH, so a direct comparison of the SRFs and WSRFs was not possible. However, the Tubachi-Takahashi model was applicable to average strength and by substituting equation (6) for equations (2) and (3) above, the SRFs values could be calculated from the Japanese work. In Fig. 7, the SRFs calculated from the Tabuchi and Takahashi equation are compared to the SRFs from the new fit provided above, the values in ASME III-NH for 100,000 h, estimates from Schubert, Klenk, and Maile [32], and the WSRF values proposed by Tabuchi and Takahashi [34].

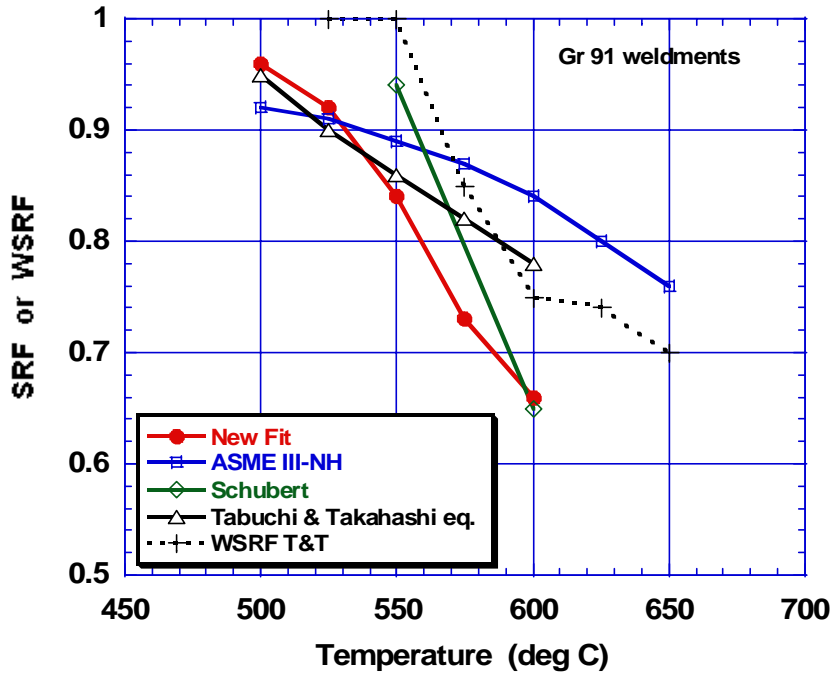


Fig. 7. Estimated Stress Rupture Factors and Weld Strength Reduction Factors for Gr 91 weldments versus temperatures for 100,000 h duration

In Fig. 7, two trends are clear. First, at temperatures below 525°C (975°F) which are of interest for nuclear pressure vessels, the SRFs will exceed 0.9 by any estimation method. Second, at temperatures of 600°C (1110°F) and above, which are of primary interest to fossil and petrochemical applications, the SRFs and WSRFs will depend on the database, analysis method, and criterion selected in the evaluation. The work of Tabuchi and Takahashi deserves special attention and appears to provide a conservative alternative to the new fit undertaken here and an improvement to the current SRF values in ASME III-NH.

Further work on Gr 91 weldments was published in 2007. Tabuchi et al. investigated GTA weldments with a “high” Ni filler metal for times to 10,000 h [35]. Again, Type IV failures occurred in the fine-grained HAZ of the base metal. At 600°C (1110°F), the slope of the log stress-log life curve for weldments between 1000 and 10,000 h was near -4, and behavior at both 600 and 650°C (1110 and 1200°F) was fairly close to the trend

estimated from the “new fit” model presented here. The estimated SRFs for 10,000 h at 550, 600, and 650°C (1020, 1110, and 1200°F) were 0.83, 0.65, and 0.58, respectively. Yamazaki, Hongo, and Watanabe examined the creep behavior of thick section Gr 91 GTA weldments for times to 10,000 h [36]. Their findings differed slightly from Tabuchi et al. [35] in that ruptures at 550°C (1020°F) and times to 1000 h at higher temperatures occurred in the weld metal. At 10,000 h the estimated SRFs at 550, 600, and 650°C (1020, 1110, and 1200°F) were 0.87, 0.67, and 0.67, respectively.

DISCUSSION OF EVALUATION

A number of factors that were important to the specification of SRFs for Gr 91 weldments were not considered in any detail. These factors were mentioned early in the report and will be discussed here, briefly.

The base metal composition could be important, as exemplified by the work of Brett and coworkers on materials with high Ni/Al ratios [29-31]. None of the base metal compositions included in this study fell into the high ratio category. Some base metal chemistries, however, could result in the weldment exceeding the A_{c1} if high PWHT temperatures are used [37]. An effect on weldment behavior could be expected if the material exceeded the critical temperature. The highest PWHT used for this study was 788°C (1450°F) which is judged to be a safe temperature for the normal range of chemistries.

Product thickness could be important since the base metal properties are known to be sensitive to thickness. In ASME Section II Part D, products thicker than 75 mm (3 in.) have lower allowable stresses than thinner products for some temperatures. Thus, depending on the thickness, one might observe different SRFs for the same temperature-time conditions. The database considered here included only one thick product and only five data at 593°C (1100°F) were produced on the thick material. European and Asian researchers undertook more testing of weldments from thick products but no clear pattern emerged. However, it is significant that Tabuchi and Takahashi did not consider thin products in their development of WSRFs [34].

The filler metal composition could be important. Sometimes, Ni is added to filler metal for improved toughness. When the Ni + Mn exceed 1.2%, the A_{c1} , martensite start, and martensite finish temperatures are lowered. The creep strength of the weld metal may be affected by untempered martensite produced from the retained austenite after tempering [38]. This will extend the region of failures in the weld metal, which normally occur at short times and high stresses. A few data from high Ni + Mn welds were included in the database used here. Half of the welds in the database were standard 9Cr-1Mo steel. This weld metal is expected to be weaker than 9Cr-1Mo-V. The deletion of rupture data short of 100 h eliminated some failures in the weld metal of the weldment. But not all of the specimens were available in the archives for inspection, so there is a possibility that some shorter time Gr 9 weld metal failures were retained in the processed database.

No detailed evaluation was undertaken to establish a relationship between the welding processes and the SRFs. The lot-centered analysis undertaken here produced Larson Miller parametric constants unique to each lot and it appeared that the SMA welds produced the strongest weldments (lowest lot constant) while the GTA welds produced the weakest weldments (highest lot constants). However, the SMA welds were most often made with the Gr 9 filler and the GTA welds were made with the Gr 91 filler metal. Other factors such as the base metal processing, weld configuration, number of passes, and PWHT conditions were not examined.

Most of the test results included in database were produced on 0.6-mm (1/4-in) diameter specimens. Some testing of full-thickness weldments is considered to be important to capture the effect of geometric restraint on the stress state in the HAZ. A few multiaxial tests were performed of the type described by Corum [39] and these generally supported the usefulness of the small specimen test results. Fortunately, testing of full-section weldments was undertaken by the Japanese [25, 26, 34, 35].

The selection of SRFs for inclusion in ASME III-NH Table 1.14.10 E-1 will require deliberation and action by the appropriate ASME Code committees. It is expected that when the factors are chosen they will apply to the S_{mt} values rather than the S_o values in ASME III-NH. In this respect, no consideration has been given in this report to the development of minimum strength values for weldments. The minimum values for weldments were discussed by Brinkman, et al. [10], and Tabuchi and Takahashi determined minimum strength values in their work [34].

CONCLUSIONS AND RECOMMENDATIONS

A re-evaluation of the stress-rupture of weldments in Gr 91 steel indicates that the stress rupture factors (SRFs) are lower than those that formed the basis for SRFs in ASME III-NH for temperatures above 550°C (1020°F).

A review of work in Europe and Asia finds a great deal of variability in the SRFs for one research effort to another but quite often values in the range of 0.6 to 0.8 were observed at 600°C (1110°F) and higher.

The database on weldments is not adequate to develop SRFs for long times (100,000 h and greater) for temperatures above 600°C (1110°F).

More testing of weldments in sections thicker than 75 mm (3 in.) is needed.

ACKNOWLEDGEMENTS

This work was supported by ASME ST-LLC and managed by J. Ramirez. Technical oversight was provided by R. I. Jetter and C. Hoffmann. Part of the review undertaking was supported by UT-Battelle LLC under Subcontract 4000045435. The authors acknowledge the support and encouragement of W. R. Corwin and W. Ren of the Oak Ridge National Laboratory.

REFERENCES

1. McGreevy, T. E., and Jetter, R. I., "DOE-ASME Generation IV Materials Tasks," *Proceedings of PVP2006-ICPVT-11*, July 23-27, Vancouver, BC, Canada, 2006.
15. Jetter, R. I., "Subsection NH- Class 1 Components in Elevated Temperature Service," *Companion Guide to the ASME Boiler & Pressure Vessel Code*, K. R. Rao, ed., American Society of Mechanical Engineers, New York, NY, 2002, pp. 369-404.
2. Patriarca, P., Harkness, S. D., Duke, J. M., and Cooper, L. R., "U. S. Advanced Materials Development Program for Steam Generators," *Nuclear Technology*, Vol. 28, March 1976, 516-536.
3. Bodine, Jr., G. C., Chakravarti, B., Owens, C. M., Roberts, B. W., Vandergriff, D. M., and Ward, C. T., *A Program for the Development of Advanced Ferritic Alloys for LMFBR Structural Applications*, TR-MCD-015, Combustion Engineering, Inc., Windsor CT (September 1977)
4. Sikka V. K., and Patriarca, P., *Analysis of Weldment Mechanical Properties of Modified 9Cr-1Mo Steel*, ORNL/TM-9045 May 1984.
5. Sikka, V. K., Cowgill, M. G., and Roberts, B. W., "Creep Properties of Modified 9Cr-1Mo Steel," pp. 413-423 in *Proceedings of Topical Conference on Ferritic Alloys for Use in Nuclear Energy Technologies*, ASM International, Materials Park, OH, 1985.
6. King, J. F., Sikka, V. K., Santella, M. L., Turner, J. F., and Pickering, E. W., *Weldability of Modified 9Cr-1Mo Steel*, ORNL-6299, Oak Ridge National Laboratory, Oak Ridge, TN, (September 1986).
7. DiStefano, J. R., and. Sikka, V. K., *Summary of Modified 9Cr-1Mo Steel Development Program : 1975-1985*, ORNL-6303, Oak Ridge National Laboratory, Oak Ridge, TN, (October 1986).
8. Brinkman, C. R., Sikka, V. K., Horak, J. A., and Santella, M. L., Long Term Creep-Rupture Behavior of Modified 9Cr-1Mo Steel Base and Weldment Behavior, ORNL/TM-10504, Oak Ridge National Laboratory, Oak Ridge, TN, (November 1987).

9. Haneda, H., Masuyama, F., Kaneko, S., and Toyoda, T., "Fabrication and Characteristic Properties of Modified 9Cr-1Mo Steel for Header and Piping," pp. 231 to 241 in *The International Conference on Advances in Materials Technology for Fossil Power Plants*, 103 September, 1987, Chicago, IL, ASM International, Materials Park, OH, 1987.
10. Brinkman, C., R., Maziasz, P. J., Keyes, B. L. P., Upton, H. D., *Development of Stress-Rupture Reduction Factors for Weldments and the Influence of Pretest Thermal Aging to 50,000 h on the Microstructural Properties of Modified 9Cr-1Mo Steel*, ORNL/TM-11459, Oak Ridge National Laboratory, Oak Ridge, TN, (March 1990).
11. Ellis, F. V., Henry, J. F., and Roberts, B. W., "Welding, Fabrication, and Service Experience with Modified 9Cr-1Mo Steel," pp. 55-63 in *New Alloys for Pressure Vessels and Piping*, PVP-Vol. 201, ASME, New York, NY, 1990.
12. Viswanathan, R., Berasi, M., Tanzosh, J., and Thaxton, T., "Ligament Cracking and the Use of Modified 9Cr-1Mo Alloy Steel (P91) for Boiler Headers," pp. 97-104 in *New Alloys for Pressure Vessels and Piping*, PVP-Vol. 201, ASME, New York, NY, 1990.
13. Tsuchida, T., et al., "BOP Manufacturing and Properties of ASTM A 387 Grade 91 Steel Plates," pp. 105-114 in *New Alloys for Pressure Vessels and Piping*, PVP-Vol. 201, ASME, New York, NY, 1990.
14. Sjodhal, L. H., "A Comprehensive Method of Rupture Data Analysis With Simplified Models," pp. 501-516 in *Characterization of Materials for Service at Elevated Temperatures*, MPC-7, American Society of Mechanical Engineers, New York, NY 1978.
15. Sakaguchi, Y., Babcock-Hitachi K. K., "Creep Rupture Properties of Mod. 9Cr-1Mo Weldment," paper presented at *First International Conference on Improved Coal-Fired Power Plants*, EPRI, November, Palo Alto, CA, 1987.
16. Toyoda, T., Haneda, H., Sada, T., and Masuyama, F., "Development of Thick Wall Pipes and Headers of Modified 9Cr Steel (9Cr-1Mo)," pp. 36-1 to 36-19 in *Second International Conference on Improved Coal-Fired Power Plants*, EPRI, Palo Alto CA, 1989.
17. Taguchi, K., et al., "Creep, Fatigue, and Creep-Fatigue Properties of Modified 9Cr-1Mo Steel Weldments," pp. 295-301 in *Structural Integrity, NDE, Risk and Material Performance for Petroleum, Process and Power*, PVP-Vol. 336, ASME, New York, NY, 1996.
18. Ellis, F. V. and Zielke, W. H., "Creep-Rupture Properties of Modified 9Cr-1Mo Weld Metal," pp. 121-128 in *Service Experience, Fabrication, Residual Stresses and Performance*, PVP-Vol. 427, ASME, New York, NY, 2001.

19. Santella, M. L., Swindeman, R. W., Reed, R. W., and Tanzosh, J. M., "Martensite Formation in 9Cr-1Mo-V Steel Weld Metal and Its Effect on Creep Behavior," paper presented at the *EPRI Conference on 9Cr Materials Fabrication and Joining Technologies*, Myrtle Beach, SC, July 2001.
20. Heuser, H., and Jochum, C., "Properties of Matching Filler Metals for P91, E911 and P92," pp. 249-265 in *Proceedings of the 3rd Conference on Advances in Material Technology for Fossil Power Plants*, The Institute of Materials, London, 2001.
21. Zang, Z., Marshall, A. W., and Holloway, G. B., "Flux Cored Arc Welding: The High Productivity Welding Process for P91 Steels," pp. 267 to 281 in *Proceedings of the 3rd Conference on Advances in Material Technology for Fossil Power Plants*, The Institute of Materials, London, 2001.
22. Middleton, C. J., Brear, J. M., Munson, R., and Viswanathan, R., "An Assessment of the Risk of Type IV Cracking in Welds to Header, Pipework and Turbine Components Constructed from the Advanced Ferritic 9% and 12% Chromium Steels," pp. 69 to 78 in *Proceedings of the 3rd Conference on Advances in Material Technology for Fossil Power Plants*, The Institute of Materials, London, 2001.
23. Tanoue, T., Nonaka, I., Umaki, H., Susuki, K., and Higuchi, K., "Proposal of Creep Damage Evaluation Procedures for Power Boilers Mod. 9Cr-1Mo Weldments (First Report: Uniaxial Loading)," pp. 319 to 328 in *Proceedings of the 3rd Conference on Advances in Material Technology for Fossil Power Plants*, The Institute of Materials, London, 2001.
24. Nonaka, I., Ito, T., Takemasa, F., Saito, K., Miachi, Y., and Fujita, A., "Full Size Internal Pressure Creep Tests for Welded P91 Hot Reheat Elbows," pp. 75-83 in *Experience with Creep-Strength Enhanced Ferritic Steels and New and Emerging Computational Methods*, PVP-Vol. 476, ASME, New York, NY 2004.
25. Nonaka, I., Ito, T., Takemasa, F., Saito, K., Miachi, Y., and Fujita, A., "Full Size Internal Pressure Creep Tests for Welded P91 Hot Reheat Piping," pp. 65-74 in *Experience with Creep-Strength Enhanced Ferritic Steels and New and Emerging Computational Methods*, PVP-Vol. 476, ASME, New York, NY 2004.
26. Masuyama, F., and Komai, N., "Creep Failure Behavior of Creep-Strength Enhanced Ferritic Steels," pp. 107 to 114 in *Experience with Creep-Strength Enhanced Ferritic Steels and New and Emerging Computational Methods*, PVP-Vol. 476, ASME, New York, NY 2004.
27. Masuyama, F., "Creep Rupture Life and Design Factors for High Strength Ferritic Steels," pp. 983-996 in *Creep & Fracture in High Temperature Components*, ECCC Creep Conference, September 12-14, 2005, DEStech Publications, Inc., Lancaster, PA.

28. Cohn, M. J., Patterson, S. R., and Coleman, K., "Creep Rupture Properties of Grade 91 Weldments," pp. 217-230 in *Advances in Materials Technology for Fossil Power Plants*, ASM International, Materials Park, OH, 2005
29. Brett, S. J., Bartes, J. S., and Thomson, R. C., "Aluminium Nitride Precipitation in Low Strength Grade 91 Power Plant Steels," pp. 1183 to 1197 in *Advances in Materials Technology for Fossil Power Plants*, ASM International, Materials Park, OH, 2005.
30. Brett, S. J., Oates, D. L., and Johnston, C., "In-Service Type IV Cracking in a Modified 9Cr (Grade 91) Header," pp. 563 to 572 in *Creep & Fracture in High Temperature Components*, ECCC Creep Conference, September 12-14, 2005, DEStech Publications, Inc., Lancaster, PA.
31. Allen, D. J., On, E., Harvey, B., and Brett, S. J., "FourCrack-An Investigation of the Creep Performance of Advanced High Alloy Steel Welds," pp. 772-791 in *Creep & Fracture in High Temperature Components*, ECCC Creep Conference, September 12-14, 2005, DEStech Publications, Inc., Lancaster, PA.
32. Schubert, J., Klenk, A., and Maile, K., "Determination of Weld Strength Factors for the Creep Rupture Strength of Welded Joints," pp. 792-805 in *Creep & Fracture in High Temperature Components*, ECCC Creep Conference, September 12-14, 2005, DEStech Publications, Inc., Lancaster, PA.
33. Becht IV, C., "New Weld Joint Strength Reduction Factors in the Creep Regime in ASME B31.3 Piping," paper PVP2005-71016 presented at the *ASME Pressure Vessels and Piping Conference*, July 17-21, 2005, Denver, CO.
34. Tabuchi, M., and Takahashi, Y., "Evaluation of Creep Strength Reduction Factors for Welded Joints of Modified 9Cr-1Mo Steel," paper presented at the *ASME Pressure Vessels and Piping Division Conference*, July 23-27, 2006, Vancouver, BC, Canada
35. Tabuchi, M., Hongo, H., Li, Y., Watanabe, T., and Takahashi, Y., "Evaluation of Microstructures and Creep Damages in HAZ of P91 Steel Weldment," paper PVP2007-26495 presented at the *ASME Pressure Vessels and Piping Division Conference*, July 22-26, 2007, San Antonio, TX
36. Yamazaki, M., Hongo, H., Watanabe, T., "Rupture Behavior of Multi-pass Welded Joints of Heat Resistant Steel Subjected to Creep Loading," paper PVP2007-26495 presented at the *ASME Pressure Vessels and Piping Division Conference*, July 22-26, 2007, San Antonio, TX
37. Masuyama, F., and Nishimura, N., "Phase Transformation and Properties of Gr 91 at Around Critical Temperature," pp. 85 to 91 in *Experience with Creep-Strength Enhanced Ferritic Steels and New and Emerging Computational Methods*, PVP-Vol. 476, ASME, New York, NY 2004.

38. Santella, M. L., Swindeman, R. W., Reed, R. W., and Tanzosh, J. M., "Martensite Formation in 9Cr-1Mo-V Steel Weld Metal and Its Effect on Creep Behavior," paper presented at the *EPRI Conference on 9Cr Materials Fabrication and Joining Technologies*, Myrtle Beach, SC, July 2001.
39. Corum, J. M., "Evaluation of Weldment Creep and Fatigue Strength-Reduction Factors for Elevated-Temperature Design," *Journal of Pressure Vessel Technology*, 1990, Vol. 112, No. 4, pp. 333-339.

APPENDIX 1

A LISTING OF PRODUCTS, FILLER METALS, AND WELD PROCESSES

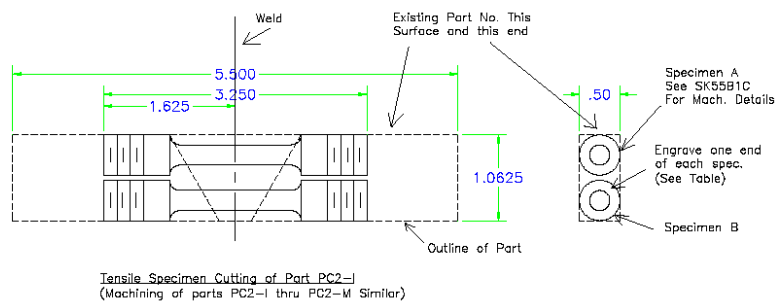
| ID | Product | Heat | Condition | Thickness | Weld | Process | Wire | Heat | Passes | PWHT | Specimen | Comment |
|-------------|---------|----------|----------------|----------------|-----------------|---------|----------|---------------|--------------|--------------|-------------|---------|
| | | | | (in.) | prep | | | | | (deg F) | | |
| PC-2 | Plate | Quaker | NT | 1 1/16 | 90° V | GTA | std 9Cr | Y3738F505 | 37 | 1450 | 1.25 TW | DWG W1 |
| PC-4 | Plate | F5349Y | NT | 5/8" | V | GTA | Gr91 | F5349Y | 16 | 1400 | 1.25 TW | DWG W2 |
| PC-5 | Tube | F5349Y | NT | 5/8" | 75° V | GTA | Gr91 | F5349Y | 4 | 1400 | 1.25 TW | DWG W2 |
| PC-9 | Plate | F5349Y | NT | 5/8" | 90° V | GTA | Gr91 | F5349Y | 24 | 1350 | 1.25 TW | DWG W2 |
| PC-10 | Plate | F5349Y | NT | 5/8" | 90° V | GTA | std 9Cr | Y3738F505 | 20 | 1350 | 1.25 TW | DWG W2 |
| PC-13 | Plate | F5349Y | NT | 3/4" | V | GTA | std 9Cr | Y3738F505 | 34 | | 1 1/4 all W | DWG W3 |
| PC-16 | Plate | F5349Y | NT | 3/4" | V | GTA | Gr91 | XA3664 | 20 | 1350 | 1 1/4 all W | DWG W3 |
| PC-32 | Plate | 30182 | NT | 5/8" | V | GTA | Gr91 | 30182 | 9 | 1350 | 1.25 TW | DWG W2 |
| PC-35 | Plate | 30182 | NT | 5/8" | 75° V | GTA | Gr91 | 30182 | | | 2.25 TW | DWG W4 |
| PC-36A 1-8 | Plate | 30394 | NT | 1" | 60° V | GTA | Gr91 | 30394 | 25 | as-welded | 2.25 TW | DWG W4 |
| PC-36B 9-16 | Plate | 30394 | NT | 1" | 60° V | GTA | Gr91 | 30394 | 25 | 1350 | 2.25 TW | DWG W4 |
| PC-39 | Plate | 30394 | 1038/677 | 1" | 60° V | GTA | Gr91 | 30394 | 17 | 1400 | 2.25 TW | DWG W4 |
| PC-42 | Plate | 30394 | 1038/704 | 1" | | GTA | Gr91 | 30394 | 6 | | 2.25 TW | DWG W4 |
| PC-45 | Plate | 30394 | NT | 1" | 60° V | GTA | Gr91 | 30394 | 9 | 1400 | 1.25 TW | DWG W2 |
| PC-52 | Plate | 30384 | NT | 1" | V | GTA | Gr91 | C2616 (30383) | 11 | 1350 | 1.25 TW | DWG W1 |
| PC-58A | Tube | 30394 | NT | 3" OD 1/2 wall | 60° V | GTA | std 9Cr | A1977F-505 | 10 | 1350 | 1.25 TW | DWG W6 |
| PC-58B | Tube | 30394 | NT | 3" OD 1/2 wall | 60° V | GTA | std 9Cr | A1977F-505 | 10 | as-welded | 1.25 TW | DWG W5 |
| PC-59 | Tube | 30394 | NT | 3" OD 1/2 wall | 60° V | SMA | std 9Cr | CAOIG-505 | 26 | | 1.25 TW | DWG W6 |
| PC-63 | Tube | sumi. | NT | 3" OD 1/2 wall | 60° V | SMA | std 9Cr | CAOIG-505 | 26 | 1350 | 1.25 TW | DWG W5 |
| PC-65 | Tube | sumi. | NT | 3" OD 1/2 wall | 60° V | SMA | std 9Cr | CAOIG-505 | 28 | 1350 | 1.25 TW | DWG W5 |
| PC-67B | Plate | 30176 | NT | 1" | 75° V | SMA | std 9Cr | 8N20AMUX24 | 31 | 1350 | 1.25 TW | DWG W1 |
| PC-71 | Plate | 30176 | NT | 1" | | SA | std 9Cr | E4390-505 | 13 | 1350 | 1 1/4 all W | DWG W6 |
| PC-72 | Plate | 30383 | NT | 2" | | SA | std 9Cr | E4390-505 | 37 | 1350/2h | 1 1/4 all W | DWG W7 |
| PC-73 | Plate | 30383 | NT | 2" | 3/4 Root-15° | SA | std 9Cr | E4390-505 | 69 | 1350/2h | 1 1/4 all W | DWG W7 |
| PC-74 | Plate | 30394 | NT | 1" | 60° V | SMA | std 9Cr | mix10153R5804 | 30 | 1350 | 1.25 TW | DWG W2 |
| PC-75 | Plate | 30394 | NT | 1" | 60° V | SMA | Gr91 | mix10166R5804 | 32 | 1350 | 1.25 TW | DWG W2 |
| PC-76 | Plate | 30176 | NT | 1" | 3/4 Root-15° | SA | std 9Cr | E4390-505 | 15 | 1350 | | |
| PC-77 | Plate | 30383 | NT | 2" | 1 Root-15° | SA | std 9Cr | 33669-505 | 63 | 1350/2h | 1 1/4 all W | DWG W7 |
| PC-80A | Plate | 30383 | NT | 2" | 3/4 Root-15° | SA | Gr91 | C2616 (30383) | 50 | 1350/2h | 2.25 TW | DWG W8 |
| PC-80B | Plate | 30383 | NT | 2" | 3/4 Root-15° | SA | Gr91 | C2616 (30383) | 50 | 1900/1400/2h | 2.25 TW | DWG W8 |
| PC-86 | Plate | 30394 | NT | 1" | 3/4 Root-15° | SA | std 9Cr | ...E-505 | 19 | 1350 | 1.25 TW | DWG W1 |
| PC-90 | Tube | sumitomo | NT | 3" OD 1/2 wall | 60° V | SMA | std 9Cr | CEM10292 | 20 | 1350 | 1.25 TW | DWG W6 |
| PC-93 | Plate | 10148 | NT | 7.6" | 5/8 Root-7 1/2" | SA | std 9Cr | 33669-505 | 145 | 1350/6h | 2.25 TW | DWG W9 |
| PC-93 | Plate | 10148 | NT | 7.6" | 5/8 Root-7 1/2" | SA | std 9Cr | 33669-505 | 145 | 1350/6h | 1.25 TW | DWG W9 |
| PC-93 | Plate | 10148 | NT | 7.6" | 5/8 Root-7 1/2" | SA | std 9Cr | 33669-505 | 145 | 1350/6h | 1 1/4 all W | DWG W9 |
| PC-94 | Tube | 59020 | NT | 3" OD 1/2 wall | 60° V | SMA | std 9Cr | CEM10292 | 12 | 1350 | 1.25 TW | DWG W5 |
| PC-95 | Tube | 59020 | NT | 3" OD 1/2 wall | 60° V | SMA | std 9Cr | CEM10292 | 17 | 1350 | 1.25 TW | DWG W6 |
| PC-98 | Plate | 30394 | NT | 1" | C | SA | std 9Cr | ... E-505 | 20 | | | |
| PC-99 | Plate | 30394 | NT | 1" | V | GTA | std 9Cr | E4390-505 | 30 | 1350 | 1.25 TW | DWG W2 |
| PC-100 | Plate | 30394 | NT | 1" | 60° V | GTA | | | 18 | | | |
| PC-102 | Tube | 59020 | NT | 3" OD 1/2 wall | V | SMA | std 9Cr | CEM10292 | 10 | 1350 | 2.8 TW | DWG W10 |
| VS1 | Pipe | | NT | 1/2" wall | | SMA | | M9412 | | 1350 | 2.25 TW | DWG W11 |
| PC-104 | Plate | 30394 | NT | 1" | 60° V | GTA | std 9Cr | A1977F-505 | 30 | 1250 | 2.25 TW | DWG W1 |
| PC-104 | Plate | 30394 | NT | 1" | V | GTA | std 9Cr | A1977F-505 | 30 | 1300 | 2.25 TW | DWG W1 |
| ETEC-1 | Pipe? | NT | 9" OD 1/2 wall | | | GTA | ERNiCr-3 | | 1350 | 2.25 TW | DWG W2 | |
| ETEC-2 | Pipe? | NT | 9" OD 1/2 wall | | | GTA | ERNiCr-3 | | 1350/950/2Kh | 2.25 TW | DWG W2 | |
| PC-109 | Plate | 10148 | 1900/1150 | 2" | V | SAW | std 9Cr | D3612F505 | 1400/1.5 | 2.5 all W? | DWG W1 | |
| PC-110 | Plate | 30176 | 1900/1150 | 1" | V | GTA | std 9Cr | 33669 | 1400 | 2.25 TW | DWG W1 | |
| PC-111 | Plate | 30394 | 1900/1150 | 1" | V | GTA | std 9Cr | 33669 | 1400/1.5 | 1.25 TW | DWG W1 | |
| 302B | Tube | | NT | 3" OD 1/2 wall | V | SMA | Gr91 | M9412 | 1350 | | | |
| 303B | Tube | | NT | 3" OD 1/2 wall | V | SMA | std 9Cr | CAOIG | 1350 | | | |
| 304B | Tube | | NT | 3" OD 1/2 wall | V | SMA | Gr22 | CAADJ | 1350 | 1.25 TW | DWG W5 | |
| SW-1 | Plate | 10148 | NT | 2" | | SA | std 9Cr | D3612F505 | 1350/2h | 2.5 TW | DWG W1 | |
| SWM-2 | Plate | | 1900/1400 | 1" | | SMA | std 9Cr | | 1400/2h? | 2.5 TW | DWG W2 | |
| PC-129 | Plate | 30176 | NT | 1" | | GTA | Gr91? | 21078? | 1350 | 1 1/4 all W | DWG W12 | |
| PC-132 | Plate | 30176 | 1900/1400 | 1" | | SMA | std 9Cr? | Kobe | 1400 | 2.25 TW | DWG W1 | |
| PC-150 | Plate | 30176 | 1900/1150 | 1" | | GTA | Gr91? | 21648? | 1350 | 2.25 TW | DWG W1 | |
| PC-166 | Plate | 30176 | 1900/1400 | 1 1/8" | | SA | std 9Cr | USW-21648 | 23 | 1375/1h | 2.25 TW | DWG W1 |
| LKNS-1 | Plate | Lukens | 1900/1400 | 2" | | SA | Gr91 | MTS3 | 44 | 1425/8h | 1.25 TW | |
| LKNS-2 | Plate | Lukens | 1900/1400 | 2" | | SA | Gr91 | MTS3 | 44 | 1425/8h | 1 1/4 all W | |
| LKNS-3 | Plate | Lukens | 1900/1400 | 2" | | SA | Gr91 | MTS3 | 44 | 1904/1364 | 1.25 TW | |
| LKNS-4 | Plate | Lukens | 1900/1400 | 2" | | SA | Gr91 | MTS3 | 44 | 1904/1364 | 1 1/4 all W | |
| LKNS-5 | Plate | Lukens | 1900/1400 | 2" | | SA | Gr91 | MTS3 | 44 | 1904/1436 | 1.25 TW | |
| LKNS-6 | Plate | Lukens | 1900/1400 | 2" | | SA | Gr91 | MTS3 | 44 | 1904/1436 | 1 1/4 all W | |
| 9R | Plate | 51383 | 1922/1418 | 3/4" | V | FCA | Gr91 | 25B52-9R | 1400/4h | 1 1/4 all W | | |
| 9R | Plate | 51383 | 1922/1418 | 3/4" | V | FCA | Gr91 | 25B52-9R | 1400/4h | 1.25 TW | | |
| 10R | Plate | 51383 | 1922/1418 | 3/4" | V | FCA | Gr91 | 25B52-10R | 1400/4h | 1 1/4 all W | | |
| 10R | Plate | 51383 | 1922/1418 | 3/4" | V | FCA | Gr91 | 25B52-10R | 1400/4h | 1.25 TW | | |
| W4R-1 | Plate | 30394 | 1900/1400 | 1" | V | FCA | Gr91 | 25B52-4R | 1400/4h | 1 1/4 all W | | |
| W4R-1 | Plate | 30394 | 1900/1400 | 1" | V | FCA | Gr91 | 25B52-4R | 1400/4h | 1.25 TW | | |
| W4R-2 | Plate | 30394 | 1900/1400 | 1" | V | FCA | Gr91 | 25B52-4R | 1400/4h | 1 1/4 all W | | |
| W4R-2 | Plate | 30394 | 1900/1400 | 1" | V | FCA | Gr91 | 25B52-4R | 1400/4h | 1.25 TW | | |
| W5R-1 | Plate | 30394 | 1900/1400 | 1" | V | FCA | Gr91 | 25B52-5R | 1400/4h | 1.25 TW | | |
| W5R-1 | Plate | 30394 | 1900/1400 | 1" | V | FCA | Gr91 | 25B52-5R | 1400/4h | 1.25 TW | | |
| W5R-2 | Plate | 30394 | 1900/1400 | 1" | V | FCA | Gr91 | 25B52-5R | 1400/4h | 1 1/4 all W | | |
| W5R-2 | Plate | 30394 | 1900/1400 | 1" | V | FCA | Gr91 | 25B52-5R | 1400/4h | 1.25 TW | | |

Note: NT corresponds to 1900°F normalizing and 1400°F tempering

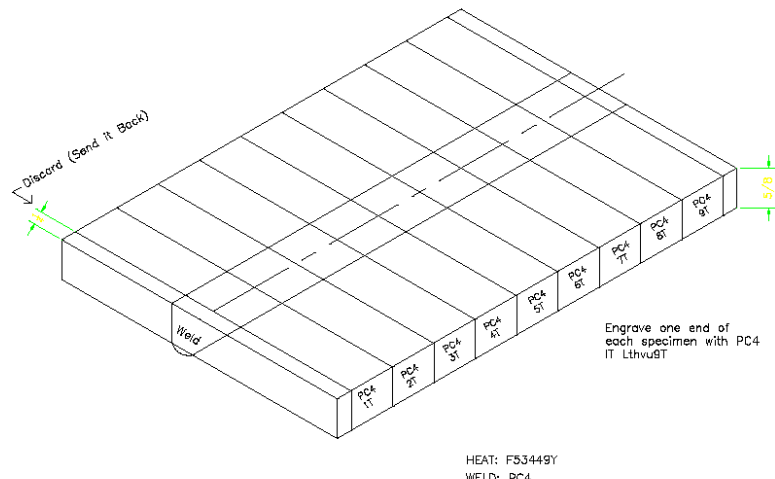
Note: NT TW indicates a cross weld specimen with HAZ in the test section

APPENDIX 2

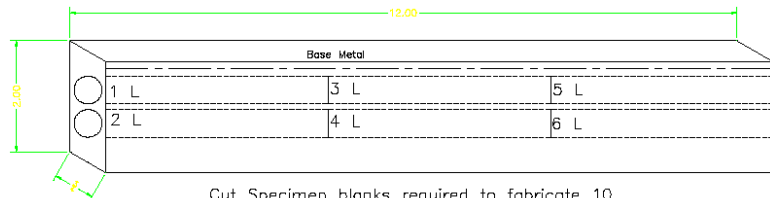
SKETCHES OF TYPICAL WELD METAL AND
WELDMENT SPECIMEN LOCATIONS



DRAWING #1

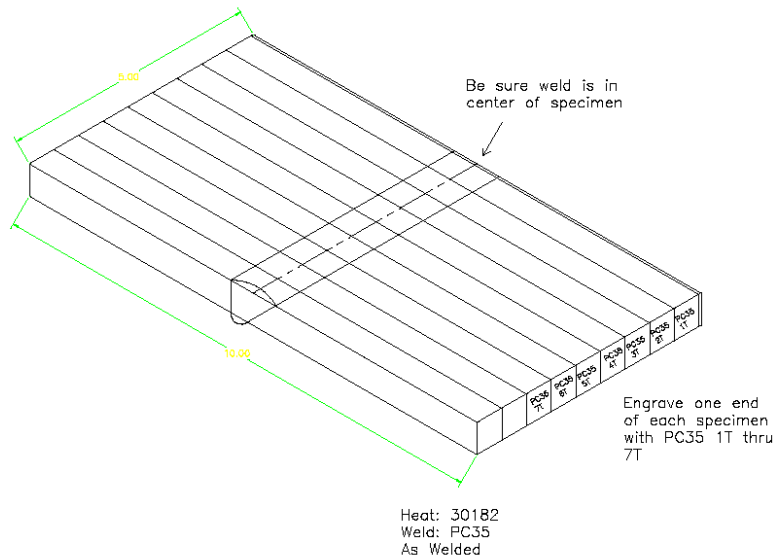


DRAWING #2



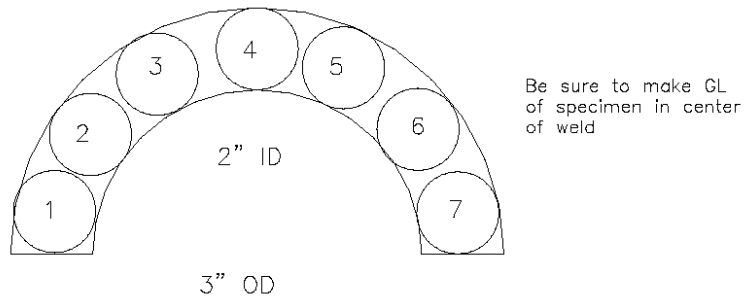
Cut Specimen blanks required to fabricate 10 specimens as per dwg sk55B1C Engrave one end of each specimen with PC13 1L thru 6L

DRAWING #3



DRAWING #4

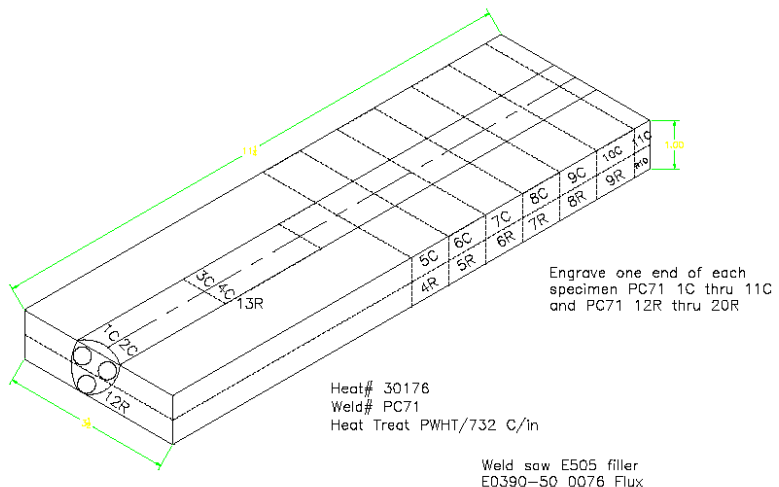
Heat #: 30394 PC58A
Heat Treatment: As welded



Cut Specimen blanks required
to make parallel specimens
as per dwg sk55BIC provided

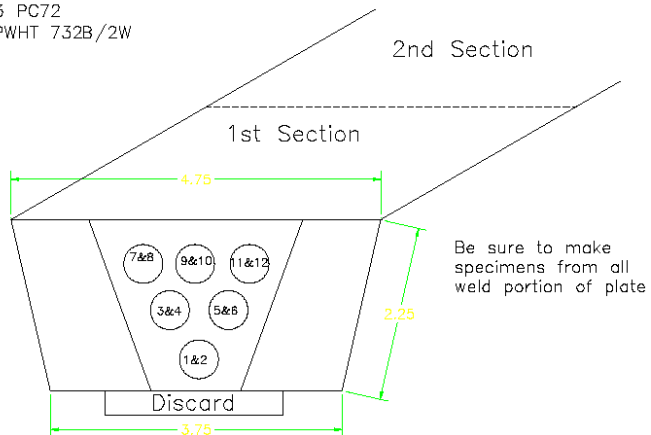
Engrave one end of each specimen with
PC58A 1L thru 7L

DRAWING #5



DRAWING #6

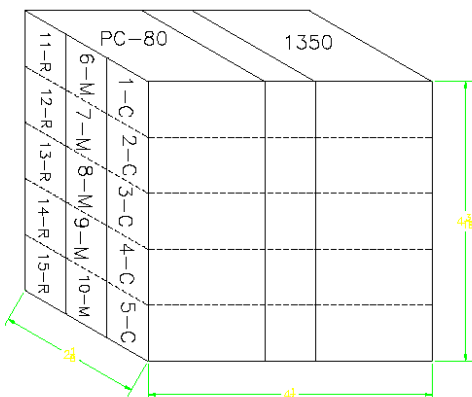
Material: 9CR-1Mo
Heat #: 30383 PC72
Heat Treat: PWHT 732B/2W



Engrave one end of each specimen with P72
1R thru 2R, PC72 3M thru 6M, PC72 7C thru
12C

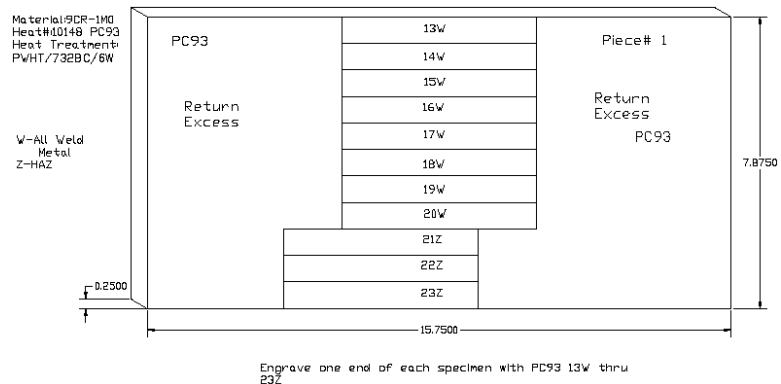
DRAWING #7

Material: 9CR-1Mo
Heat: PC-80
Heat Treatment:
PWHT/1350/2hrs.



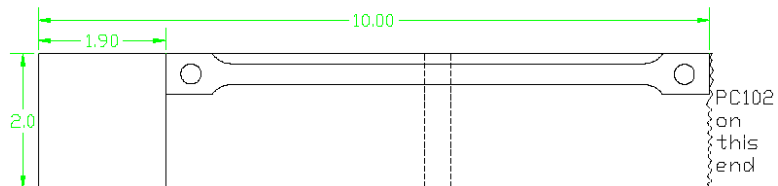
Engrave one end of each specimen with
PC-80 1-C thru 5-C, PC-80 6-M thru 10-M,
PC-80 11-R thru 15-R

DRAWING #8



DRAWING #9

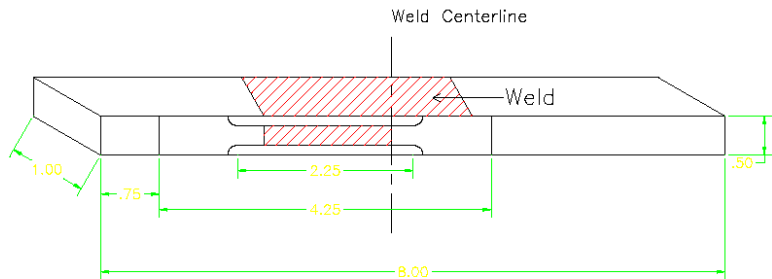
Material: 9CR-1MO
Heat#: NKK59020 PC102
Heat Treat: PWHT/732BC/1M



Engrave one end of each specimen with
PC102- thru 4L

DRAWING #10

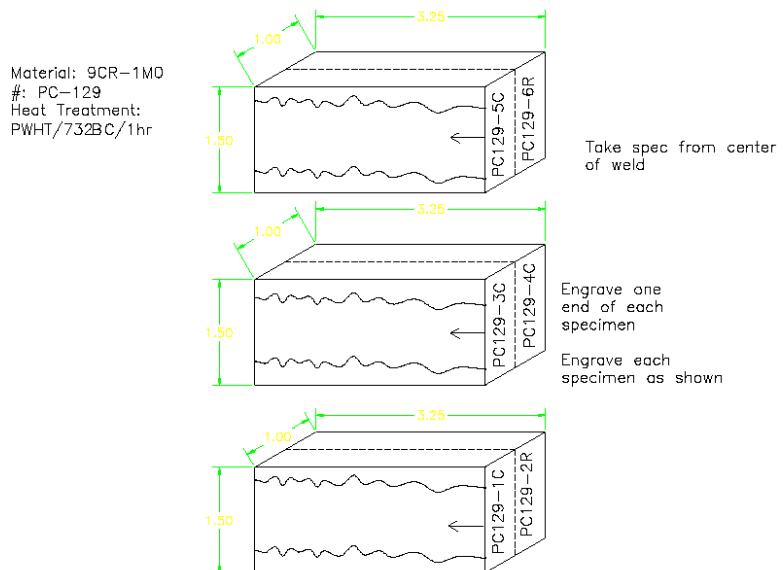
Material- 9CR-1MO
 Heat- VSI
 Heat Treatment-
 PWHT/732BC/1hr



Material- Modified 9C-1MO steel
 Instruction- Make sure that the specimen is cut out as shown in the sketch. If deviated the specimen will be useless.
 VSI 1 through VSI 7

VKS-2

DRAWING #11



DRAWING #12

APPENDIX 3

CHEMISTRIES FOR FILLER METALS OR DEPOSITED WELD METAL

| Weld ID | Product (in.) | Wire | C | Mn | P | S | Si | Ni | Cr | Mo | V | Cb | Ti | Cu | Al | N2 |
|---------|------------------|---------------------------|-------|------|-------|-------|------|------|-------|------|-------|--------|-------|------|-------|-------|
| PC-2 | 1 1/16 Plate | std 9CrMo | | | | | | | | | | | | | | |
| PC-4 | 5/8 Plate | F5349-deposit | 0.072 | 0.41 | 0.01 | 0.015 | 0.36 | 0.11 | 8.69 | 0.95 | 0.21 | 0.057 | 0.007 | 0.09 | 0.001 | 0.012 |
| PC-5 | 1/2 Tube | F5349-wire chem | 0.10 | 0.43 | 0.01 | 0.013 | 0.36 | 0.12 | 8.83 | 0.94 | 0.208 | 0.0588 | 0.01 | 0.09 | 0.001 | 0.011 |
| PC-9 | 5/8 Plate | F5349-wire chem | 0.10 | 0.43 | 0.01 | 0.013 | 0.36 | 0.12 | 8.83 | 0.94 | 0.208 | 0.0588 | 0.01 | 0.09 | 0.001 | 0.011 |
| PC-10 | 5/8 Plate | std 9CrMo-deposit | 0.074 | 0.49 | 0.01 | 0.013 | 0.41 | 0.12 | 9.0 | 0.96 | 0.054 | 0.019 | 0.006 | 0.04 | <.001 | 0.02 |
| PC-13 | 5/8 Plate | std 9CrMo-Y3730F505 | | | | | | | | | | | | | | |
| PC-16 | 5/8 Plate | std 9CrMo-XA3664 | | | | | | | | | | | | | | |
| PC-32 | 5/8 Plate | 30162 wire | | | | | | | | | | | | | | |
| PC-35 | 5/8 Plate | 30162 wire | | | | | | | | | | | | | | |
| PC-36 | 1 Plate | 30394 wire | | | | | | | | | | | | | | |
| PC-39 | 1 Plate | 30394 wire | | | | | | | | | | | | | | |
| PC-42 | 1 Plate | 30394 wire | | | | | | | | | | | | | | |
| PC-45 | 1 Plate | 30394 wire | | | | | | | | | | | | | | |
| PC-52 | 1 1/2 Plate | 30383-wire C2618 | | | | | | | | | | | | | | |
| PC-56A | 3 OD Tube | std 9CrMo-A1977F505 | | | | | | | | | | | | | | |
| PC-58B | 3 OD Tube | std 9CrMo-A1977F505 | | | | | | | | | | | | | | |
| PC-59 | Tube | std 9CrMo-CAOIG-wire chem | 0.052 | 0.62 | 0.005 | 0.007 | 0.14 | <.01 | 9.27 | 0.87 | 0.03 | | | | | 0.05 |
| PC-63 | Tube | std 9CrMo-CAOIG-wire chem | 0.052 | 0.62 | 0.005 | 0.007 | 0.14 | <.01 | 9.27 | 0.87 | 0.03 | | | | | 0.05 |
| PC-64 | | std9 CrMo-3N30AMX19 | 0.099 | 0.75 | 0.011 | 0.011 | 0.26 | 0.06 | 8.05 | 0.97 | | | | | | |
| PC-65 | Tube | std 9CrMo-CAOIG-wire chem | 0.052 | 0.62 | 0.005 | 0.007 | 0.14 | <.01 | 9.27 | 0.87 | 0.03 | | | | | 0.05 |
| PC-67B | 1 Plate | std 9CrMo-AN20AMZ24 | 0.078 | 0.69 | 0.006 | 0.015 | 0.29 | 0.07 | 8.1 | 0.97 | | | | | | |
| PC-71 | 1 Plate | std 9CrMo-E4390-E505 | 0.08 | 0.69 | 0.015 | 0.006 | 0.29 | 0.07 | 8.1 | 0.97 | | | | | | |
| PC-72 | 2 Plate | std 9CrMo-E4390-E505 | | | | | | | | | | | | | | |
| PC-73 | 2 Plate | std 9CrMo-E4390-E505 | | | | | | | | | | | | | | |
| PC-74 | 1 Plate | mix 19153R 5804 | | | | | | | | | | | | | | |
| PC-75 | 1 Plate | mix 19156R 5804 | | | | | | | | | | | | | | |
| PC-77 | 2 Plate | std 9CrMo-33669-E505 | | | | | | | | | | | | | | |
| PC-80 | 2 Plate | 30383 wire | 0.089 | 0.53 | 0.012 | 0.003 | 0.48 | 0.09 | 8.25 | 1.04 | 0.20 | 0.071 | 0.004 | 0.04 | 0.007 | 0.048 |
| PC-86 | 1 Plate | std 9CrMo | 0.036 | 0.45 | 0.016 | 0.009 | 0.34 | 0.22 | 8.75 | 0.98 | 0.036 | 0.006 | 0.004 | 0.3 | 0.007 | 0.012 |
| PC-90 | Tube | std 9CrMo CEM 10292 | | | | | | | | | | | | | | |
| PC-93 | 8 Plate | std 9CrMo-33669-E505 | 0.076 | 0.55 | 0.008 | 0.007 | 0.35 | 0.08 | 8.38 | 0.96 | 0.01 | 0.007 | 0.005 | 0.05 | 0.012 | 0.019 |
| PC-94 | Tube | std 9CrMo CEM 10292 | | | | | | | | | | | | | | |
| PC-95 | Tube | std 9CrMo CEM 10292 | | | | | | | | | | | | | | |
| PC-99 | Plate | std 9CrMo -E505 | 0.011 | 0.4 | 0.016 | 0.012 | 0.28 | 0.2 | 8.78 | 1.02 | 0.051 | 0.006 | 0.001 | 0.18 | 0.003 | 0.036 |
| PC-99 | Plate | std 9CrMo E4390 E505 | | | | | | | | | | | | | | |
| PC-100 | Plate | std 9CrMo | 0.038 | 0.5 | 0.016 | 0.009 | 0.38 | 0.14 | 8.99 | 1.08 | 0.048 | 0.007 | 0.002 | 0.18 | 0.003 | 0.052 |
| PC-102 | Tube | std 9CrMo CEM 10292 | | | | | | | | | | | | | | |
| V51 | Pipe | M9412 | | | | | | | | | | | | | | |
| PC-104 | Plate | std 9CrMo A1977 E505 | | | | | | | | | | | | | | |
| ETEC | Pipe | ERNiCr-3 | | | | | | | | | | | | | | |
| PC-109 | Plate | std 9CrMo D3612F E505 | | | | | | | | | | | | | | |
| PC-110 | Plate | std 9CrMo-33669-E505 | | | | | | | | | | | | | | |
| PC-111 | Plate | std 9CrMo-33669-E505 | | | | | | | | | | | | | | |
| 302B | Tube | M9412 | | | | | | | | | | | | | | |
| 303B | Tube | std 9CrMo-CAOIG-wire chem | 0.052 | 0.62 | 0.005 | 0.007 | 0.14 | <.01 | 9.27 | 0.87 | 0.03 | | | | | 0.05 |
| SW-1 | Plate | std 9CrMo D3612F E505 | | | | | | | | | | | | | | |
| SW-2 | Plate | std 9CrMo | | | | | | | | | | | | | | |
| PC-129 | Plate | | | | | | | | | | | | | | | |
| PC-132 | Plate | | | | | | | | | | | | | | | |
| PC-150 | Plate | | | | | | | | | | | | | | | |
| PC-156 | Plate | std 9CrMo USW 21648 | | | | | | | | | | | | | | |
| LNK5 | 2 Plate | Thermanik MTS3 | 0.11 | 0.57 | 0.012 | 0.01 | 0.15 | 0.74 | 9.39 | 0.9 | 0.22 | 0.034 | 0.002 | 0.04 | 0.016 | 0.051 |
| 4R | 1 Plate | | 0.13 | 0.13 | 0.012 | 0.009 | 0.34 | 0.3 | 8.8 | 1.0 | 0.16 | 0.03 | | 0.01 | <.01 | 0.04 |
| 5R | 1 Plate | | 0.13 | 0.89 | 0.012 | 0.008 | 0.33 | 1.0 | 10.0 | 1.1 | 0.2 | 0.05 | | 0.01 | <.01 | 0.06 |
| 4R | 1 Plate | | 0.1 | 0.57 | 0.014 | 0.008 | 0.25 | 0.85 | 10.25 | 1.07 | 0.21 | 0.04 | | 0.01 | 0.01 | 0.04 |
| 10R | 1 Plate | | 0.1 | 0.56 | 0.014 | 0.008 | 0.26 | 0.82 | 9.84 | 1.05 | 0.22 | 0.05 | | 0.01 | 0.01 | 0.04 |

APPENDIX 4

A COMPILATION OF STRESS RUPTURE TESTING DATA ON Gr 91 WELDMENTS AND Gr 9 and Gr 91 WELD METALS

| TN | Weld | SN | Condition | Temp (deg C) | Stress (MPa) | RL (h) | EI (%) | RA (%) | Type | Failure | Comment |
|-------|---------|------|--------------|-----------------|-----------------|-----------|-----------|-----------|----------|----------|--------------|
| | | | | | | | | | Specimen | Location | |
| 20728 | PC-2 | 1-T | 788 pwht | 649 | 117.2 | 4.5 | 22.5 | 91.0 | cross | weld | neck |
| 20733 | PC-2 | 2-T | 788 pwht | 649 | 82.7 | 336 | 6.8 | 36.4 | cross | | |
| 20744 | PC-2 | 3-T | 788 pwht | 538 | 220.6 | 17.2 | 20.5 | 88.3 | cross | weld | neck |
| 20773 | PC-2 | 7-T | 788 pwht | 538 | 179.3 | 85.2 | 27.1 | 89.1 | cross | weld | neck |
| 20785 | PC-2 | 8-T | 788 pwht | 538 | 151.7 | 12238D | | | cross | | discontinued |
| 20991 | PC-4 | 2-T | 760 pwht | 649 | 117.2 | 35.3 | 18.0 | 73.1 | cross | | |
| 20993 | PC-4 | 3-T | 760 pwht | 649 | 82.7 | 307.2 | 13.4 | 49.3 | cross | | |
| 20997 | PC-4 | 4-T | 760 pwht | 538 | 234.4 | 290 | 18.0 | 75.4 | cross | | |
| 20998 | PC-5 | 2-T | 760 pwht | 649 | 117.2 | 25.9 | 13.9 | 80.7 | cross | HAZ | neck |
| 21003 | PC-5 | 3-T | 760 pwht | 649 | 82.7 | 194.1 | 13.2 | 72.5 | cross | HAZ | neck |
| 21215 | PC-9 | 2-L | 732 pwht | 649 | 117.2 | 30.2 | 19.8 | 68.3 | cross | HAZ | neck |
| 21225 | PC-9 | 4-L | 732 pwht | 649 | 82.7 | 308.3 | 14.4 | 37.9 | cross | HAZ | shear |
| 21236 | PC-9 | 5-L | 732 pwht | 538 | 234.4 | 201 | 17.2 | 73.5 | cross | HAZ | neck |
| 21257 | PC-10 | 2-L | 732 pwht | 649 | 117.2 | 45.2 | 12.4 | 54.1 | cross | HAZ | neck |
| 22981 | PC-10 | 4-L | 732 pwht | 593 | 158.6 | 537.9 | 12.8 | 54.5 | cross | | |
| 22995 | PC-10 | 5-L | 732 pwht | 593 | 172.4 | 238.2 | 12.5 | 60.3 | cross | | |
| 21418 | PC-13 | 1-L | | 649 | 117.2 | 89.9 | 33.4 | 82.8 | weld | weld | neck |
| 21490 | PC-13 | 2-L | | 649 | 82.7 | 1068.4 | 32.7 | 80.1 | weld | weld | neck |
| 21492 | PC-13 | 3-L | | 538 | 275.8 | 379.8 | 28.4 | 83.3 | weld | weld | neck |
| 21519 | PC-16 | 1-L | 732 pwht | 538 | 275.8 | 10505D | | | weld | | discontinued |
| 23233 | PC-16 | 2-L | 732 pwht | 649 | 117.2 | 2834D | | | weld | | discontinued |
| 21954 | PC-32 | 3-T | 732 pwht | 649 | 103.4 | 2037.8 | 19.6 | 78.3 | cross | | |
| 22060 | PC-32 | 4-T | 732 pwht | 593 | 193.1 | 35.2 | 22.1 | 72.9 | cross | weld | |
| 22072 | PC-32 | 5-T | 732 pwht | 593 | 158.6 | 163.7 | 18.7 | 77.1 | cross | | |
| 22086 | PC-32 | 6-T | 732 pwht | 538 | 234.4 | 385.4 | 18.0 | 83.4 | cross | | |
| 22093 | PC-32 | 7-T | 732 pwht | 538 | 275.8 | 50.4 | 18.2 | 84.0 | cross | | |
| 22099 | PC-32 | 8-T | 732 pwht | 538 | 234.4 | 682.9 | 19.8 | 84.5 | cross | | |
| 22434 | PC-36 | 3-T | as-welded | 593 | 193.1 | 770.9 | 3.2 | 16.6 | cross | | |
| 22478 | PC-36 | 13-T | 732 pwht | 593 | 193.1 | 292 | 5.1 | 41.3 | cross | | |
| 22529 | PC-39 | 3-T | 760 pwht | 649 | 117.2 | 72.4 | 3.7 | 27.6 | cross | | |
| 22530 | PC-39 | 4-T | 760 pwht | 593 | 193.1 | 297.4 | 4.9 | 20.2 | cross | | |
| 22534 | PC-39 | 6-T | 760 pwht | 649 | 103.4 | 103.1 | 3.4 | 25.2 | cross | | |
| 22549 | PC-36 | 14-T | 732 pwht | 593 | 89.6 | 1850.1 | 2.7 | 6.2 | cross | | |
| 22550 | PC-39 | 7-T | 760 pwht | 593 | 158.6 | 1447.7 | 2.6 | 11.3 | cross | | |
| 22559 | PC-35 | 7-T | NT | 593 | 179.3 | 460.8 | 8.6 | 9.8 | cross | | |
| 22596 | PC-42 | 3-T | 1038/704/24h | 593 | 193.1 | 17.7 | 18.7 | 84.3 | cross | | |
| 22609 | PC-42 | 4-T | 1038/704/24h | 593 | 158.6 | 319.8 | 18.9 | 86.3 | cross | | |
| 22627 | PC-42 | 6-T | 1038/704/24h | 593 | 144.8 | 1136 | 16.0 | 85.4 | cross | | |
| 22836 | PC-45 | 1-T | 760 pwht | 593 | 158.6 | 2317.5 | 4.1 | 9.7 | cross | | |
| 22860 | PC-45 | 2-T | 760 pwht | 593 | 124.1 | 4765.1 | 3.2 | 27.6 | cross | | |
| 22916 | PC-52 | 5-R | 732 pwht | 593 | 158.6 | 813.2 | 5.3 | 23.6 | cross | FL | shear |
| 22934 | PC-52 | 5-C | 732 pwht | 593 | 158.6 | 1537.7 | 2.4 | 16.8 | cross | FL | shear |
| 22935 | PC-52 | 7-R | 732 pwht | 593 | 144.8 | 2318.9 | 4.9 | 22.3 | cross | FL | shear |
| 22937 | 394L | 2-L | as-welded | 593 | 144.8 | | | | cross | HAZ | neck |
| 22938 | 394L | 1-L | as-welded | 593 | 158.6 | | | | cross | HAZ | neck |
| 22945 | 394L | 4-L | as-welded | 538 | 220.6 | | | | cross | HAZ | neck |
| 22946 | 394L | 3-L | as-welded | 538 | 179.3 | | | | cross | HAZ | neck |
| 22948 | 394L | 5-L | as-welded | 538 | 206.9 | | | | cross | HAZ/FL | neck |
| 22449 | 394L | 6-L | as-welded | 565 | 172.4 | | | | cross | HAZ | neck |
| 22950 | 394L | 7-L | as-welded | 565 | 124.1 | | | | cross | FL | shear |
| 23736 | 394L | 11-L | 732 pwht | 677 | 41.4 | 1331.8 | 12.1 | 59.1 | cross | HAZ | neck |
| 23022 | PC-58-B | 3-L | 732 pwht | 593 | 172.4 | 554.8 | 15.2 | 78.2 | cross | HAZ | neck |
| 23023 | PC-58-B | 4-L | 732 pwht | 593 | 158.6 | 1203.1 | 9.7 | 53.2 | cross | FL | shear |
| 23025 | PC-58-B | 5-L | 732 pwht | 538 | 206.9 | 26800.2 | 6.3 | 18.4 | cross | FL | shear |
| 23026 | PC-58-B | 6-L | 732 pwht | 538 | 186.2 | 49057.6 | 3.1 | 7.8 | cross | FL | shear |
| 23034 | PC-58-B | 7-L | 732 pwht | 593 | 144.8 | 2646.7 | 7.3 | 40.5 | cross | FL | shear |
| 23115 | PC-59 | 3-L | as-welded | 593 | 158.6 | 1268 | 5.2 | 19.9 | cross | FL | shear |
| 23116 | PC-59 | 4-L | as-welded | 649 | 103.4 | 132.8 | 5.8 | 16.4 | cross | FL | shear |
| 23124 | PC-59 | 5-L | as-welded | 649 | 89.6 | 357.4 | 5.8 | 11.4 | cross | FL | shear |
| 23161 | PC-59 | 6-L | as-welded | 593 | 172.4 | 857.7 | 16.1 | 43.3 | cross | FL | shear |
| 23236 | PC-63 | 1-L | 732 pwht | 593 | 172.4 | 582.1 | 8.0 | 15.5 | cross | FL | shear |
| 23457 | PC-63 | 5-L | 732 pwht | 649 | 89.6 | 334.1 | 4.5 | 16.7 | cross | FL | shear |

| TN | Weld | SN | Condition | Temp (deg C) | Stress (MPa) | RL (h) | EI (%) | RA (%) | Type | Failure | Comment |
|-------|----------|------|--------------|-----------------|-----------------|-----------|-----------|-----------|----------|----------|------------|
| | | | (deg C) | | | | | | Specimen | Location | |
| 23295 | PC-63 | 4-L | 732 pwht | 593 | 144.8 | 3363.6 | 3.6 | 8.8 | cross | | |
| 23271 | PC-71-TW | 7-C | 732 pwht | 593 | 172.4 | 132 | 9.4 | 59.4 | cross | HAZ/FL | neck |
| 23276 | PC-71-W | 2-C | 732 pwht | 593 | 172.4 | 1627.3 | 13.3 | 32.3 | weld | weld | shear |
| 23283 | PC-71-TW | 16-R | 732 pwht | 593 | 172.4 | 185.9 | 7.8 | 57.8 | cross | HAZ/FL | neck |
| 23285 | PC-71-TW | 15-R | 732 pwht | 538 | 206.9 | 17202.9 | 7.0 | 29.5 | cross | FL | shear |
| 23430 | PC-71-W | 3-C | 732 pwht | 593 | 144.8 | 1784.5 | 20.0 | 36.3 | weld | weld | dbl shear |
| 23368 | PC-74 | 3-T | 732 pwht | 593 | 172.4 | 63.3 | 18.6 | 77.2 | cross | weld | neck |
| 23385 | PC-74 | 4-T | 732 pwht | 593 | 144.8 | 197.8 | 16.9 | 74.8 | cross | weld | neck |
| 23386 | PC-75 | 4-T | 732 pwht | 593 | 144.8 | 2642.9 | 2.0 | 6.9 | cross | weld | neck |
| 23384 | PC-75 | 3-T | 732 pwht | 593 | 172.4 | 1459.5 | 2.9 | 3.3 | cross | | |
| 23709 | PC-80 | 16-C | 760/2h pwht | 677 | 55.2 | 4923.9 | 5.0 | 25.0 | cross | HAZ | shear |
| 23963 | PC-81 | 10-C | 732/40h | 593 | 172.4 | 297.5 | 24.0 | 85.5 | cross | HAZ | neck |
| 24001 | PC-81 | 1-C | 732/2h | 593 | 172.4 | 1507 | 15.5 | 79.8 | cross | HAZ | neck |
| 24013 | PC-81 | 12-C | 732/40h | 649 | 62.1 | 5084.5 | 2.7 | 13.4 | cross | weld | brittle |
| 23485 | PC-90 | 3-L | 732 pwht | 649 | 117.2 | 77.9 | 4.6 | 7.2 | cross | FL | shear |
| 23486 | PC-90 | 4-L | 732 pwht | 649 | 89.6 | 450 | 5.1 | 15.6 | cross | FL | shear |
| 23489 | PC-90 | 5-L | 732 pwht | 593 | 172.4 | 585.6 | 9.7 | 8.6 | cross | FL | shear |
| 23493 | PC-90 | 6-L | 732 pwht | 593 | 144.8 | 2547.8 | 10.2 | 48.2 | cross | weld | neck |
| 23497 | PC-90 | 7-L | 732 pwht | 649 | 75.8 | 839.5 | 3.1 | 1.2 | cross | FL | shear |
| 23498 | PC-90 | 8-L | 732 pwht | 649 | 131.0 | 26 | 11.3 | 16.2 | cross | FL | shear |
| 23501 | PC-90 | 9-L | 732 pwht | 538 | 234.4 | 2783.1 | 17.1 | 71.7 | cross | weld | neck |
| 23502 | PC-90 | 10-L | 732 pwht | 593 | 193.1 | 86.2 | 17.2 | 61.6 | cross | HAZ/FL | neck |
| 23504 | PC-90 | 11-L | 732 pwht | 593 | 206.9 | 15278.8 | 18.3 | 79.7 | cross | HAZ | neck |
| 23549 | PC-93 | 8-R | 732/6h pwht | 593 | 144.8 | 1070.4 | 11.4 | 79.3 | cross | HAZ | neck |
| 23703 | PC-93 | 2-C | 732/6h pwht | 593 | 144.8 | 238.2 | 14.0 | 84.5 | cross | weld | neck |
| 23771 | PC-93 | 29-Z | 732/6h pwht | 593 | 124.1 | 3186.2 | 18.5 | 76.9 | cross | HAZ | neck |
| 23791 | PC-93 | 31-Z | 732/6h pwht | 593 | 144.8 | 9835.6 | 4.4 | 29.0 | cross | weld | neck |
| 23786 | PC-93 | 30-Z | 732/6h pwht | 593 | 110.3 | 1949.7 | 21.1 | 88.6 | cross | HAZ | neck |
| 23543 | PC-94 | 3-L | 732 pwht | 649 | 75.8 | 881.8 | 4.4 | 17.6 | cross | FL | shear |
| 23630 | PC-94 | 4-L | 732 pwht | 677 | 41.4 | 2577.8 | 13.5 | 74.0 | cross | weld | neck |
| 23634 | PC-94 | 5-L | 732 pwht | 677 | 66.2 | 666.8 | 10.7 | 34.0 | cross | FL | shear |
| 23551 | PC-95 | 4-L | 732 pwht | 649 | 69.0 | 2521.3 | 7.3 | 13.7 | cross | FL | shear |
| 23540 | PC-95 | 3-L | 732 pwht | 593 | 144.8 | 2223 | 11.5 | 52.0 | cross | weld? | neck |
| 23632 | PC-102 | 3-L | 732 pwht | 649 | 75.8 | 510.4 | 4.2 | 48.9 | cross | FL | shear |
| 23644 | PC-102 | 4-L | 732 pwht | 593 | 144.8 | 2468.1 | 3.7 | 48.9 | cross | FL | shear/neck |
| 23812 | PC-104B | 1-C | 677 pwht | 649 | 75.8 | 996.1 | 4.1 | 36.2 | cross | FL/HAZ | shear/neck |
| 25655 | PC-109 | 6-R | 760/1h | 593 | 110.0 | 2691.6 | 3.8 | 16.1 | cross | weld | 0.505 spec |
| 25754 | PC-109 | 3-C | 760/1h | 538 | 230.0 | 87.4 | 6.3 | 7.1 | cross | weld | 0.505 spec |
| 25797 | PC-109 | 7-R | 760/1h | 593 | 110.0 | 2301.1 | 3.8 | 5.8 | cross | weld | 0.505 spec |
| 23979 | PC-110 | 20-R | 760/1h | 593 | 172.4 | 168.1 | 8.0 | 77.2 | cross | HAZ | neck |
| 23992 | PC-110 | 21-R | 760/1h | 593 | 144.8 | 1079.3 | 5.7 | 63.2 | cross | HAZ | neck |
| 23997 | PC-110 | 19-C | 760/1h | 593 | 172.4 | 103.2 | 8.6 | 71.5 | cross | HAZ | neck |
| 23999 | PC-110 | 22-R | 760/1h | 593 | 124.1 | 2277.6 | 4.1 | 39.5 | cross | HAZ/FL | neck/shear |
| 24005 | PC-110 | 24-T | 760/1h | 593 | 172.4 | 1502.9 | 15.0 | 83.7 | base | base | neck |
| 24006 | PC-110 | 25-T | 760/1h | 593 | 144.8 | 8086.8 | 13.7 | 79.4 | base | base | neck |
| 24363 | PC-110 | 26-T | 760/1h | 538 | 179.3 | 61348D | | | base | base | |
| 25403 | PC-110 | 3-C | 760/1h | 538 | 186.2 | 18748D | | | cross | | |
| 25409 | PC-110 | 11-R | 760/1h | 538 | 175.8 | 16585D | | | cross | | 1038/621 |
| 25411 | PC-110 | 4-C | 760/1h | 593 | 134.5 | 759.6 | 6.7 | 88.3 | cross | FL | shear |
| 25484 | PC-110 | 12-R | 760/1h | 593 | 110.3 | 4158.7 | 6.3 | 42.6 | cross | HAZ/FL | neck/shear |
| 25485 | PC-110 | 5-C | 760/1h | 593 | 103.4 | 9296.3 | 93.0 | 54.0 | cross | HAZ | neck |
| 23684 | PC-111 | 3-R | 760/1.5 pwht | 593 | 144.8 | 2304.2 | 3.8 | 43.7 | cross | | |
| 23762 | PC-111 | 1-R | 732 pwht | 593 | 172.4 | 838.2 | 6.8 | 69.4 | cross | | |
| 25401 | PC-111 | 3-C | 760/1h | 538 | 193.1 | 16941D | | | cross | | 1038/621 |
| 25405 | PC-111 | 11-R | 760/1h | 593 | 151.7 | 2146.6 | 7.6 | 50.0 | cross | HAZ | neck |
| 25410 | PC-111 | 12-R | 760/1h | 538 | 179.3 | 16439D | | | cross | | 10338/621 |
| 25493 | PC-111 | 4-C | 760/1h | 593 | 137.9 | 6415.8 | 3.5 | 7.0 | cross | FL | shear |
| 25535 | PC-111 | 5-C | 760/1h | 538 | 165.5 | 13701D | | | cross | | 1038/621 |
| 25604 | PC-111 | 6-C | 760/1h | 593 | 117.2 | 10728D | | | cross | | 1038/621 |
| 25613 | PC-111 | 13-C | 760/1h | 593 | 124.1 | 2955.3 | 5.7 | 50.7 | cross | HAZ | neck |
| 24163 | PC-129 | 1-C | 732/1h | 649 | 131.0 | 3615.3 | 8.7 | 14.5 | cross | FL | shear |
| 24219 | PC-129 | 3-C | as-welded? | 593 | 144.8 | | | | cross | weld | brittle |

| TN | Weld | SN | Condition | Temp (deg C) | Stress (MPa) | RL (h) | EI (%) | RA (%) | Type Specimen | Failure Location | Comment |
|-------|---------|-------|-------------|--------------|--------------|---------|--------|--------|---------------|------------------|---------------|
| 24279 | PC-129 | 2-R | 732/1h | 538 | 206.9 | 63150D | | | cross | | |
| 24273 | PC-132 | 3-C | 760/1h | 593 | 172.4 | 116.3 | 7.8 | 76.0 | cross | HAZ | neck |
| 24278 | PC-132 | 4-C | 760/1h | 593 | 144.8 | 579.9 | 5.8 | 54.0 | cross | FL | shear |
| 24285 | PC-132 | 5-C | 760/1h | 593 | 124.1 | 3568.1 | 4.3 | 25.9 | cross | FL | shear |
| 24293 | PC-132 | 8-R | 760/1h | 538 | 206.9 | 9268.3 | 11.6 | 80.0 | cross | HAZ | neck |
| 24376 | PC-132 | 9-R | 760/1h | 538 | 179.3 | 47271 | 4.3 | 22.9 | cross | FL | shear |
| 24545 | PC-150 | 1-C | 732/1h | 593 | 144.8 | 1503.5 | 1.9 | 16.9 | cross | FL | shear |
| 24551 | PC-150 | 2-C | 732/1h | 593 | 124.1 | 5037.4 | 1.2 | 12.0 | cross | FL | shear |
| 24621 | PC-150 | 3-C | 732/1h | 593 | 110.3 | 8635.7 | 1.2 | 9.6 | cross | FL | shear |
| 24625 | PC-150 | 4-C | 732/1h | 538 | 193.1 | | | | cross | FL | shear |
| 24631 | PC-150 | 5-C | 732/1h | 649 | 75.8 | 711.5 | 1.6 | 14.7 | cross | FL | shear |
| 24666 | PC-156 | 1-C | 746/1h | 593 | 144.8 | 499.4 | 4.3 | 42.5 | cross | FL | shear |
| 24962 | PC-156 | 4-C | 746/1h | 593 | 82.7 | 19972.7 | 2.4 | 7.5 | cross | FL | shear |
| 24722 | PC-156 | 3-C | 746/1h | 593 | 103.4 | 4707.4 | 2.7 | 24.0 | cross | FL | shear |
| 24971 | PC-156 | 5-C | 746/1h | 538 | 206.9 | 9739.4 | 5.7 | 54.0 | cross | FL | shear |
| 24959 | PC-156? | 6-C? | 746/1h | 593 | 82.7 | | | | cross | FL | shear |
| 24978 | PC-156 | 6-C | 746/1h | 538 | 193.1 | | | | cross | FL | shear |
| 24687 | PC-158 | 2-C | 746/1h | 593 | 124.1 | 1075 | 2.8 | 29.5 | cross | FL | shear |
| 24689 | PC-163 | CAST? | 1040/760/1 | 593 | 172.4 | 2540 | 13.3 | 83.5 | | | neck |
| 24721 | PC-163 | CAST? | 1040/760 | 593 | 144.8 | 10419 | | | | | |
| 25348 | PC-163 | CAST? | 1040/760 | 538 | 206.9 | 164.2 | 14.0 | 85.6 | | | |
| 23687 | VSI | 3 | 732 pwht | 677 | 55.2 | 463.9 | 8.4 | 71.8 | cross | HAZ | neck |
| 23718 | ETEC | 4 | 732 pwht | 510 | 275.8 | 8046.2 | 2.6 | 12.8 | cross | weld | DMW |
| 23733 | ETEC | 5 | 1050 | 593 | 96.5 | 14041.7 | 2.0 | 26.8 | cross | HAZ/FL | DMW |
| 23756 | ETEC | 1 | 732 pwht | 593 | 172.4 | 1367.8 | 5.5 | 64.1 | cross | HAZ | DMW neck |
| 23759 | ETEC | 7 | 732 pwht | 649 | 75.8 | 1091.7 | 3.2 | 53.6 | cross | HAZ | DMW neck |
| 23769 | ETEC | 15 | 732 pwht | 593 | 124.1 | 5013.8 | 1.4 | 7.5 | cross | FL | DMW interface |
| 24038 | ETEC | 16 | 732 pwht | 649 | 48.3 | 13646.8 | | 3303.0 | cross | FL | DMW shear |
| 29891 | LNKS | W2(P) | 774/8h pwht | 600 | 186.2 | 38.5 | 30.6 | 44.4 | all weld | all weld | neck |
| 29901 | LNKS | WA-1 | 774/8h pwht | 600 | 150.0 | 660 | 26.2 | 70.4 | all weld | all weld | neck |
| 29986 | LNKS | WA-2 | 774/8h pwht | 600 | 150.0 | 653 | | | all weld | all weld | neck |
| 29911 | LNKS | WB-1 | 774/8h pwht | 600 | 120.0 | 6351 | 14.7 | 31.0 | all weld | all weld | neck |
| 29189 | LNKS | W5 | 774/8h pwht | 593 | 137.9 | 1584 | 29.3 | 72.6 | | | |
| 29944 | LNKS | W3(P) | 774/8h pwht | 650 | 100.0 | 468 | 14.5 | 30.5 | all weld | all weld | neck |
| 29951 | LNKS | W1(P) | 774/8h pwht | 550 | 200.0 | 7529 | 29.1 | 73.5 | all weld | all weld | neck |
| 29904 | LNKS | WA-3 | 774/8h pwht | 600 | 120.0 | 56.5 | | | cross | HAZ | |
| 29879 | LNKS | W1-1 | 1040/740 NT | 600 | 186.2 | 965 | 10.1 | 12.3 | all weld | all weld | |
| 29892 | LNKS | TW1-3 | 1040/740 NT | 600 | 186.2 | 706 | | 50.9 | cross | HAZ | |
| 29871 | LNKS | W1-2 | 1040/740 NT | 600 | 186.2 | 760 | | 19.2 | cross | HAZ | |
| 29900 | LNKS | WE-1 | 1040/780 NT | 600 | 150.0 | 1402 | | | all weld | all weld | |
| 29918 | LNKS | WF-1 | 1040/780 NT | 600 | 120.0 | 9251 | 7.8 | 8.2 | all weld | all weld | |
| 29928 | LNKS | WF-3 | 1040/780 NT | 600 | 150.0 | 872 | | 76.6 | cross | HAZ | |
| 29918 | LNKS | WE-3 | 1040/780 NT | 600 | 120.0 | 6066 | | 45.4 | cross | HAZ | |
| 29978 | 9R | 9AWT | 760/4h pwht | 593 | 172.4 | 4987 | 11.1 | 18.5 | all weld | all weld | |
| 29981 | 9R | 9AWC | 760/4h pwht | 649 | 103.4 | 1741 | 12.2 | 21.8 | all weld | all weld | |
| 29980 | 9R | 9T1 | 760/4h pwht | 593 | 172.4 | 468.4 | | 53.0 | cross | HAZ | |
| 29975 | 10R | 10AWC | 760/4h pwht | 593 | 172.4 | 5458 | | | all weld | all weld | |
| 29982 | 10R | 10AWT | 760/4h pwht | 593 | 155.1 | 7780 | | | all weld | all weld | |
| 29979 | 10R | 10T1 | 760/4h pwht | 593 | 172.4 | 262.5 | | 85.8 | cross | HAZ | |
| 29984 | 10R | 10T2 | 760/4h pwht | 649 | 124.1 | 61.3 | | 41.0 | cross | HAZ | |
| 29991 | W4 | W4C-1 | 760/4h pwht | 600 | 150.0 | 5632 | 4.8 | 9.0 | all weld | all weld | drop preheat |
| 30017 | W4 | W4C-4 | 760/4h pwht | 600 | 186.2 | 1193 | 8.3 | 9.6 | all weld | all weld | drop preheat |
| 30052 | W4 | W4C-3 | 760/4h pwht | 600 | 100.0 | 1567 | 5.2 | 6.7 | all weld | all weld | drop preheat |
| 29992 | W4 | W4H-1 | 760/4h pwht | 600 | 150.0 | 3373 | 3.5 | 6.8 | all weld | all weld | hold preheat |
| 30019 | W4 | W4H-3 | 760/4h pwht | 600 | 186.2 | 698.4 | 8.4 | 20.4 | all weld | all weld | hold preheat |
| 30055 | W4 | W4H-2 | 760/4h pwht | 650 | 100.0 | 871.2 | 5.1 | 7.1 | all weld | all weld | hold preheat |
| 29996 | W4 | W4T-3 | 760/4h pwht | 600 | 150.0 | 203 | | 66.8 | cross | HAZ | hold preheat |
| 30027 | W4 | W4T-4 | 760/4h pwht | 600 | 120.0 | 1266 | | 29.3 | cross | HAZ | hold preheat |
| 30064 | W4 | W4T-2 | 760/4h pwht | 650 | 100.0 | 93 | | 45.6 | cross | HAZ | hold preheat |

| TN | Weld | SN | Condition | Temp (deg C) | Stress (MPa) | RL (h) | EI (%) | RA (%) | Type Specimen | Failure Location | Comment |
|-------|------|---------|-------------|-----------------|-----------------|-----------|-----------|-----------|------------------|---------------------|--------------|
| 30132 | W4 | NTW4-2 | NT/760/4h | 600 | 150.0 | 528.1 | 15.3 | 50.5 | all weld | all weld | re-NT |
| 30135 | W4 | NTW4-5 | NT/760/4h | 650 | 100.0 | 1531 | | | all weld | all weld | re-NT |
| 30134 | W4 | NTW4-11 | NT/760/4h | 600 | 186.2 | 30.3 | 30.3 | 81.6 | all weld | all weld | re-NT |
| 29989 | W5 | W5C-1 | 760/4h pwht | 600 | 150.0 | 1977 | 13.5 | 28.6 | all weld | all weld | drop preheat |
| 30016 | W5 | W5C-6 | 760/4h pwht | 600 | 186.2 | 417 | 18.9 | 62.8 | all weld | all weld | drop preheat |
| 30053 | W5 | W5C-3 | 760/4h pwht | 650 | 100.0 | 1267 | 5.7 | 27.5 | all weld | all weld | drop preheat |
| 29990 | W5 | W5H-4 | 760/4h pwht | 600 | 150.0 | 9152 | 5.3 | 13.1 | all weld | all weld | hold preheat |
| 30018 | W5 | W5H-3 | 760/4h pwht | 600 | 186.2 | 440.8 | 10.0 | 23.1 | all weld | all weld | hold preheat |
| 30032 | W5 | W5H-1 | 760/4h pwht | 650 | 100.0 | 3106 | 7.7 | 17.7 | all weld | all weld | hold preheat |
| 30028 | W5 | W5T-2 | 760/4h pwht | 600 | 186.2 | 62 | | 82.6 | cross | | hold preheat |
| 30000 | W5 | W5T-3 | 760/4h pwht | 600 | 150.0 | 937 | | 22.3 | cross | | hold preheat |
| 30065 | W5 | W5T-4 | 760/4h pwht | 650 | 100.0 | 128.6 | | 30.5 | cross | | hold preheat |
| 30133 | W5 | NTW5-2 | NT/760/4h | 600 | 186.2 | 821.8 | 19.9 | 55.6 | all weld | all weld | re-NT |

CREEP-RUPTURE DATA SOURCES, DATA ANALYSIS PROCEDURES, AND THE
ESTIMATION OF STRENGTH FOR ALLOY 800H AT 750°C AND ABOVE

PART 1: STRESS-RUPTURE

R. W. Swindeman
Cromtech Inc
Oak Ridge, TN 37830-7856

M. J. Swindeman
University of Dayton Research Institute
Dayton, OH 45469-0110

B. W. Roberts
BW Roberts Consultants
Chattanooga, TN 37416

B. E. Thurgood
Bpva Engineering
San Diego, CA 92131

D. L. Marriott
Stress Engineering Services
Mason, OH 45040

March, 2007

ABSTRACT

Databases summarizing the creep-rupture properties of alloy 800H and its variants were reviewed and referenced. For the most part, the database was judged to be adequate to meet the needs for time-dependent properties in the extension of alloy 800H in ASME Section III Subsection NH (III-NH) to 900°C (1650°F) and 600,000 hours. Procedures for analyzing creep and stress-rupture data for III-NH were reviewed and compared to the current procedure endorsed by the ASME Section II on Materials. The stress-rupture database for alloy 800H in the temperature range of 750 to 1000°C (1382 to 1832°F) was assembled and used to estimate the average and minimum strength for times to 600,000 hours.

INTRODUCTION

A three-year collaborative effort has been established between the Department of Energy (DOE) and the American Society of Mechanical Engineers (ASME) to address technical issues related to codes and standards applicable to the Generation IV Nuclear Energy Systems Program [1]. A number of tasks have been identified that will be managed through the ASME Standards Technology, LLC (ASME ST-LLC) and involve significant industry, university, and independent consultant activities. One of the tasks the *Verification of Allowable Stresses in ASME Section III, Subsection NH With Emphasis an Alloy 800H and Grade 91 Steel*. A subtask is the assessment of the data needed to extend the ASME Section III coverage of alloy 800H to 900°C (1650°F). To this end a review is provided here that identifies data sources and analytical procedures that have been used in code-related work on alloy 800 over the last thirty years. This review is followed by an evaluation of the long-time stress-rupture characteristics in the temperature range of 750 to 900°C (1382 to 1650°F).

IDENTIFICATION OF MATERIALS

Alloy 800H is one of three classes (or “grades”) of 33Ni-42Fe-21Cr alloy that are listed in ASME Section II and approved for construction of pressure boundary components. These are identified as UNS N08800, UNS N08810, and UNS N08811 for alloy 800, alloy 800H, and alloy 800HT, respectively. There are other variants identified in international construction codes and databases. Often, the specifications for these variants fall within the ASME SB specifications so valuable information may be obtained from these sources. The history of the development of the three SB grades of alloy 800 has been provided by INCO alloys [2, 3]. Variants of alloy 800 were examined for both irradiation resistance [4] and steam generator requirements [5] and by 1975 several restricted chemistry versions of alloy 800 were available. Further evaluations were performed in Europe on the Sanicro 30 and Sanicro 31 alloys with emphasis on the influence of carbon, titanium, and aluminum [6]. By 1989 three variants of alloy 800 were available in the German codes [7], and the German code KTA 3221.1 that was issued in 1993 provided design data for three materials: alloy 800 DE, alloy 800 Rk, and alloy 800H [8].

ASME III-NH identifies the permitted SB specifications and associated product forms for alloy 800H (UNS N08810) in Table I-14.1. The ladle composition for the alloy 800H material may be compared to the other grades mentioned above in Table 1. Alloy 800 differs from alloy 800H in permitting carbon levels below 0.05%, annealing temperatures below 1121°C (2050°F), and finer grain size with ASTM grain size numbers above 5. Alloy 800HT requires carbon to be at least 0.06%, the aluminum plus titanium to be in the range of 0.85 to 1.2%, and the annealing temperature to be at least 1149°C (2150°F). The Japanese specification for alloy 800H is virtually identical to the ASME SB specification for alloy 800H. The three specifications identified in the German code KTA 3221.1 are included in Table 1. The German specifications require narrower ranges for nickel and chromium content. For grades 800 DE and 800 Rk, lower carbon is

permitted and the maximum carbon is reduced relative to the ASME SB specifications. The ranges for aluminum and titanium are reduced and the maximum for both elements is reduced. The KTA 3221.1 specifications allow higher aluminum and titanium for the alloy 800 H grade. Both the minimum and maximum values are higher than for the ASME SB specification. All specifications, except for alloy 800 and alloy 800 DE, require grain sizes of ASTM No. 5 or coarser. The German specifications place additional requirements on phosphorus, nitrogen, cobalt, and niobium. Additional product form chemistry requirements apply but they will not be presented here. The similarity in the chemical requirements for ASME and Japanese versions of alloy 800H suggest that data produced on materials from these sources should be interchangeable and useful in extending ASME III-NH to higher temperatures. Care is needed with respect to using data produced from material in conformance with the German specifications to assure that the material falls with the ASME SB specification for alloy 800H.

Table 1. Comparison of chemistries for variants of alloy 800

| Element | ASME N08800 800 | ASME N08810 800H | ASME N08811 800HT | DIN 800 DE | DIN 800 Rk | DIN 800 H | JIS-G-4904 |
|-----------------|-----------------------|------------------------|-------------------------|---------------|---------------|--------------|------------|
| Ni | 30.0-35.0 | 30.0-35.0 | 30.0-35.0 | 30.0-32.5 | 30.0-32.5 | 30.0-34.0 | 30.0-35.0 |
| Cr | 19.0-23.0 | 19.0-23.0 | 19.0-23.0 | 19.0-22.0 | 19.0-22.0 | 19.0-22.0 | 19.0-23.0 |
| Fe | 39.5 min | 39.5 min | 39.5 min | bal | bal | bal | |
| C | 0.10 max | 0.05-0.10 | 0.06-0.10 | 0.03-0.06 | 0.03-0.08 | 0.05-0.10 | 0.05-0.10 |
| Mn | 1.50max | 1.50 max | 1.50 max | <1.5 | <1.5 | <1.5 | 1.50 max |
| S | 0.015 max | 0.015 max | 0.015 max | <0.010 | <0.010 | <0.010 | 0.015 max |
| Si | 1.0 max | 1.0 max | 1.0 max | <0.70 | <0.70 | <0.70 | 1.0 max |
| Cu | 0.75 max | 0.75 max | 0.75 max | <0.15 | <0.45 | <0.45 | 0.75 max |
| Al | 0.15-0.60 | 0.15-0.60 | 0.15-0.60 | 0.15-0.40 | 0.20-0.50 | 0.40-0.75 | 0.15-0.60 |
| Ti | 0.15-0.60 | 0.15-0.60 | 0.15-0.60 | 0.20-0.40 | 0.20-0.50 | 0.25-0.65 | 0.15-0.60 |
| Al+Ti | | 0.85-1.20 | | <0.60 | <0.70 | | |
| P | | | | <0.015 | <0.015 | <0.015 | |
| N | | | | <0.03 | <0.03 | <0.03 | |
| Co | | | | <0.02 | <0.45 | <0.45 | |
| Nb | | | | <0.1 | <0.1 | | |
| ASTM GS No. | ≤5 | ≤5 | | | | ≤5 | |
| Euronorm 103 GS | | | 3 to 7 | 1 to 5 | 1 to 5 | | |

AVAILABLE SOURCES FOR CREEP AND STRESS-RUPTURE DATA

Although sufficient tensile and creep-rupture data existed in the 1960s to gain ASME Boiler and Pressure Vessel (BPV) Code acceptance, Huntington Alloys Inc. (HAI) assembled an expanded database for alloy 800 from U.S. and European sources for a re-evaluation of strength needed for further BVP code action in 1974. This information was intended for use in nuclear programs in [2, 9]. At that time, the European data provided to HAI included 302 creep-rupture tests. It is known that there were three specifications involved. In two of these specifications, the maximum carbon content was 0.030% and in the third the carbon range was 0.035 to 0.060%. Also, different limits were set for the

titanium and aluminum contents. These data, provided by HAI for use by General Atomic Company (GA), Westinghouse-Tampa (W-T), and ORNL, were retained at ORNL and included both Grade 1 (alloy 800) and Grade 2 (alloy 800H) materials. Some creep data were provided by HAI in the ASTM McBee card format. Other listings were in tables and hand plots. The temperatures for approximately 130 creep tests on alloy 800H ranged from 538 to 1093°C (1000 to 2000°F). The creep data were used by Sterling at GA to develop a creep law needed for construction of isochronous stress-strain curves [10].

To further assist in expanding the data base, ORNL placed a subcontract with Sandvik in 1976 to supply stress-rupture data and technical papers describing development work on SANICRO 30 and SANICRO 31 alloys [11]. Over 600 rupture tests were listed for a variety of chemistries, melting practices, fabrication practices, product forms, and heat treatments. The SANICRO 30 heats were too low in carbon to qualify as alloy 800H but 19 of the 39 lots of SANICRO 31 exhibited chemistries that conformed to alloy 800H. Most lots of SANICRO 31 met the alloy 800H heat treating requirements. Testing temperatures ranged from 550 to 700°C (1022 to 1296°F). The emphasis of the research was for usage around 600°C [11-14].

In 1978, three reports produced by W-T were combined in a review of the status of alloy 800 for steam generators [15]. The stress-rupture compilation included 162 results from tests in the range of 482 to 982°C (900 to 1800°F). Although the emphasis was on the properties of Grade 1, material (N08800), an interesting discussion of tertiary creep limit was included that bears on the tertiary creep limit of ASME III-NH. Much of this material was presented at Petten International Conference in 1978 [16, 17].

Also in 1978, Booker, Baylor, and Booker re-assembled and analyzed the creep-rupture database for alloy 800H (N08810) [18]. They examined creep behavior, tertiary creep characteristics, and stress-rupture. They reported creep data for 8 lots tested in the range of 538 to 871°C (1000 to 1600°F). These included two product forms of a single heat (plate and tubing) and one lot whose chemistry did not conform to alloy 800H due to low carbon content. The creep data included the time to end “primary creep,” the minimum creep rate, and the time to tertiary creep as defined by the 0.2% offset strain from the minimum creep rate projection. They showed creep curves for 72 tests. Many of the creep data compiled were taken from the HAI data package [2, 9]. In their report, Booker et al. listed 485 stress-rupture data supplied by Sandvik for Sanicro 31 [11]. Included were 156 stress-rupture data for lots that conformed to the alloy 800H specification. Booker et al. performed extensive analyses of the creep data and proposed formulations to describe the temperature-stress dependencies of creep, rupture, and tertiary limits.

A revised data compilation of creep, rupture, and tensile data for alloy 800 (N08800) was issued by HAI in 1980 [19]. This compilation included the European test results that were accumulated in 1974. The listing of tensile data included results for 71 lots of cold drawn (CD) tubes, 2 lots of cold drawn (CD) rounds, and 10 lots of hot rolled (HR) plates. Creep-rupture data were included for the same product forms. A total of 228 test data covered the temperature range of 450 to 982°C (842 to 1800°F).

The accumulation of creep and stress-rupture data on variants of alloy 800 continued during the early 1980s. Andersson reported data on effects of composition, heat treatment, and cold work on the tensile and stress-rupture of alloy 800H at 600°C (1112°F) [6], while Milička reported data on effects of prestraining on creep behavior of alloy 800H near 700°C (1292°F) [20]. The data in both papers were provided in graphical rather than tabular form.

In 1982, stress-rupture data were added to the data base accumulated by GA for a re-evaluation of the strength of alloy 800H. These included 40 data from five lots of tubing produced by Sumitomo Ltd and 39 data from Babcock & Wilcox Company on bar and tubing. Data were restricted to the temperature range of 538 to 816°C (1000 to 1500°F). Analysis of the data was undertaken by ORNL, Mar-Test Inc, and GA and led to the revision of allowable stress intensities for ASME Section III Code Case N-47 [21]. The data and results of the analysis were summarized in a report by Booker [22].

Creep-rupture of alloys 800 and 800H in air and helium were reported by Trester et al. in 1982 for temperatures in the range of 649 to 900°C (1200 to 1650°F) [23]. This work addressed such issues as the effect of carburization and aging on the yield and ultimate strengths, ductility and toughness, and creep-rupture behavior. The report included a review of other work on helium effects and provided 45 references. Stress-rupture data from tests in “wet” helium were reported from four sources over the temperature range 649 to 760°C (1200 to 1400°F). Stress-rupture data from tests in “dry” helium were reported from three sources over the temperature range 649 to 816°C (1200 to 1500°F). Control data from tests in air were included. Creep curves were provided for 14 tests performed in air and helium at temperatures from 649 to 900°C (1200 to 1650°F).

Testing (tensile and stress-rupture) of alloy 800H forging at 649°C (1200°F) were begun at GA [24, 25]. Also in the mid-1980s, a program supported by GA Technologies Inc. was undertaken by ERA Technology Ltd to explore the effect of compositional and fabrication factors on the tensile and creep-rupture behavior of alloy 800 [26]. Primarily, the efforts were concerned with low carbon and low aluminum plus titanium variants, but one series addressed alloy 800H. Creep-rupture tests on alloy 800H were performed on tubes from four casts and bars from two casts. The test temperatures ranged from 800 to 1000°C (1482 to 1832°F) for times to beyond 10,000 hours. Creep strains were determined by interruption of the tests for room temperature measurements. Data for 77 tests were provided in graphs and tables.

In the mid 1980s, a number of papers addressing HTGR materials technology were provided in a special issue of Nuclear Technology [27]. Materials included alloys 800H, 617, X, and other candidates. Papers covered the status of the materials development work, the selection of metallic materials, microstructural characterization, creep properties, fatigue properties, tensile properties, fracture mechanics, gas/metal reactions, friction and wear, hydrogen permeation, irradiation behavior, design codes, and nondestructive evaluation. Several papers included evaluations of alloy 800H. In

particular, Sainfort et al. included stress-rupture curves for alloy 800H in helium and air to 750°C (1382°F) [28], Lee provided summary data for stress-rupture, minimum creep rate, and time to tertiary creep in air and helium at 649 and 760°C (1200 to 1400°F) [29], and Schubert et al. provided summary data for stress-rupture and time to 1 percent creep for temperature to 950°C (1742°F) [30]. Data were provided as plots.

In the 1980s there was interest in using alloy 800H for advanced fossil energy applications. Here, alloy 800H was used in process heaters and heat recovery systems. Smolik and Flinn, for example, examined the stress-rupture of pressurized tubes in air, inert environments, and oxidizing/sulfidizing environments at 871°C (1600°F) [31]. Over 40 tests ranging to beyond 3400 hours were included in the work and data were provided in a tabular form. About the same time, Taylor, Guttmann, and Hurst reported results of stress-rupture testing of solution annealed, aged, and carburized alloy 800H at 800°C (1472°F) [32]. Degischer et al. described the effect of solution temperature and aging on the creep behavior of two heats of alloy 800H at 800°C (1472°F) [33]. Creep data were provided as log creep rate versus log creep strain.

The very-high temperature gas cooled (VHTGR) reactor program undertook an extensive environmental creep testing effort in the 1980s at the General Electric Company [34]. The activity examined two heats of alloy 800H. One heat was tested in both air and HTGR helium and the other heat in only air. Temperatures for 40 tests ranged from 750 to 1050°C (1382 to 1922°F) and times extended to beyond 10,000 hours. The reported data included the time to 1% total strain, the minimum creep rate, the time to the onset of tertiary creep, the time to 0.2% offset tertiary creep strain, and rupture life. Notched-bar stress rupture testing was undertaken. The authors included an assessment of the data availability for alloy 800H as a function of temperature to determine the data requirements for code qualification to 954°C (1750°F).

The MHTGR-NPR program re-kindled interest in restricted chemistry versions of alloy 800H in the US [35]. In particular, there was interest in a version of alloy 800H with carbon near the minimum requirement of the specification (0.05%) and aluminum plus titanium at 0.5% or greater. As part of the program, efforts were made to re-assemble the database and re-evaluate compositional effects. Sources included the HAI compilations [2, 9], the ERA Technology Ltd work [25], the Sandvik tests [11], and the Petten database [36]. The Petten database was quite extensive and covered several variants of alloy 800, cold work effects, and environmental effects mostly derived from European research efforts. No tabular data were provided. Papers by Diehl and Bodmann [7, 37] provided further insight into the nature of the European data base. Diehl and Bodmann summarized an examination of the specifications and strength characteristics of the variants of alloy 800 contained in the Hochtemperatur-Reaktorbau GmbH (HRB) material data bank. The HRB creep-rupture data included 4735 tests on 289 materials (lots) over the temperature range of 450 to 1205°C (842 to 2200°F). The variants were designated Alloy 800-Rk, Alloy 800-NT, and Alloy 800HT and distinguished from one another on the basis of chemistry, heat treatment, and grain size. The stress-rupture data based re-assembled by McCoy for the MHTGR-NPR work included some of these US, European, and Japanese data [38]. Most of the 79 heats and lots conformed to alloy

800H specification. A total of 838 rupture data were compiled in tabular form for temperatures from 538 to 816°C (1000 to 1500°F). Supplemental creep-rupture testing of a “reference” heat of alloy 800H was begun in 1990 [39]. A few tests in the temperature range of 538 to 816°C (1000 to 1500°F) were completed on base metal and weldment specimens before the MHTGR-NPR work was terminated. Additional testing of the alloy 800H reference heat was undertaken by Swindeman in 1992 [40]. Here, temperatures were in the range of 700 to 982°C (1292 to 1800°F).

A model for creep behavior of alloy 800HT was published by El-Magd et al. in 1996 [41]. The creep data were provided as log creep rate versus log time and log creep rate for temperatures in the range of 700 to 900°C (1292 to 1650°F).

Four significant contributions to the creep-rupture data base for alloy 800H were produced by the National Institute for Materials Science (NIMS) [41, 42, 43, 45]. Data were provided for 6 lots of tubing over the temperature range of 550 to 1000°C (1022 to 1832°F) [41]. Similarly, data were provided for 6 lots of plate materials over the same temperature range [42]. Data included minimum creep rate, the time to 1% total strain, the time to tertiary creep based on the 0.2% offset from the minimum creep rate projection, and rupture life. Data at the lower temperatures extended to nearly 200,000 hours [43]. Creep data for a single bar product were provided along with relaxation data for temperatures to 800°C (1472°F) [45].

Finally, the status of the database at Petten was investigated recently. There were 1089 “creep” test results available for alloy 800H with temperatures ranging from 500 to 1000°C (932 to 1832°F). The data appear to be from German work on the HGR program.

DATA ANALYSIS PROCEDURES

The materials data currently provided in ASME Section II that are applicable to ASME III-NH include physical properties (Tables TE-1 through TE-5, Tables TCD, Tables TM-1 through TM-4, and Tables NF-1 and NF-2), short-time tensile properties (Table U, Table Y-1), buckling charts, and design stress intensity values (Tables 2A, 2B, and 4) corresponding to criteria identified in Appendix 2 of Section II. ASME III-NH provides additional materials data in the tables of Appendix 1-14. For purposes of high-temperature design, ASME III-NH includes stress-rupture tables, fatigue tables, creep-fatigue damage envelopes, creep-buckling charts, and isochronous stress versus strain curves in Appendix 1-14 and Appendix T. For alloy 800H, the coverage extends to 760°C (1400°F) and for times to 3×10^5 hours. Fatigue curves extend to 10^6 cycles. The effects of service-aging on the yield strength and ultimate strength are included. Stress-rupture data for weld filler metals are included.

It is a matter of ASME policy that strength values for all “Code Books” be set or approved by BPV Section II. For new materials or extended coverage of existing materials, ASME often subcontracts with a consultant to derive the strength values for code cases or the appropriate tables in Section II-D. The strength values are based on the

criteria developed by the specific construction code. Appendix 1 in Section II-D identifies the criteria for establishing the allowable stress for Tables 1A and 1B in Section II-D. Appendix 2 in Section II-D identifies the criteria for establishing the allowable stress intensity values for Tables 2A, 2B, and 4 in Section II-D. However, Tables 2A and 2B do not cover temperatures where time-dependent properties control the allowable stress intensities. The criteria for establishing these time-dependent stress intensities are specified in ASME Section III, Subsection NH paragraph NH-3221 and differ from those ASME Section II-D Appendix 1 in several ways: (a) Appendix 1 has a creep rate criterion which is 100% of the stress to produce a creep rate if 0.01%/1000h, while paragraph NH-3221 has a total (elastic, plastic, primary plus secondary creep) strain criterion which is 100% of the minimum stress to produce 1% total strain in a specific time, say 100,000 hours; (b) Appendix 1 has a rupture strength criterion of F_{avg} times the average stress to produce rupture in 100,000 hours, while paragraph NH-3221 calls for 67% of the minimum stress to produce rupture in a specific time, say 100,000 hours; (c) Appendix 1 has a second rupture strength criterion of 80% of the minimum stress to produce rupture in 100,000 hours, while NH-3221 calls for 80% of the minimum stress to cause initiation of tertiary creep in a specific time, say 100,000 hours. The factor F_{ave} used in Appendix 1 has the value 0.67 or less and depends on the slope of the stress-rupture curve around 100,000 hours [46].

Over the years, the methods of data analysis needed to produce the tables and charts in ASME Sections II, III, and III-NH have evolved and will continue to evolve. Several of the references identified above provide analysis procedures and it is beneficial to review some of these procedures as well as alternatives. First, the current procedures for processing creep and stress-rupture data for ASME II will be reviewed.

Current ASME Section II Procedures for Setting Time-Dependent Stress Allowables

The minimum data requirements for approval of new materials for elevated temperature construction are outlined in Appendix 5 of ASME Section II Part D. Generally, the data package is submitted as part of a code case that is applicable to a specific construction code, such as Section I or Section VIII, which covers high-temperature structural components. In addition to the construction code, the draft code case is concurrently submitted to Section II, which has the responsibility for setting stresses, and Section IX, which has the responsibility of approving the applicable rules for welded construction. As described above, consultants working under subcontracts to ASME process the data and develop stresses conforming to each of the criteria set forth in Appendix 1 of ASME Section II Part D. Although the consultants have not been restricted to the use of any specific procedure, the time-dependent allowable stresses for every new material approved in codes cases or incorporated into II-D for the last twelve years have been based on the Larson-Miller temperature-time parametric correlation method that employs a stress-dependent activation energy. Thus:

$$(1/t_R) = A \exp[-f_1(S)/RT] \quad (1)$$

Where t_R is rupture life or reciprocal creep rate, A is a constant, $f_l(S)$ is a function of stress, R is the universal gas constant, and T is absolute temperature. Taking the log to base ten and rearranging produces the familiar Larson Miller parameter (LMP):

$$LMP = T (C + \log t_R) = f_l(S)/2.303R \quad (2)$$

Where C is $\log A$ and identified as the Larson-Miller parametric constant.

Typically, a stress function $f(S)$ is formulated as a polynomial in log stress:

$$f(S) = f_l(S)/2.303R = a_0 + a_1 \log S + a_2 (\log S)^2 + a_3 (\log S)^3 + \dots \quad (3)$$

where a_i is a series of constants that depend on the number of terms in the polynomial. Using a least squares fitting method in which $\log t_R$ is the dependent variable and T and $\log S$ are independent variables, the optimum values for C and a_i are determined. Although not explicitly required by Appendix 1 of ASME Section II-D, the consultants may employ a “lot-centered” procedure developed by Sjodahl that calculates a lot constant (C_h) for each lot along with the Larson-Miller constant, C, which represents the average lot constant (C_{ave}) for the heats (46). However, only C_{ave} is used to determine the S_{Rave} and S_{Rmin} values specified in Appendix 1. To determine S_{Rave} , eq. (2) be solved for S at 100,000 hours. The determination of S_{Rmin} in Appendix 1 requires that eq. (2) be solved for S at 100,000 h after adjusting C by 1.65 multiples of the standard error of estimate (SEE) in $\log t_R$. This minimum represents the 95% lower bound to the stress-rupture data. Thus, only a single analysis for rupture life is needed to assess two of the three time-dependent criteria in Appendix 1. The factor F_{ave} only applies to S_{Rave} and requires an estimate of the slope of the $\log S$ versus $\log t_R$ curve, n, at 100,000 hours. The F_{ave} value may be found by evaluating the partial derivative $[\partial f(S)/\partial(\log t_R)]_T$ at 100,000 hours. The value of F_{ave} is then given by the antilog of $(-1/n)$. It has a defined upper limit of 0.67. Alternatively, F_{ave} may be determined as the ratio of the 10^5 h strength to the 10^6 hour strength needed to produce a factor of 10 on life at 100,000 hours. Some insight into an MPC procedure for F_{ave} accepted by ASME has been provided by Prager, who provides an analysis for alloy 800H as an example [47]. He found that the F_{ave} for alloy 800H range from 0.640 at 816°C (1500°F) to 0.585 at 982°C (1800°F). The third criterion, S_c , rarely controls the allowable stresses in Tables 1A and 1B. Generally, it is only necessary to provide sufficient data to demonstrate that S_c does not control. Using eq. (2) and eq. (3), the procedures for the determination of S_c are similar to S_{Rave} , except that t_R is replaced by $1/mcr$, where mcr is the minimum creep rate. Although the lot constants, variants within a lot, variants between lots, and SEE of the $\log t_R$ can be produced in the analytical procedure required by ASME, it is important to recognize that the ASME II-D does not explicitly provide such information in the minutes of the responsible subgroup or in the stress tables. The minutes of ASME Section II show which time-dependent criterion controls the allowable stresses but Tables 1A and 1B in ASME Section II-D only show the controlling stresses.

ASME Subsection NH Procedures for Setting Time-Dependent Stress Intensities

The procedures used to produce the stress intensity values and minimum rupture strength values in the ASME III-NH Table I-14.4 and I-14.6 have not been standardized. However, the documentation of data used in the analyses and the details of the analytical procedures are contained in the minutes of the ASME Subgroup on Elevated Temperature Design. In some instances reports and open literature publications provide additional information on these topics.

As mentioned above, the ASME III-NH time-dependent criteria considered for Table I-14.4 include (1) 67% of the minimum rupture strength as a function of temperature and time, (2) 80% of the minimum stress to produce the onset of tertiary creep as a function of temperature and time, (3) the minimum stress to produce 1% total strain as a function of temperature and time. Table I-14.6 provides the minimum rupture strength as a function of temperature and time. In contrast, the isochronous stress-strain curves in Appendix T of ASME III-NH represent the “average stress” vs strain trend for temperatures and times covered by the code. For consistency within the ASME code, the same stress-rupture model developed for the ASME Section II-D tables should be used for the determination of the stresses for criterion (1) and Table I-14.6 in ASME III-NH. Unfortunately, this consistency is not always assured.

With respect to alloy 800H, as mentioned above, the original development of stress intensity values were described by Sterling [10]. A review of the procedures and an offering of alternate procedures were provided by Booker and co-workers [18, 48]. It was determined that the stress-rupture data did not support the values in the code case. Working with HAI, ORNL, and others, GA Technologies revised the stress tables for CC N-47 [21]. Two of the three criteria for time-dependent stress-intensity values were addressed. For the determination of the minimum stress to rupture, S_{Rmin} , a correlation for the average rupture life was first developed that was a modification of the Larson-Miller parameter:

$$T [-b_o + \log(t_R+3)] = b_1 + b_2 \log S. \quad (4)$$

Here, on the left side of eq. (4) b_o is the negative of the LM constant, C , in eq. (2) and the 3 hours are added to the rupture life, t_R , to improve the fit of the model to the data at short times. The right side of eq. (4) is a two-term polynomial in which the a_i terms of eq. (3) are labeled b_1 and b_2 . This stress function is a simple power law and permits eq. (4) to be solved for stress in a straightforward procedure. The minimum rupture stress is obtained by introducing 1.65 multiples of the standard error of estimate, SEE, into the rewritten eq. (4):

$$\log S_{Rmin} = \{[\log(t_R+3) + 1.65 \text{ SEE} - b_o] T - b_1\} / b_2. \quad (5)$$

The values provided in ASME III-NH Table I-14.6C were produced by this equation.

A correlation between the time to tertiary creep, based on the 0.2% offset definition, and the rupture life was used to develop a method to address the second of the three time-dependent criteria for setting allowable stress intensities. This correlation was a simple power law written in logarithmic form below:

$$\log t_3 = \log A + B \log t_R \quad (6)$$

Where A and B are constants. Using eq. (6), a rupture life, t' , corresponding to the t_3 of interest, was calculated and used in eq. (5) to determine the corresponding minimum stress for the initiation of tertiary in the time, t_3 .

In CC 1592, the minimum stress to produce 1% total strain, $S_{1\%}$, did not control S_t for alloy 800H and no revisions were made in developing CC N-47 or ASME III-NH. A re-analysis of $S_{1\%}$, was undertaken by Booker, Baylor, and Booker in 1976 [18]. Due to the difficulty in determining the minimum strength from the database, they defined $S_{1\%}$, as 80% of the average stress to produce 1% strain as a function of temperature and time. They showed that the $S_{1\%}$ did not control the S_t or S_{mt} above 593°C (1100°F) [18].

A Norton-Bailey power-law creep model was developed by Sterling for the time-dependent component of the isochronous stress-strain curves [10]. Here:

$$\varepsilon_c = D S^n t^m, \quad (7)$$

where ε_c is creep strain and D, n, and m are constants. Sterling observed that the time to a given strain followed a “linear Larson-Miller type stress and temperature dependence.” For analysis purposes, he wrote eq. (7) as:

$$\log t = (u_1/T) \log S + (u_2/T + u_3) \log \varepsilon_c + (u_4/T + u_5), \quad (8)$$

where u_i are constants determined by a least squares analysis. As mentioned above, this equation forms the basis for the time-dependent component of the isochronous curves in Appendix T. It represents average creep behavior. Accepting the assertion of Booker, Baylor, and Booker, one could calculate $S_{1\%}$ using the 80% factor and eq. (8).

A Few Other Data Analysis Procedures

Early work by HAI clearly demonstrated that the time dependency of rupture strength for alloy 800H follows a power law. Evaluations by Wattier [21], Prager [47], Booker [48], and Nippon Kokan [49] support the power law stress dependency with the Larson-Miller time-temperature parametric correlation.

Following Pepe [49], McCoy used the Minimum Commitment Method (MCM) procedure [50] for correlating stress-rupture life data for alloy 800H but provided no information regarding the parametric values or the stress dependency of the rupture life [38]. However, the MCM procedure produced isothermal stress-rupture curves for alloy 800H that approximated a power law for temperatures above 649°C (1200°F).

Although the Europeans have extensive experience in working with time-temperature parametric methods, they have favored isothermal stress-time correlations for determining average and minimum strengths. In the German code development, isothermal extrapolations are restricted to a factor of three in time [30]. This rule requires an extensive long-time data base since they provide allowable stresses for design up to 200,000 hours [51]. With respect to the nuclear construction codes, the papers by Diehl and Bodmann provide some insight into data processing procedures [7, 37]. Here, “the relationships between the characteristics of the creep and creep-rupture properties and the metallurgical parameters were investigated by multilinear regression analyses.” These investigations involved isothermal data divided into groups (time segments). The regression analyses helped to identify three variants of alloy 800 (800 DE, 800 Rk, and 800 HT) differing by chemistry and heat treatment (grain size). Then, stress-rupture curves and stress versus time to 1% total creep curves were produced for each variant. In contrast to the power law stress-life trend observed for alloy 800H, the log stress versus log time curves turn downward with increasing time for all variants. Of the three variants in the German code, only 800 HT is permitted for service above 700°C (1292°F). The duration of the data permitted the extension of allowable stresses to 100,000 hours. Stress values for 300,000 hours are provided in the KTA 3221 table but a note indicates that the extrapolation in time is beyond a factor of three.

Data correlation was undertaken at NIMS of the long-time tests results on alloy 800H [42, 43, 44]. The NIMS analysts favored the Manson-Haferd parameter in combination with a polynomial in log stress such as eq. (3). Although data for several lots approached or exceeded 100,000 hours, only four or five stresses were included at each temperature, and the estimation of the long time strength of each lot was based on the interpolation of the parametric fit to the data. Correlations included the strength-temperature dependence of rupture life, time to 1% total strain, minimum creep rate, and time to 0.2% offset tertiary creep.

EVALUATION OF THE STRESS-RUPTURE OF ALLOY 800H AT 750°C AND HIGHER

This section summarizes analyses that estimated the average and minimum rupture strength values for times to 300,000 hours and beyond. The evaluation consisted of the selection of applicable data, selection of analysis methods, estimation of stresses, and comparison of results with values from which ASME Section II-D and Subsection III-NH tables were derived.

Selection of Data:

Stress rupture data were accumulated for more than one hundred lots of alloy 800H and its variants. The criteria for selecting usable data from this database were these:

Chemistry: Carbon in the range of 0.05 to 0.1%,
Al+Ti in the range of 0.5 to 1.2%
Grain size: ASTM Grain Size Number 5 or lower
Anneal: Annealed at 1120°C or higher
Data Range: Temperatures of 750°C and higher
Products: Plate, Bar, Pipe, and Tubes

From the database, 37 lots were selected which produced 351 data at 750°C and higher. Histograms showing the distribution of carbon and Al+Ti for the lots are provided in Figures 1 and 2. A histogram for the grain size distribution is shown in Figure 3. The distribution of temperatures is shown in Figure 4. The distribution of rupture lives is shown in Figure 5.

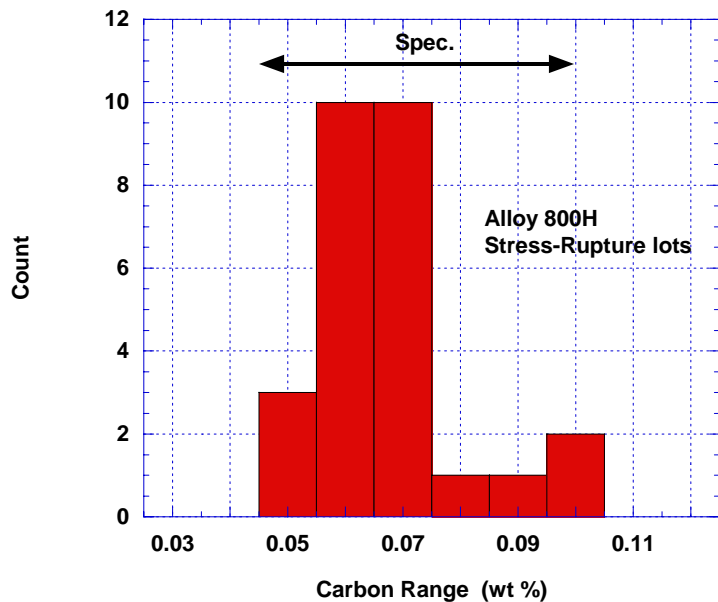


Figure 1. Distribution of carbon contents in 37 lots of alloy 800H

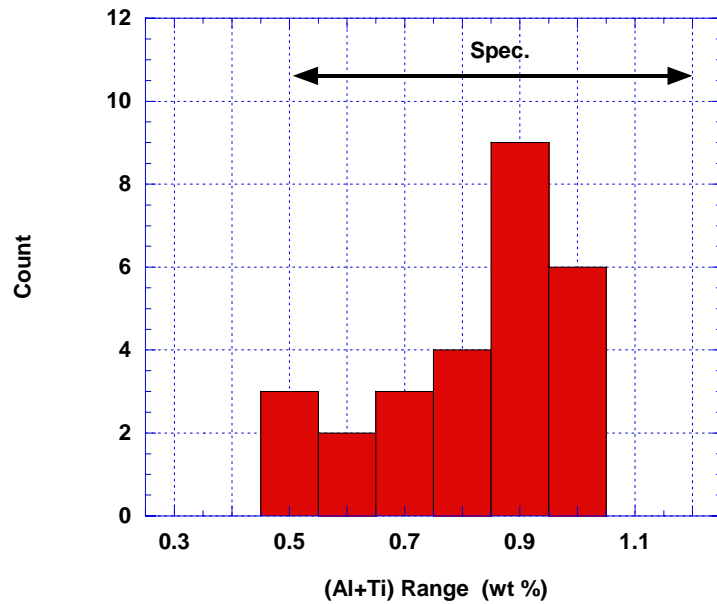


Figure 2. Distribution of Al+Ti contents in 37 lots of alloy 800H

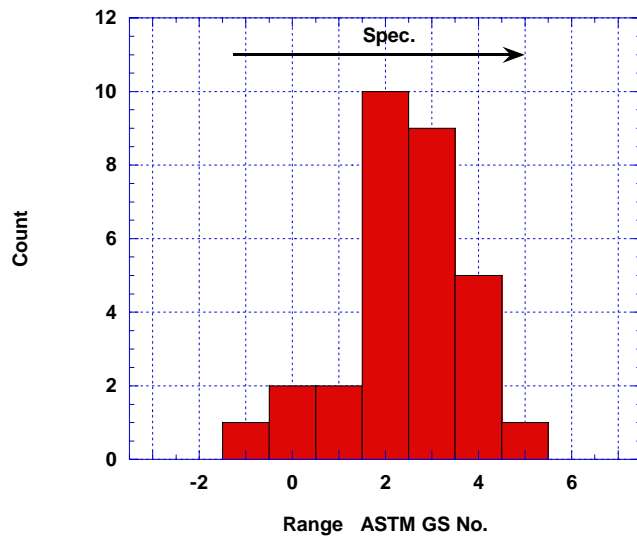


Figure 3. Distribution of grain sizes in 37 lots of alloy 800.
(ASME GS No. 00 was assigned a value of -1)

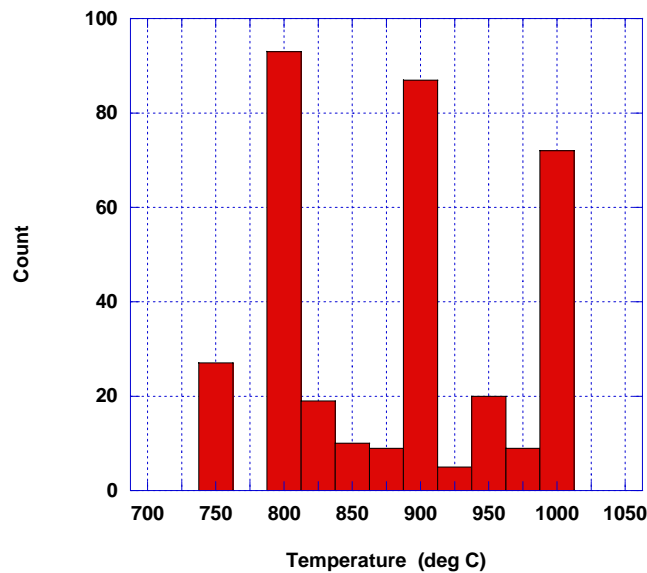


Figure 4. Distribution of testing temperatures for 37 lots of alloy 800H

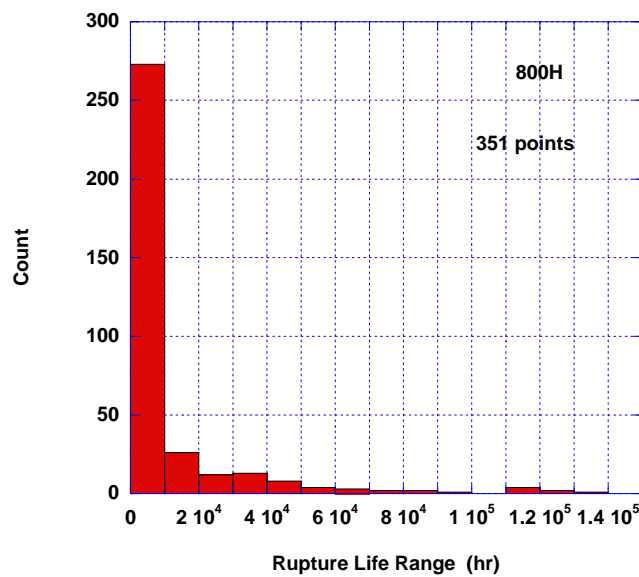


Figure 5. Distribution of rupture lives for 37 lots of alloy 800H

Selection of Analysis Methods:

As described in the review section of this report, many analysis methods were examined over the years [18, 21, 22, 38, 39, 42, 43, 44, 46, 47, 48, 49, 50]. Since it was the intent of the effort reported here to extend the current Subsection III-NH stress allowable stress intensities (Table I-14.4C) and minimum stress values (Table I-14.5C) to higher temperatures and longer times, an analysis consistent with previous “code” analyses was needed. Also, it was judged to be necessary that the analysis would produce values close to those in ASME Section II-D 1B when the criteria in Table I-100 in II-D were invoked. The detailed analysis procedures used to set the II-D values were not published nor were they in the Code committee minutes. However, a paper by Prager provided general guidelines for the evaluation of alloy 800H for temperatures above 760°C [47]. Here, the Larson-Miller (LM) time-temperature parametric approach was selected and parametric constant of 15.21805 was reported. Other parametric approaches were cited.

For the analysis reported here, the Larson-Miller parameter, in combination with a polynomial in log stress, was selected. See equations 2 and 3 above. Both global and lot-centered approaches were included.

Results:

The fit of the LM parameter to the high-temperature data is shown in Figure 6. The optimized parametric constant, C, was 15.12487. This number was close to the value reported by Prager (15.21805). The coefficients for the stress function were as follows:

$$\begin{aligned}a_0 &= 29648.78 \\a_1 &= -7334.877 \\a_2 &= 1903.854 \\a_3 &= -619.4775\end{aligned}$$

The standard error of estimate for the fit was approximately 0.29 log cycle (in life). A histogram showing the distribution of the residuals (log tr – calculated log life) is shown in Figure 7, while the variation of residuals with life, stress, and temperature are shown in Figures 8, 9, and 10, respectively. The plots revealed no gross trends, although a few test data at 800 and 900°C appeared to exceed the life expectations by significant margins.

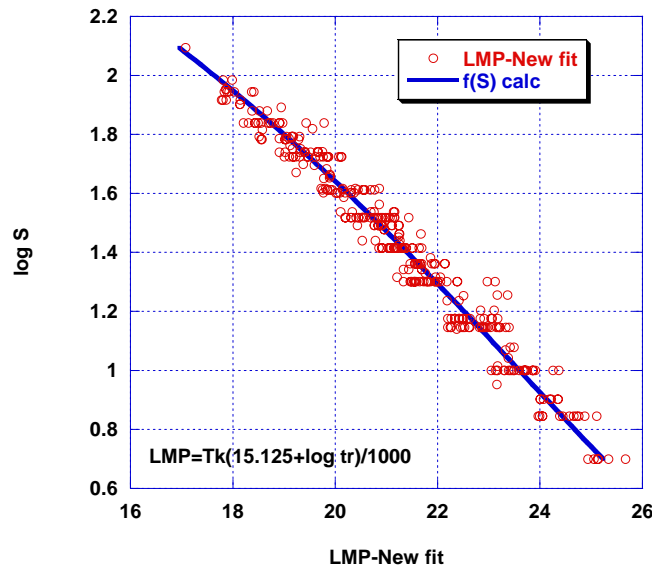


Figure 6. Log stress versus Larson Miller parameter for alloy 800H

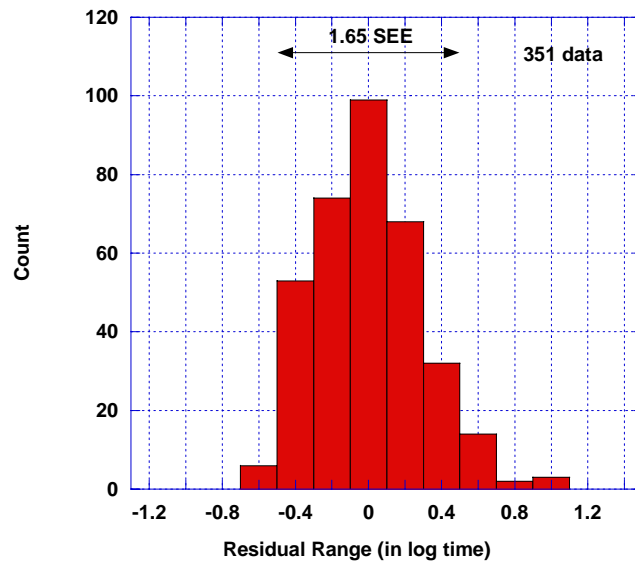


Figure 7. Histogram of residuals for fit of LM parameter for alloy 800H

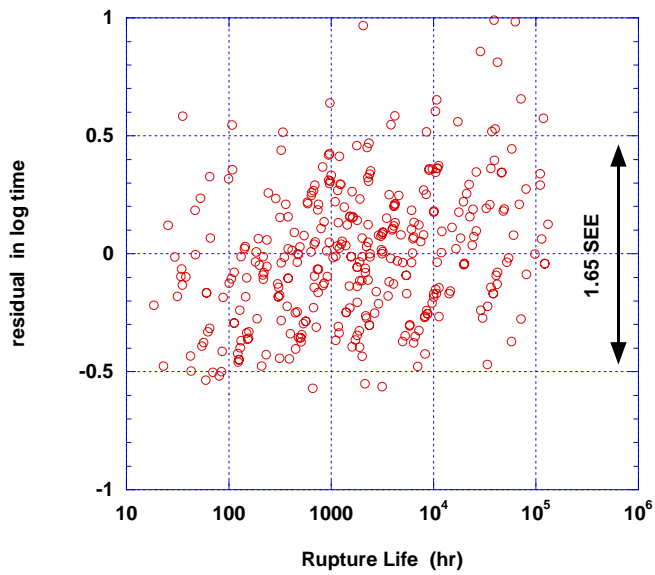


Figure 8. Residuals versus rupture life for LM parameter fit to alloy 800H

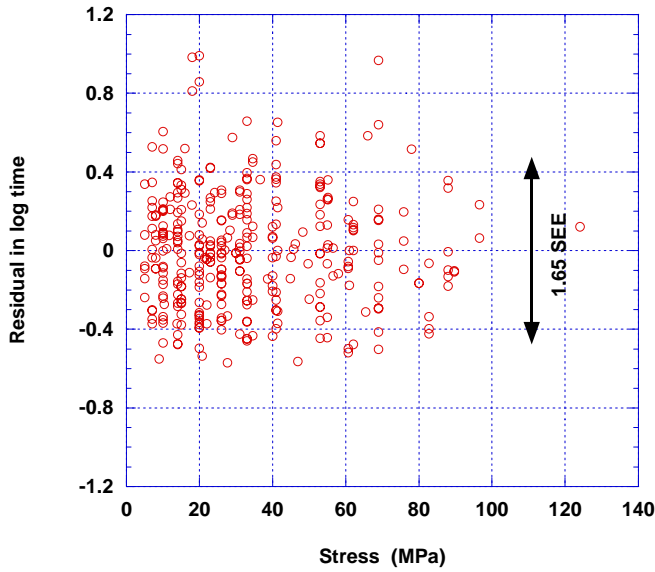


Figure 9. Residuals versus stress for LM parameter fit to alloy 800H

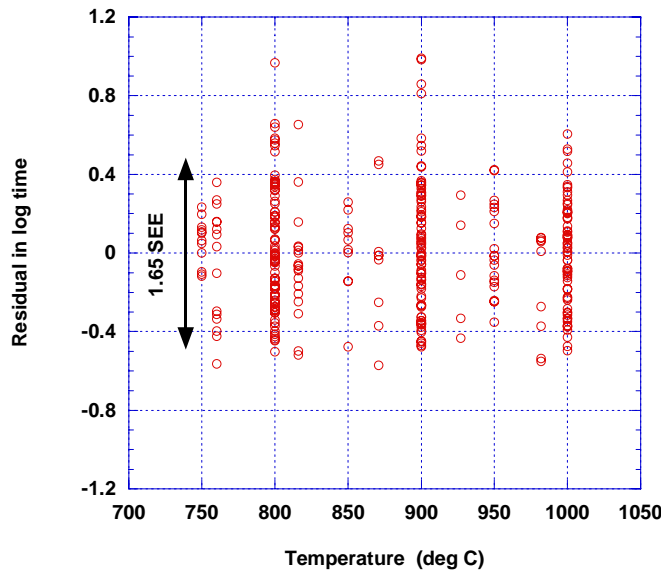


Figure 10. Residuals versus temperature for LM parameter fit to alloy 800H

It was expected that the lot-centering method would improve the fit to the data and permit some quantitative estimates of the influence of chemistry or microstructure on strength. However, the method was not very satisfactory. First, a single lot of plate product from the NIMS file (fdA) was examined. This material produced a C value of 18.02. Then the analysis of the NIMS file for six plate products was undertaken. This lot-centered analysis changed the LM constant for lot fdA to 16.45. Then all 37 lots were analyzed. The LM constant for lot fdA dropped to 15.66. The average LM constant for 37 lots was 15.93, somewhat higher than the value for the “global” analysis described above. The table below provides data for three lots- one from each of three groups.

Table 1. Effect of Data Selection on the LM Constants, C,
for Three Lots in a Lot-Centered Analyses

| Lot | Group | Group C _{ave} | C-in-Group | C-in-All |
|---------|-------------|------------------------|------------|----------|
| fdA | ----- | ----- | ----- | 18.02* |
| fdA | NIMS plates | 16.48 | 16.45 | 15.66** |
| HH8099A | ----- | ----- | ----- | 17.07* |
| HH8099A | HAI | 17.47 | 17.43 | 15.89** |
| AED | ----- | ----- | ----- | 11.52* |
| AED | UK | 11.05 | 10.95 | 15.82** |

*value as a single lot analysis, **value for the lot within the 37 lots

Clearly, the UK lots that included bar and tube products were distinctly different from the HAI and NIMS lots and contributed to the lower value of C for the average of the 37 lots (15.92). One reason for the significant change in the C value between the single lot analysis and the multi-lot analysis was associated with the restriction on the stress function, $f(S)$. One stress function was “forced” on all lots in the lot-centered analysis. More sophisticated lot-centering methods were available that would relax this restriction but these were not used in this work [50]. The global approach was selected as being the most representative of the current “Code” methodology. The times and stresses were estimated from the LM constant and polynomial coefficients given above for the global analysis.

The “average strength,” S_{Rave} , and “minimum strength,” S_{Rmin} , for 100,000 hours were calculated for temperatures from 750 to 900°C. The minimum strength was based on the stresses corresponding to a rupture curve displaced to shorter life from the average curve by 1.65 multiples of SEE in log time. These S_{Rave} and S_{Rmin} values are listed in Table 2.

Table 2. Calculated stresses for 100,000 hours (MPa)

| Temperature (°C) | Average Strength | Minimum Strength |
|------------------|------------------|------------------|
| 750 | 34.9 | 28.8 |
| 775 | 28.6 | 23.3 |
| 800 | 23.3 | 18.8 |
| 825 | 18.9 | 15.2 |
| 850 | 15.3 | 12.2 |
| 875 | 12.4 | 9.77 |
| 900 | 9.97 | 7.84 |

The minimum strength values for these and other temperature-time combinations could be added directly to Table I-14.6C in III-NH. Also, one of the criteria for Table I-14.5C is 67% of the minimum strength for the temperature-time combination in the table. However, values based on the minimum strength may not be the controlling value. The other criteria require information from the creep analyses (1% creep and tertiary creep criteria) and were not considered here but will appear in Part 2 of this report.

Comparisons:

The minimum strength value at 750°C may be compared directly with a value in ASME III-NH which lists 29 MPa at 100,000 hours. Rounding the 28.8 MPa in Table 2 produces the same strength as in ASME III-NH Table I-14.6C.

As mentioned above, the analysis for III-NH would need to produce results that are consistent with Table 1B of ASME II-D. Table 3 below is an expansion of Table 2 and provides a comparison with values in ASME II-D. The second column provides the F_{ave} values that were needed to replace the 0.67 factor applied in II-D at lower temperatures to

S_{Rave} and produce a margin on life of at least ten. These values are plotted against temperature in Figure 11. Here, it may be seen that the values approach 0.67 at low temperatures but have not reached it at 750°C. Prager reported values in the range of 0.63 to 0.60 as the temperature increased from 870 to 980°C [47]. The table indicates that the criterion based on the minimum strength (column 4) would control at 750°C, while the criterion based on average strength (column 3) would control at higher temperatures. At most temperatures, the ASME II-D stresses were lower than those calculated from this analysis. However, the differences were not judged to be significant for III-NH. Figure 12 compares the stress calculated in this analysis with the II-D values.

Table 3. Calculated stresses for 100,000 hours (MPa) which form the basis for the time-dependent allowable stresses in ASME II-D.

| Temp. (°C) | F_{ave} | $F_{ave}S_{Rave}$ | $0.8S_{Rmin}$ | II-D |
|------------|-----------|-------------------|---------------|------|
| 750 | 0.663 | 23.2 | 23.0 | 22.6 |
| 775 | 0.650 | 18.6 | 18.7 | 18.3 |
| 800 | 0.638 | 14.9 | 15.1 | 15.0 |
| 825 | 0.628 | 11.9 | 12.1 | 11.9 |
| 850 | 0.619 | 9.48 | 9.74 | 9.03 |
| 875 | 0.612 | 7.57 | 7.82 | 7.35 |
| 900 | 0.608 | 6.06 | 6.27 | 5.86 |

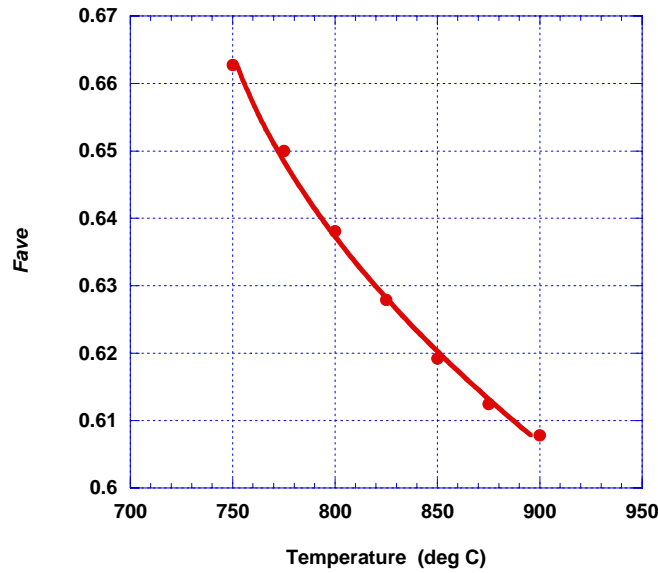


Figure 11. F_{ave} versus temperature for alloy 800H

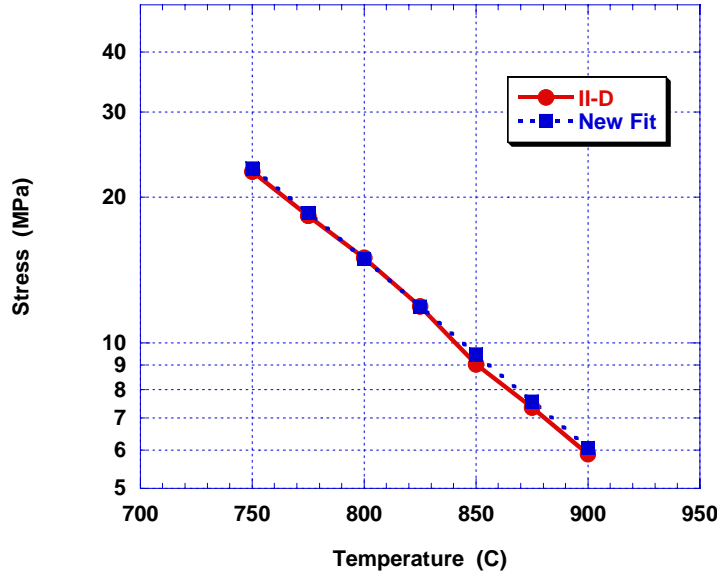


Figure 12. Comparison of ASME II-D stresses with the new fit for alloy 800H

As mentioned in the review section of this report, other methods of analysis have been used to estimate the long-time strength of alloy 800H. Several of these did not extend to the temperatures of interest in this work. McCoy, however, using the Minimum Commitment Method (MCM) provided estimates to 816°C [38]. McCoy also cited strength estimates by Pepe who examined several parametric procedures extending into high temperatures [50]. NIMS employed the Manson-Haferd parametric procedure to estimate the strength of individual lots over a broad temperature range [42, 43]. These results may be compared to the analysis report here for 800°C and are shown in Table 4 below. The strength at 800°C represented by this work falls within the scatter of the other predictive procedures.

Table 4. Comparison of the average strength of alloy 800H at 800°C and 100,000 hours from a number of sources.

| Source | Strength (MPa) | Number of lots | Parameter | Products |
|-----------|----------------|----------------|-----------|----------|
| This work | 23.3 | 37 | L-M | all |
| NIMS | 25.3 | 6 | M-H | plates |
| McCoy | 26.5 | 69 | MCM | all |
| Pepe | 21.0 | 30 | MCM | all |
| Pepe | 23.9 | 30 | L-M | all |
| Pepe | 22.1 | 30 | O-S-D | all |

L-M Larson-Miller; M-H Manson-Haferd; MCM Minimum Commitment Method; O-S-D Orr-Sherby-Dorn

Example of the addition to III-NH Table I-14.6C:

Figure 13 plots the calculated minimum stress rupture curves for temperatures of 750°C to 900°C. Included in the plot are the current III-NH values for 750°C. The curves extrapolate the times to at least 600,000 hours and cover stresses to as low as 6 MPa at 900°C.

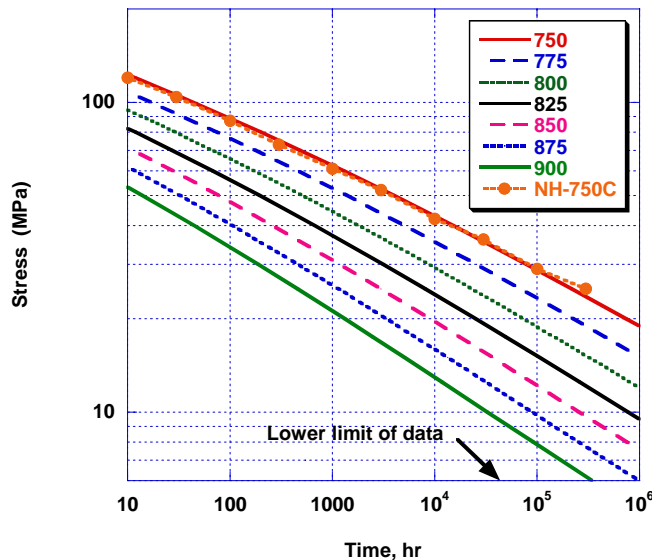


Figure 13. Minimum stress-to-rupture versus time for alloy 800H

SUMMARY AND RECOMMENDATIONS

The sources for high-temperature creep-rupture data for alloy 800H and its variants were reviewed and the development allowable stresses for pressure code construction was traced with emphasis on ASME Section III, Subsection-NH.

Criteria for setting stresses and data analysis procedures needed to develop allowable stresses were reviewed. Procedures used by ASME Section II were compared with those of ASME Section III, Subsection-NH.

The materials covered in references provided in this report were carefully reviewed to show compliance with the requirements of the alloy 800H specifications applicable to ASME Section III, Subsection-NH, and a subset was selected for the estimation of long-time rupture strength in the temperature range 750 to 900°C (1382 to 1650°C).

Sufficient data existed to permit the extension of the time-dependent allowable stress intensity values in ASME III-NH to 900°C (1650°F) and 600,000 hours.

ACKNOWLEDGEMENTS

This work was supported by ASME ST-LLC and managed by J. Ramirez. Technical oversight was provided by R. I. Jetter and C. Hoffmann. Part of the review undertaking was supported by UT-Battelle LLC under Subcontract 4000045435. The authors acknowledge the support and encouragement of W. R. Corwin and W. Ren of the Oak Ridge National Laboratory.

REFERENCES

1. T. E. McGreevy and R. I. Jetter, "DOE-ASME Generation IV Materials Tasks," *Proceedings of PVP2006-ICPVT-11*, July 23-27, 2006, Vancouver, BC, Canada.
2. "INCOLOY alloy 800 Data for Use in Design of Gas Cooled and Liquid Metal Fast Reactors," personal communication, J. M. Martin of Huntington Alloys to J. M. Duke, Westinghouse Electric Company, Tampa, FL (January 12, 1975).
3. *INCOLOY alloys 800/800H/800HT A History*, INCO Alloys International, Inc., Huntington, WV (not dated).
4. D. G. Harman, *Post Irradiation Tensile and Creep-Rupture Properties of Several Experimental Heats of Incoloy 800 at 700 and 760°C*, ORNL-TM-2305, Oak Ridge National Laboratory, Oak Ridge, TN (December 1968).
5. "Specification of Ni-Fe-Cr (Alloy 800) for Application in Sodium Heated Steam Generators," personal communication, J. M. Duke, Westinghouse Electric Company, Tampa, FL to P. Patriarca, Oak Ridge National Laboratory, Oak Ridge, TN (August 1975).
6. T. Andersson, "Effects of Composition, Heat Treatment, and Cold Work on Structure and Properties of Alloy 800," paper presented at 21 emas Journees des Aciers Speciaux, Saint-Etienne, France, April 27-28 1982.
7. H. Diehl and E. Bodmann, "Alloy 800: New Stress Rupture and Creep Data for Pressurized Components in High Temperature Reactors," *Nuclear Engineering and Design*, Vol. 119 (1990) 195-206.
8. *Regeln des Kemtechnischen Ausschusses (KTA-Regeln) KTA 3221.1: Metallische HTR-Komponenten*, KTA-Sitzung am 15.06.1993.
9. "Technical Meeting on Microstructure and Properties of Alloy 800," personal communication, T. H. Bassford, Huntington Alloys Inc. Huntington, WV to P. Patriarca, Oak Ridge National Laboratory, Oak Ridge, TN (November 1976).

10. S. A. Sterling, *A Temperature-Dependent Power Law for Monotonic Creep*, GA-A13027 (Rev), General Atomic Corp. San Diego, CA, June 1974, Revised March 1976.
11. *Creep Rupture Data & Documents Published*, Report 1976-09-21, Sandvik AB, Sandviken, Sweden, 1976.
12. L. Egnell, "Status Review of Alloy 800 Paper No. 21 Design Data," presented at the British Nuclear Energy Society Materials Conference, 25-26 September 1974.
13. L. Egnell and N. G. Persson, "Creep-Rupture Ductility of Alloy 800," paper presented at the *18eme Colloque de Metallurgie- Le nickel et son role specifique dans certains types d'alliage*, Saclay, France, June 23-25, 1975.
14. A. Plumtree and N-G. Persson, "Influence of γ' Precipitation on the Creep Strength and Ductility of an Austenitic Fe-Ni-Cr Alloy," *Metall. Trans.*
15. C. E. Sessions and P. J. McGeehan, "ASME & B&PV Code Recommendations of Design Stresses for Use of Annealed Alloy 800 in Elevated Temperature Nuclear Vessels," pp. 89 to 193 in *Status of Incoloy Alloy 800 Development for Breeder Reactor Steam Generators*, ORNL/Sub-4308/3, Oak Ridge National Laboratory, Oak Ridge, TN (December 1978).
16. Alloy 800 *Proceedings of the Petten International Conference*, Petten, The Netherlands, March 14-16, 1978.
17. N. G. Persson, "Mechanical Properties of Alloy 800 above 600°C, pp 135-149 in *Alloy 800*, North-Holland Publishing Company, 1978
18. M. K. Booker, V. B. Baylor, and B. P. L. Booker, *Survey of Available Creep and Tensile Data for Alloy 800H*, ORNL/TM-6029, Oak Ridge National Laboratory, Oak Ridge, TN (January 1978).
19. T. V. Schill, *INCOLOY Alloy 800 (Formerly Grade I) Annealed*, unpublished report from Huntington Alloys Inc. Huntington, WV, (March 1980).
20. K. Milička, "Internal Stress and Structure in Creep of Cold Prestrained Fe-21Cr-32Ni Alloy at 975 K," *Metal Science*, Vol. 16, September 1982, pp. 419-424.
21. "A Fourth Round Analysis of Alloy 800H Monotonic Allowable Stresses for Code Case N-47 Including Other Analyses," letter report J. B. Wattier to B. E. Thurgood, General Atomic Company, San Diego CA provided to the Working Group on Materials Behavior Subgroup on Elevated Temperature Design ASME Boiler & Pressure Vessel Committee, February 1982.

22. M. K. Booker, *Analysis of the Creep Strain-Time Behavior of Alloy 800*, ORNL/TM-8449, Oak Ridge National Laboratory, Oak Ridge, TN (May 1983).
23. P. W. Trester, W. R. Johnson, M. T. Simnad, R. D. Burnette, and D. I. Roberts, *Assessment of Effects of Fort St. Vrain HTGR Primary Coolant on Alloy 800*, EPRI NP-2548, Electric Power Research Institute, Palo Alto CA, (August 1982).
24. A. B. Smith, *Properties of Alloy 800H Tubesheet Forging*, General Atomic Company, San Diego, CA 1982.
25. J. F. King and H. E. McCoy, *Weldability and Mechanical Property Characterization of Weld Clad Alloy 800H Tubesheet Forging*, ORNL/TM-9108, Oak Ridge National Laboratory, Oak Ridge, TN (September 1984).
26. P. F. Aplin, *Alloy 800: Summary of the Accumulated Data*, ERA Report No: 85-0127, ERA Technology Ltd, Leatherhead, Surrey, UK (June 1985).
27. *Nuclear Technology*, Vol. 66, No. 1, July 1984
28. G. Sainfort, J. Sannier, M. Cappelaere, and J. Grégoire, "Mechanical Characterization of Metallic Materials for High-Temperature Gas-Cooled Reactors in Air and in Helium Environments," *Nuclear Technology*, Vol. 66, No. 1, July 1984, pp. 186-194.
29. K. S. Lee, "Creep Rupture Properties of Hastelloy-X and Incoloy-800H in a Simulated HTGR Helium Environment Containing High Levels of Moisture," *Nuclear Technology*, Vol. 66, No. 1, July 1984, pp 241-249.
30. F. Schubert, U. Bruch, R. Cook, H. Diehl, P. J. Ennis, W. Jakobeit, H. J. Penkalla, E. te Heesen, and G. Ullrich, "Creep Rupture Behavior of Candidate Materials for Nuclear Process Heat Applications," *Nuclear Technology*, Vol. 66, No. 1, July 1984, pp. 227-239.
31. G. R. Smolik and J. E. Flinn, *Behavior of Pressurized Incoloy 800H Tubes in Environments Pertaining to Coal Gasification*, EGG-MS-6852, Idaho National Engineering Laboratory, Idaho Falls, ID (May 1985).
32. N. G. Taylor, V. Guttmann, and R. C. Hurst, "The Creep Ductility and Fracture of Carburized Alloy 800H at High Temperatures," pp. 475-485 in *High Temperature Alloy*, Elsevier Applied Science, London, UK, 1985.
33. H. P. Degischer, H. Aigner, H. Lahodny, and K. Spiradek, "Qualification of Stationary Creep of the Carbide Precipitating Alloy 800H," pp. 487-498 in *High Temperature Alloy*, Elsevier Applied Science, London, UK, 1985.

34. D. H. Baldwin, O. F. Kimball, and R. A. Williams, *Design Data for Reference Alloys: Inconel 617 and Alloy 800H*, HTGR-041, General Electric Company, Sunnyvale, CA (April 1986).
35. H. E. McCoy, *Interim Report on Mechanical Properties Data Analysis of Low Carbon Alloy 800 in Support of ASME Code Case N-47 Code Stress Allowables (INCO and ERA Interim Data Sets)*, unpublished report, Oak Ridge National Laboratory, Oak Ridge, TN (April 1991).
36. P. McCarthy, *Alloy 800 Data Presentation*, Technical Note P/A2/87/13, ERA Technology Ltd, Leatherhead, Surrey, UK, (December 1985).
37. H. Diehl and E. Bodmann, “Alloy 800 Specifications in Compliance with Component Requirements,” *Journal of Nuclear Materials*, Vol. 171 (1990) 63-70.
38. H. E. McCoy, *Use of the MCM for Analysis of Alloy 800H Rupture Data*, ORNL/TM-12430, Oak Ridge National Laboratory, Oak Ridge, TN (September 1993).
39. H. E. McCoy, *Tensile and Creep Tests on a Single Heat of Alloy 800H*, ORNL/TM-12436, Oak Ridge National Laboratory, Oak Ridge, TN (September 1993).
40. R. W. Swindeman, Unpublished Work in the Metals and Ceramics Division, Oak Ridge National Laboratory, Oak Ridge, TN 1992.
41. E. El-Magd, G. Nicolini, and M. Farag, “Effect of Carbide Precipitation on the Creep Behavior of Alloy 800HT in the Temperature Range 700°C to 900°C,” *Metallurgical and Materials Transactions*, Vol. 27A March 1996, 747-756.
42. *Data Sheets on the Elevated-Temperature Properties of Iron Based 21Cr-32Ni-Ti-Al Alloy for Heat Exchanger Seamless Tubes (NCF 800H TB)*, NRIM Creep Data Sheet No. 26B, National Research Institute for Metals, Sengen, Tsukuba-shi, Ibaraki, Japan (September 1998).
43. *Data Sheets on the Elevated-Temperature Properties of Iron Based 21Cr-32Ni-Ti-Al Superalloy for Corrosion-Resisting and Heat-Resisting Superalloy Plates (NCF 800H-P)*, NRIM Creep Data Sheet No. 27B, National Research Institute for Metals, Sengen, Tsukuba-shi, Ibaraki, Japan (March 2000).
44. *Long-Term Creep Rupture Data Obtained After Publishing the Final Edition of the Creep Data Sheets*, NMIS Creep Data Sheet No. 50, National Institute for Materials Science, Sengen, Tsukuba-shi, Ibaraki, Japan (March 2004).

45. *Data Sheets on the Elevated-Temperature Stress Relaxation Properties of Iron Based 21Cr-32Ni-Ti-Al Alloy for Corrosion-Resisting and Heat-Resisting Superalloy Bar (NCF 800H-B)*, NIMS Creep Data Sheet No. 47, National Institute for Materials Science, Sengen, Tsukuba-shi, Ibaraki, Japan (March 1999).
46. L. H. Sjodhal, A Comprehensive Method of Rupture Data Analysis With Simplified Models, pp. 501-516 in *Characterization of Materials for Service at Elevated Temperatures*, MPC-7, American Society of Mechanical Engineers, New York NY, 1978.
47. M. Prager, "Proposed Implementation of Criteria for Assignment of Allowable Stresses High in the Creep Range, pp 273-293 in *Structural Integrity, NDE, Risk and Material Performance for Petroleum, Process and Power*, PVP-Vol. 336, American Society of Mechanical Engineering, New York, NY 1996.
48. M. K. Booker, "An Analytical Representation of the Creep and Creep-Rupture Behavior of Alloy 800H," pp. 1-27 in *Characterization of Materials for Service at Elevated Temperatures*, MPC-7, American Society of Mechanical Engineers, New York NY 1978.
49. S. S. Manson and U. Muralidharan, "Analysis of Creep Rupture Data for Five Multiheat Alloys by the Minimum Commitment Method Using Double Heat Centering," pp. 1-6 in *Progress in Analysis of Fatigue and Stress Rupture*, MPC-23, American Society of Mechanical Engineers, New York NY 1984.
50. J. J. Pepe, *Materials Property Data: Applications and Access*, PVP 111, American Society of Mechanical Engineers, New York NY 1986.
51. R. A. McFarlane and G. Baylac, "Creep Design Rules Proposed for EN 13445," pp. 161-166 in *Pressure Vessel Technology 2003*, Grafisches Zentrum an der Technischen Universität Wien, Austria, 2003.

A REVIEW OF AVAILABLE TENSILE AND CREEP-RUPTURE DATA SOURCES
AND DATA ANALYSIS PROCEDURES FOR DEPOSITED WELD METAL AND
WELDMENTS OF ALLOY 800H

Robert W. Swindeman

Cromtech Inc

Oak Ridge, TN 37830

Michael J. Swindeman

University of Dayton Research Institute

Dayton, OH 45469

Blaine W. Roberts

BW Roberts Consultants

Chattanooga, TN 37416

Brian E. Thurgood

Bpva Engineering

San Diego, CA 92131

Douglas L. Marriott

South Lebanon OH

August, 2007

ABSTRACT

Databases summarizing the tensile and creep-rupture properties of deposited weld metal and weldments for alloy 800H were reviewed and referenced. Procedures for analyzing creep-rupture data for temperatures of 750°C (1382°F) and higher were reviewed and used to estimate the weld strength reduction factors (SRFs) as a function of time and temperature for temperatures to 900°C (1650°F). The database was judged to be inadequate to meet the needs for the extension of the use of filler metal for alloy 800H in ASME Section III Subsection NH to 900°C (1650°F). Five appendices were included that 1) listed the data used in the evaluation of the SRFs, 2) provided the values for parametric constants in the models, 3) provided an example of the calculated SRFs for alloy 82, 4) recommended supplemental creep-rupture testing to expand the database and improve the estimation of SRFs for long-time service, 5) provided a summary of a parametric Finite Element Analysis (FEA) study of cross-weld samples.

INTRODUCTION

A two-year collaborative effort has been established between the Department of Energy (DOE) and the American Society of Mechanical Engineers (ASME) to address technical issues related to codes and standards applicable to the Generation IV Nuclear Energy Systems Program [1]. A number of tasks have been identified that will be managed through the ASME Standards Technology, LLC (ASME ST-LLC) and involve significant industry, university, and independent consultant activities. Task 1 in this effort has several goals. The first goal is to assess the status of the databases for alloy 800H and its weldments and identify the data needed, if any, to extend the ASME Section III-NH coverage of alloy 800H to 900°C (1650°F) for service life for times approaching 600,000 hours. The second goal is to review the database for grade 91 steel and its weldments and identify the data needed, if any, to provide confidence that the steel will meet the performance requirements for service to times approaching 600,000 hours. Task 1 is primarily concerned with Code criteria related to tensile and creep rupture properties. Other tasks in the DOE-ASME project address cyclic service conditions. This report is the fourth in a series of reports that concerned alloy 800H [2-4]. The first three addressed the tensile, stress-rupture, and creep databases for alloy 800H. This report reviews the database for deposited weld metal and weldments.

IDENTIFICATION OF MATERIALS

Alloy 800H is one of three classes (or “grades”) of 33Ni-42Fe-21Cr alloy that are listed in ASME Section II and approved for construction of pressure boundary components. The three grades are identified as UNS N08800, UNS N08810, and UNS N08811 for alloy 800, alloy 800H, and alloy 800HT, respectively. Alloy 800 (N0880) corresponds to a relatively fine-grained annealed condition normally used at lower temperatures where creep strength is not an important consideration. Alloy 800H (N08810) corresponds to a relatively coarse-grained material (ASTM grain size number 5 or greater) with a carbon range of 0.05 to 0.10% which is typically annealed around 1150°C (2175°F). This material is approved for construction to 982°C (1800°F) under the rules of ASME Section VIII. Alloy 800HT (N08811) requires carbon to be at least 0.06%, the aluminum plus titanium to be in the range of 0.85 to 1.2%, and the annealing temperature to be at least 1149°C (2150°F). This stronger version of alloy 800H is used when creep strength is important and relaxation cracking is not of great concern. Other variations of alloy 800 exist in the German Code KTA 3221.1 [5], and these are described briefly in an earlier report [2]. Only alloy 800H is permitted under the rules in ASME III-NH and an additional restriction requires the Al+Ti content to be in the range of 0.4 to 1.2%. The specific grade of base metal and its associated properties are important considerations in this review which includes the data produced on weldments that may rupture in the base metal heat affected zone or the base metal itself.

Typical base metal chemistries are provided in Table 1. Included are three ASTM grades, three DIN grades, and one Japanese grade.

Table 1. Comparison of chemistries for variants of alloy 800

| Element | ASME | ASME | ASME | DIN | DIN | DIN | JIS-G-4904 | | |
|-----------------|-----------|-----------|-----------|------------|-------------|--------------|---------------|---------------|--------------|
| | N08800 | N08810 | N08811 | <u>800</u> | <u>800H</u> | <u>800HT</u> | <u>800 DE</u> | <u>800 Rk</u> | <u>800 H</u> |
| Ni | 30.0-35.0 | 30.0-35.0 | 30.0-35.0 | 30.0-32.5 | 30.0-32.5 | 30.0-34.0 | 30.0-35.0 | | |
| Cr | 19.0-23.0 | 19.0-23.0 | 19.0-23.0 | 19.0-22.0 | 19.0-22.0 | 19.0-22.0 | 19.0-22.0 | 19.0-23.0 | |
| Fe | 39.5 min | 39.5 min | 39.5 min | Bal | Bal | bal | | | |
| C | 0.10 max | 0.05-0.10 | 0.06-0.10 | 0.03-0.06 | 0.03-0.08 | 0.05-0.10 | 0.05-0.10 | | |
| Mn | 1.50max | 1.50 max | 1.50 max | <1.5 | <1.5 | <1.5 | 1.50 max | | |
| S | 0.015 max | 0.015 max | 0.015 max | <0.010 | <0.010 | <0.010 | 0.015 max | | |
| Si | 1.0 max | 1.0 max | 1.0 max | <0.70 | <0.70 | <0.70 | 1.0 max | | |
| Cu | 0.75 max | 0.75 max | 0.75 max | <0.15 | <0.45 | <0.45 | 0.75 max | | |
| Al | 0.15-0.60 | 0.15-0.60 | 0.15-0.60 | 0.15-0.40 | 0.20-0.50 | 0.40-0.75 | 0.15-0.60 | | |
| Ti | 0.15-0.60 | 0.15-0.60 | 0.15-0.60 | 0.20-0.40 | 0.20-0.50 | 0.25-0.65 | 0.15-0.60 | | |
| Al+Ti | | | 0.85-1.20 | <0.60 | <0.70 | | | | |
| P | | | | <0.015 | <0.015 | <0.015 | | | |
| N | | | | <0.03 | <0.03 | <0.03 | | | |
| Co | | | | <0.02 | <0.45 | <0.45 | | | |
| Nb | | | | <0.1 | <0.1 | | | | |
| ASTM GS No. | ≤5 | ≤5 | | | | | ≤5 | | |
| Euronorm 103 GS | | | | 3 to 7 | 1 to 5 | 1 to 5 | | | |

A number of filler metals have been used for joining similar and dissimilar metal welds with alloy 800H. Some compositions are listed in Table 2 for coated electrodes for shielded metal arc welding (SMAW) included in the AWS 5.11 specification. Only one of these filler metals, alloy A (ENiCrFe-2), is permitted in ASME III-NH, according to Table I-14.1(b), and Table I-14.10 C-1 provides stress factors for the bare electrode equivalent (ENiCrFe-2) used for SMAW. The database reviewed here includes alloy 132, alloy A, alloy 617, and 21/33/Nb which is considered to be a matching filler metal for alloy 800H. Emphasis is on alloy A.

Table 2. Comparison of chemistries for coated filler metal electrodes

| Element | alloy 132 ENiCrFe-1 (W86132) | alloy A ENiCrFe-2 (W86133) | alloy 182 ENiCrFe-3 (W86182) | alloy 617 ENiCrCoMo-1 (W86117) | 21/33/Nb |
|---------|------------------------------------|----------------------------------|------------------------------------|--------------------------------------|-----------|
| C | 0.08 max | 0.10 max | 0.10 max | 0.05-0.15 | 0.06-0.12 |
| Mn | 3.5 max | 1.0-3.5 | 5.0-9.5 | 0.3-2.3 | 1.6-4.0 |
| Fe | 11.0 max | 12.0 max | 10.0 max | 5.0 max | Rem |
| P | 0.03 max | 0.03 max | 0.03 max | 0.03 max | 0.03 max |
| S | 0.015 max | 0.02 max | 0.015 max | 0.015 max | 0.02 max |
| Si | 0.75 max | 0.75 max | 1.0 max | 0.75 max | 0.6 max |
| Cu | 0.50 max | 0.50 max | 0.50 max | 0.50 max | - |
| Ni | 62.0 min | 62.0 min | 59.0 min | Rem | 30.0-35.0 |
| Co | - | 0.12 max* | 0.12 max* | 9.0-15.0 | - |
| Ti | - | - | 1.0 max | - | - |
| Cr | 13.0-17.0 | 13.0-17.0 | 13.0-17.0 | 21.0-26.0 | 19.0-23.0 |
| Nb | 1.5-4.0 | 0.5-3.0 | 1.0-2.5 | 1.0 max | 0.08-1.5 |
| Mo | - | 0.5-2.5 | - | 8.0-10.0 | 0.5 max |

Notes: * Co 0.12 max when specified by purchaser; max for other elements is 0.50.

Compositions for bare filler metal electrodes (SFA-5.14) are listed in Table 3. Only ERNiCr-3 (alloy 82) is permitted for use by ASME III-NH, according to Table I-14.1(b), and Table I-14.10 C-2 provides stress factors for joints with this alloy.

Table 3. Comparison of chemistries for bare filler metal electrodes

| Element | alloy 82 ERNiCr-3 (N06082) | alloy 617 ERNiCrCoMo-1 (N06617) |
|---------|----------------------------------|---------------------------------------|
| C | 0.10 max | 0.05-0.15 |
| Mn | 2.5-3.5 | 0.3-2.3 |
| Fe | 3.0 max | 5.0 max |
| P | 0.03 max | 0.03 max |
| S | 0.015 max | 0.015 max |
| Si | 0.50 max | 0.75 max |
| Cu | 0.50 max | 0.50 max |
| Ni | 67.0 min | Rem |
| Co | 0.12 max* | 9.0-15.0 |
| Ti | 0.75 max | - |
| Cr | 18.0-22.0 | 21.0-26.0 |
| Nb | 2.0-3.0 | 1.0 max |
| Mo | - | 8.0-10.0 |

Notes: * Co 0.12 max when specified by purchaser;
max for other elements is 0.50.

REVIEW OF DATABASES FOR DEPOSITED FILLER METALS AND WELDMENTS

Early data on filler metals and weldments used for alloy 800 and nickel base alloys were summarized in *The Elevated-Temperature Properties of Weld-Deposited Metal and Weldments* (ASTM STP No. 226) [6]. Pages 154 to 170 of the report provided McBee-type data sheets for a number of filler metals. Two data sheets are provided for alloy 132 deposited filler metal. Two data sheets are provided for alloy 132 filler metal in alloy 800H plates. The results of short-time stress-rupture testing were given for testing in the temperature range of 760 to 982°C (1400 to 1800°F). Most weldment ruptures occurred in the weldment fusion line.

York and Flury performed a literature search for a suitable filler metals for alloy 800 and selected Incoloy 88 & 182 filler metals for joining alloy 800 [7]. It was reported that weldments from the two filler metals exhibited similar tensile and creep-rupture properties for temperatures less than 649°C (1200°F). Tensile data to 760°C (1400°F) and creep data to 649°C (1200°F) were provided. This work was in support of the fast-breeder reactor (FBR) program which had a need for a steam generator operating at less than 649°C (1200°F).

Klueh and King investigated the elevated tensile properties of ERNiCr-3 weld metal [8]. Tensile data on deposited alloy 82 filler metal to 732°C (1350°F) were reported. Again, this work was in support of the FBR program needs.

King and Reed investigated the weldability of alloy 800 [9]. They examined the hot cracking tendencies of seven heats of alloy 800 with varying carbon, aluminum, and titanium contents. The ratio (Al+Ti)/(C+Si) was found to be a reasonable predictor of cracking behavior in the Tigmajig test. No tensile or creep data were gathered.

Further studies by Klueh and King in support of the FBR program were published in 1978 and 1979 and included creep and stress-rupture behavior of ERNiCr-3 weld metal [10, 11]. Data for deposited alloy 82 filler metal were reported to 732°C (1350°F).

Sartory required a creep law for an inelastic \square atcheting analysis of a 2 1/4Cr-1 Mo steel pipe joined to type 316H stainless steel using alloy 82 filler metal [12, 13]. The creep law was developed and revised from test data on coupons machined from a dissimilar metal weld test article. Data were in the range of 510 to 566°C (950 to 1050°F).

Booker and Strizak produced cyclic data on weld-deposited alloy 82 at 649°C (1200°F) [14]. Hold times at constant stress were introduced in tensile or compression and strains were reversed by strain-rate control to produced creep reversed by plasticity or plasticity reversed by creep. Tests were also performed with creep reversals in both tension and compression. No effort was made to develop expressions for the creep behavior.

Klueh and King examined the thermal aging behavior of alloy 82 weld metal and weldments [15]. Aging was performed at 510 and 566°C (950 and 1050°F). Tensile testing was performed to 677°C (1250°F) and creep-rupture tests to 566°C (1050°F).

Nippon-Kokan (NKK) reported the properties of Tempaloy 800H tubes welded with matching filler metal and alloy 82 [16]. Information included composition, microstructures, cross weld hardness, and tensile properties for as-welded and solution-annealed weldments in 11-mm plates. The tensile data indicated higher yield strengths than for base metal for the as-welded cross-weld samples for temperatures to 1000°C (1832°F) but the same ultimate strength. No stress-rupture data for weldments are provided.

Data for pressurized alloy 800H tubes containing butt welds were reported by Stannett and Wickens [17]. Alloy 82 and 182 fillers were used. Testing was at 550 and 700°C (1022 to 1292°F). All tube burst failures occurred in the base metal.

In 1982, Klueh and J. F. King examined the elevated-temperature tensile and creep-rupture behavior of alloy 800H/ERNiCr-3 Weld Metal/2 1/4Cr-1Mo steel dissimilar-metal weldments [18]. Creep-rupture data extended to 732°C (1350°F).

McCoy and King investigated the tensile and creep-rupture properties of weld-deposited alloy A (EniCrFe-2) and alloy 82 filler metal and weldments including alloy 800H and Hastelloy X [19]. Tensile data on deposited alloy A weld metal went from 23 to 871°C (70 to 1600°F) and creep rupture data were gathered from 482 to 760°C (900 to 1400°F). Tensile and creep-rupture data for weldments were produced to 649°C (1200°F) for both filler metals. Testing data for aged weldments were included.

Lindgren, Thurgood, Ryder, and Li reviewed the mechanical properties of welds in commercial alloys for high-temperature gas-cooled reactor components in 1984 [20]. They presented creep-rupture data for several filler metals and weldments used for joining alloy 800H and dissimilar metal tubes or pipes. Included were alloy 88 and alloy 188, alloy 82 and alloy 182. Plots of stress-rupture behavior were shown for temperatures to 760°C (1400°F).

In the same issue of *Nuclear Technology*, Bassford and Hosier discussed the production and welding technology of some high-temperature nickel alloys and provided guidance and data for welding alloy 800H for applications up to 790°C (1450°F) [21]. Stress-rupture data for all-weld metal were tabulated for alloy A and alloy 82 to 982°C (1800°F).

Schubert, Bruch, Cook, Diehl, Ennis, Jakobeit, Penkalla, te Heesen, and Ullrich reviewed the creep-rupture behavior of candidate materials for nuclear process heat applications [22]. The paper provided one figure that plotted stress versus rupture life for alloy 82 and a 21/33/Nb at 850 and 950°C (1575 and 1650°F). The alloy 82 weld metal was weaker than average strength alloy 800H while the 21/33Nb matching filler metal appeared to have strength comparable to the base metal.

King and McCoy reported on the weldability and mechanical property characterization of weld-clad alloy 800H tubesheet forging. Tensile properties were provided for Inconel 82 weld-deposited cladding for temperatures to 649°C (1200°F) [23]. Data were gathered for composite and base metal samples over the same temperature range. Failure locations at 649°C (1200°F) often occurred at the weld interface.

In 1986, an INCO brochure provided a table for the stress-rupture for strength of alloy A and alloy 82 for temperatures in the range of 538 to 982°C (1000 to 1800°F) and times to 10,000 hours [24]. Also, a figure was provided for the stress-rupture of deposits from welding electrode 117 in comparison to alloy 800HT for temperatures in the range of 649 to 982°C (1200 to 1800°F) and time to 10,000 hours. About the same time, Bassford, provided tensile and stress-rupture data for alloy 117 and alloy 112 deposited weld metal and cross welds in alloy 800H [25]. Temperatures ranged to 1093°C (2000°F).

A Survey and Guidelines for High Strength Superheater Materials- Alloy 800H was compiled for the Electric Power Research Institute in 1987 [26]. This report included a “steel maker’s search on alloy 800H” by three participants: Sumitomo Metal Industries, Ltd., Nippon Steel Corp., and Nippon Kokan K. K (NKK). The reviews drew heavily on the studies of alloy 800H that were performed in support of the high-temperature gas-cooled reactor programs (in the US, UK, and Germany) and the fast breeder reactor programs in the US. In the summary section, plots for tensile data were supplied that were constructed from seven sources and ranged to 1100°C (2000°F). Several filler metals including alloys 82 and 182 were listed and both deposited metal and joint configurations were included. Stress-rupture data were provided as a stress versus Larson Miller parameter plots. Again, both deposited metal and joint data were included. However, the data did not appear to be original data but rather were derived from processed curves or tables. The review by Sumitomo Metal Industries, Ltd. Was the most extensive with respect to filler metals. Of the 193 references, there were 32 references that addressed weld metal and weldment issues. About 14 of these references reported mechanical behavior such as tensile or creep-rupture properties. About half of these were of Japanese origin. Figures were provided that were reproduced from many of these references.

McCoy produced tensile and creep test data for a heat of alloy 800H in 1993. Data for deposited alloy 82 weld metal and weldments were provided [27, 28]. Tensile data ranged to 871°C (1600°F) and creep-rupture data range to 816°C (1500°F).

DATA ANALYSIS

The materials data for base metals currently provided in ASME Section II that are applicable to Section III-NH include physical properties (Tables TE-1 through TE-5, Tables TCD, Tables TM-1 through TM-4, and Tables NF-1 and NF-2), short-time tensile properties (Table U, Table Y-1), buckling charts, and design stress intensity values (Tables 2A, 2B, and 4) corresponding to criteria identified in Appendix 2 of Section II. Section III-NH provides additional materials data in the tables of Appendix 1-14. For

purposes of high-temperature design, Section III-NH includes an extension of the tensile strength values (Table NH-3225-1) and the yield strength values (Table I-14.5), maximum allowable stress intensity values (Table I-14.2), allowable stress intensity values as a function of temperature and time (Tables I-14.3 and I-14.4), expected minimum stress-to-rupture tables (Table I-14.6), stress-rupture factors for weldments (Table I-14.10), design fatigue tables (Fig. T-1420-1), creep-fatigue damage envelopes (Fig. T-1420-2), creep-buckling charts (Fig. T-1522), and isochronous stress versus strain curves (T-1800) in Appendix 1-14 and Appendix T. For alloy 800H, the coverage extends to 760°C (1400°F) and for times to 3×10^5 hours. Fatigue curves extend to 10^6 cycles. The effects of service-aging on the yield strength and ultimate strength are included (NH-2160 and Table NH-3225-2). The Section III Code Case N201-4 contains data tables and figures that are intended to be consistent with Section III-NH. No data for deposited filler metals or weldments are provided in either Section II or Section III-NH. Instead, the stress-rupture factors for weldments are provided for some combinations of base metals and filler metals. Stress-rupture factors for weldments with alloy A (ENiCrFe-2) welds and alloy 82 (ERNiCrFe-3) joining alloy 800H are provided in Table I-14.10, as mentioned above. Values for the factors range from 1.0 to 0.59 for alloy A over the temperature range from 427 to 760°C (800 to 1400°F) and from 1.0 to 0.54 for alloy 82.

Over the years, the methods of data analysis needed to produce the tables and charts in ASME Sections II, III, and III-NH have evolved and will continue to evolve. The procedures for establishing the Section II Table 1A and 1B allowable stresses were reviewed in prior reports on this project (2-4). Also, the Section II procedures for determining the Y-1 and U values were reviewed earlier [2]. Methods for extending the S_{YI} and S_U values in Section III-NH to 900°C (1650°F) were recommended [2]. Section II procedures for establishing time-dependent allowable stresses were reviewed [3,4]. At present, however, there is no well-established procedure for determining the values for the stress-rupture factors (SRFs) for weldments provided in Section III-NH. In the case of the austenitic alloys, the SRFs have been based on the ratio of the deposited weld metal strength to the base metal strength for the specific temperatures and times provided in the stress factor table. To some extent, the weldment strength has been “considered” in establishing these ratios, but it has not been established whether small cross-weld specimen data should be included in the analysis that determines the strength ratios. In this report, deposited filler metal and weldment data will be treated separately sometimes and together at other times. Although tensile properties of weldments are not considered in the Section III-NH, the available properties are discussed below and compared to base metal properties. Then the stress-rupture properties will be compared to base metal.

Tensile data:

Procedures for analyzing the base metal tensile data to produce S_{YI} and S_U values were outlined previously [2]. The analysis makes use of a trend curve based on the ratio of elevated temperature strength to the room temperature strength as a function of temperature [29, 30]. Since few tensile data exist for the deposited weld metals, a trend curve for weld metal is of limited value in a statistical sense, but a comparison of the weld data or weldment data with the base metal trend curve enables an estimate of the

similarity or difference in short-time behavior. In this report, however the comparison will be between the available weld metal data and curves constructed from the Y-1 and recommended S_{YI} values for yield behavior and the U and recommended S_U values for the ultimate tensile strength.

Figure 1 compares the yield strength for alloy A weld metal with alloy 800H. The curve for alloy A was developed by INCO [24] while the datum points were obtained from McCoy and King [19]. The alloy 800H curve represents the Y-1 and S_{YI} trend curve anchored to the minimum specified room-temperature yield strength for alloy 800H (172 MPa). The average yield strength curve would be anchored to 225 MPa at room temperature [2]. It is clear that alloy A weld metal in the as-deposited condition is much stronger than alloy 800H. The same is true for the U and S_U trend curve as may be seen in Figure 2.

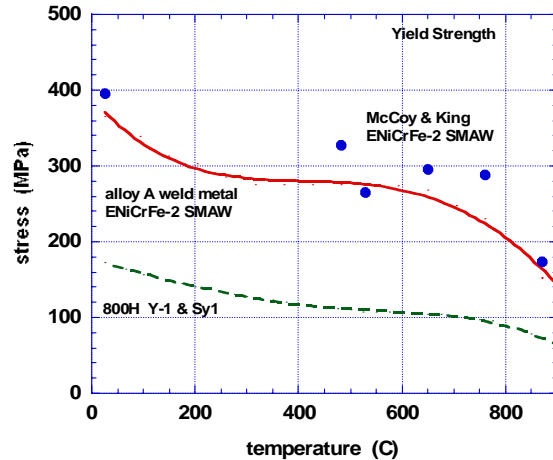


Fig. 1. Comparison of the yield strength for alloy A weld metal with alloy 800H

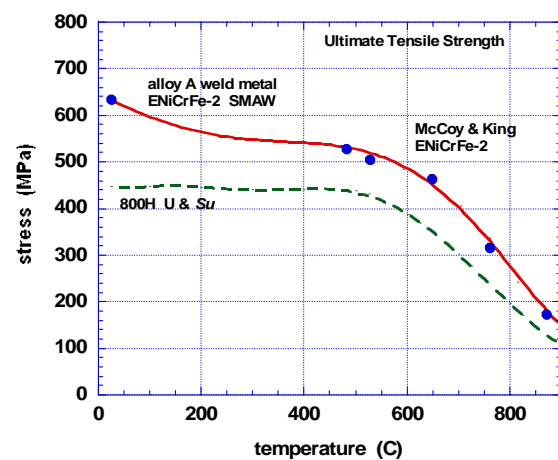


Fig. 2. Comparison of the tensile strength for alloy A weld metal with alloy 800H

Figures 3 and 4 provide data for the 21/33Nb filler metal with the Y-1 and S_{YI} trend curve curve and the U and S_U trend curve for alloy 800H base metal. Also included are the trend curves for alloy A developed by INCO. Here, it may be seen that the 21/33Nb weld metal produces slight higher yield strengths than alloy A but similar ultimate tensile strengths.

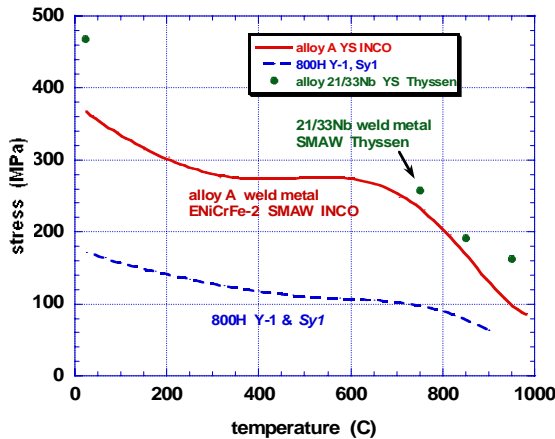


Fig. 3. Comparison of the yield strength for 21/33Nb weld metal with alloy 800H and alloy A weld deposit.

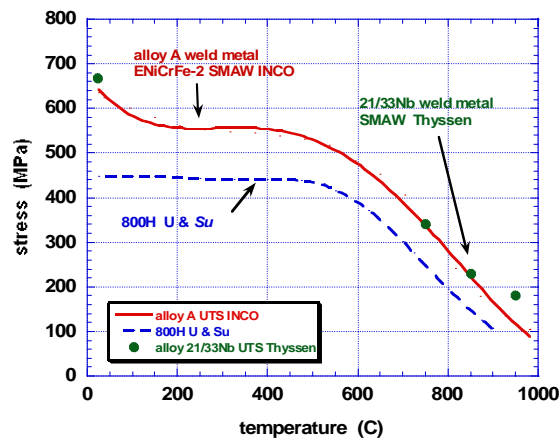


Fig. 4. Comparison of the tensile strength for 21/33NB weld metal with alloy 800H and alloy A weld deposit

Figures 5 and 6 show comparisons the strength of alloy 617 filler metal deposits with alloy A and alloy 800H. The tensile yield and ultimate strengths of deposits from the alloy 117 electrodes are much stronger than alloy A and alloy 800H. The material is clearly “overmatched” in strength with alloy 800H from this aspect.

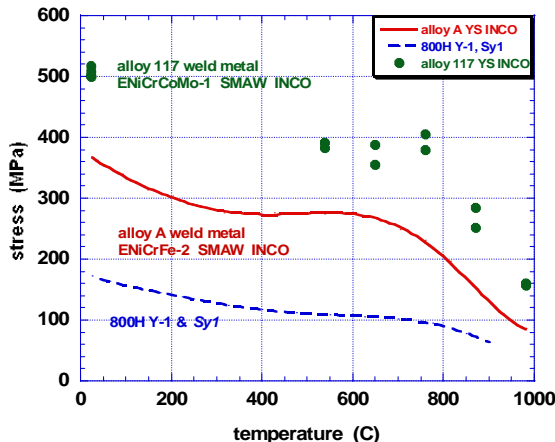


Fig. 5 Comparison of the yield strength for alloy 117 weld metal with alloy 800H

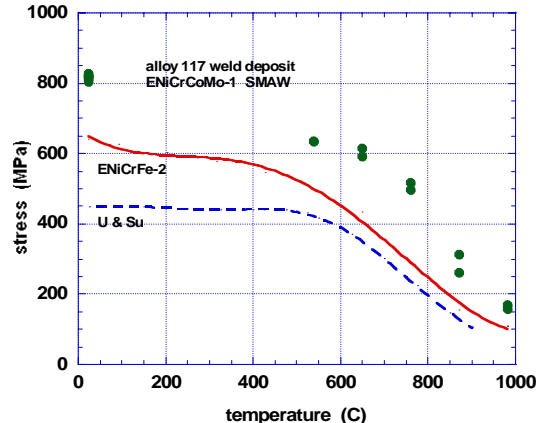


Fig. 6. Comparison of the tensile strength for alloy 117 weld metal with alloy 800H

Strength curves for the weld metal produced by the alloy 82 wire (ERNiCrFe-3) are shown in Figure 7 and 8 where they may be compared to data for the alloy 182 electrode and alloy 800H base metal. The INCO curves indicate that the weld metal deposited from the alloy 82 wire has slightly more strength than weld metal deposited from alloy 182 electrodes. The strengths of both weld metals are roughly comparable to alloy A

weld metal. Typical data produced on alloy 82 weld metal are shown in Figures 9 and 10. Yield strength data for four lots extracted from the literature exhibit considerable scatter and generally fall below the curve developed by INCO. Yield strength data remain well above the $Y-1$ and S_{y1} strength curves for alloy 800H. Ultimate tensile strength data for alloy 82 weld metal generally fall below the curve developed by INCO but are above the U and S_U strength curves for alloy 800H.

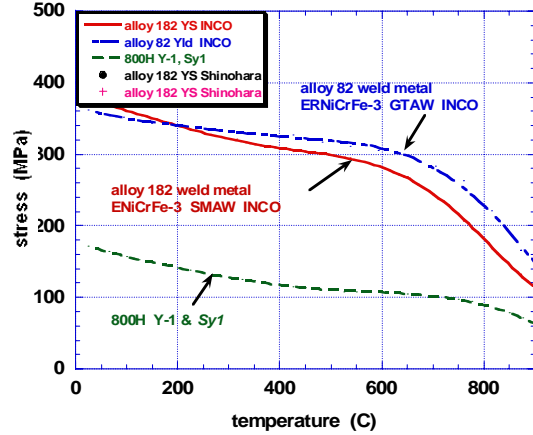


Fig. 7. Comparison of the yield strengths of SMA and GTA weld metals

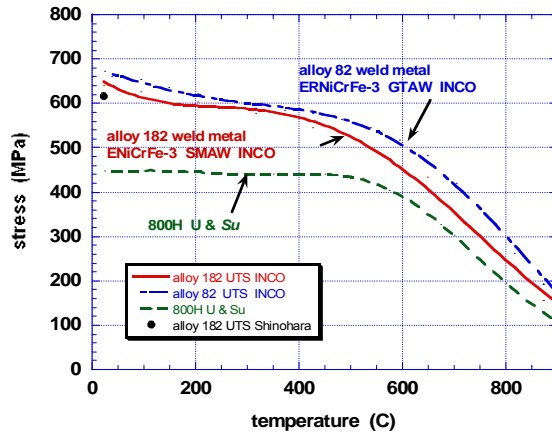


Fig. 8. Comparison of the tensile strengths of SMA and GTA weld metals.

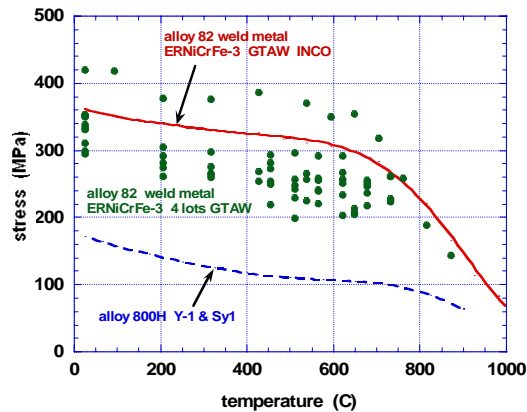


Fig. 9. Comparison of the yield strength for alloy 82 weld metal with alloy 800H

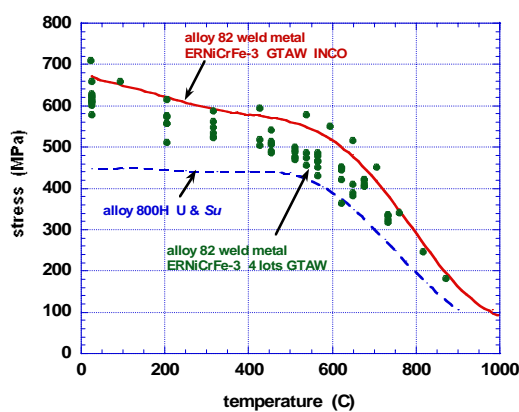


Fig. 10. Comparison of the tensile strength for alloy 82 weld metal with alloy 800H

Weldment data are shown in Figures 11 and 12. Filler metals include alloy A, alloy 182, alloy 112, alloy 117, and alloy 82. Typically, the higher yield strengths of the filler metals boost the yield strength of the weldments over that of the base metal (alloy 800H). The weldments, however, have lower yield and ultimate tensile strengths than the weld metals. Failures occur in the alloy 800H base metal somewhat removed from the fusion line for some filler metals but near the fusion line for other filler metals.

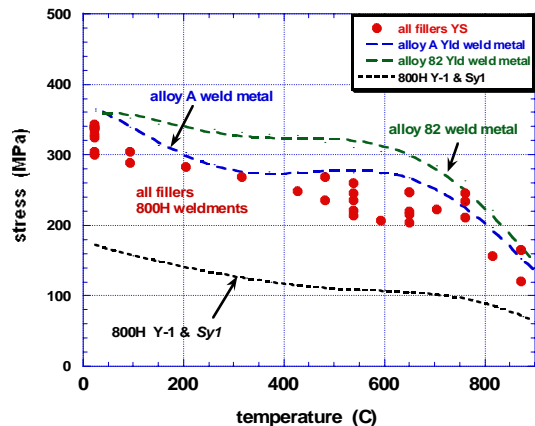


Fig. 11. Comparison of weldment yield strength with alloy 800H base metal

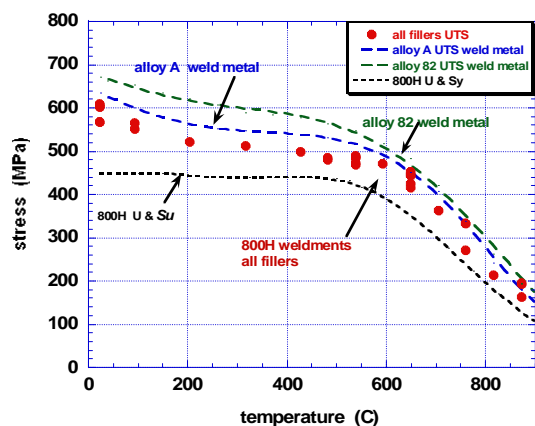


Fig. 12. Comparison of weldment tensile strength with alloy 800H base metal

With respect to extending ASME Section III-NH to 900°C (1650°F) for alloy 800H, additional tensile testing of filler metals is needed to more clearly define tensile data in the temperature range from 750 to 900°C (1382 to 1650°F).

Assembly of the Stress-Rupture Database:

In an earlier section of this report, the sources for stress-rupture data on filler metals for joining alloy 800H were reviewed. The bulk of the data in these sources was developed from programs focused on components intended for operation below 750°C (1382°F). These data were used to develop the Stress Rupture Factors (SRFs) in ASME Section III-NH Tables I-14-10 C-1 and C-2. However, it was the intent of this report to collect and evaluate the data needed to extend coverage in the tables to longer times and 900°C (1650°F). It was not intended that the current SRFs be changed, hence data below 750°C (1382°C) were assembled but only data for 732°C (1350°F) and higher were included in the analyses. Data tables are summarized in Appendix 1. The tabulated data were extracted from tables in reports, when possible, but some data were extracted from plots in papers and reports. These data lacked the precision and accuracy that was desired, but considering the overall lot-to-lot variability were considered to be better than no data at all. Since ASME III-NH only provides SRFs which are based on stress-rupture behavior, data bearing on other aspects of the time-dependent behavior of filler metals, such as time to 1% creep and the time to the initiation of tertiary creep, were not collected. Data for several types of filler metals were included. These filler metals are listed in Table 2 and Table 3 of this report. Alloy 132 (ENiCrFe-1) was an exception, and data for this filler metal were not included in Appendix 1.

Procedure for Determining the Stress Reduction Factors:

The SRFs provided in ASME III-NH have been defined as the ratios of the strength of the weldment to the strength of the base metal for the specific temperature and time at which the ratio was determined. It is assumed that the ratios were based on the average strengths of the weldment and base metal, not the minimum strengths. In actual practice, the SRFs for the austenitic stainless steels such as types 304H and 316H, were based on the ratios of the strength of the deposited filler to the strength of base metal. These strengths were obtained from the testing of coupons extracted from the deposited weld metals and base metals, but data from cross-weld test coupons and “full-thickness” weldment tests were used to validate the SRFs or make adjustments to the values. Little or no testing was performed on full-thickness weldments of alloy 800H, hence the analytical procedures for determining the SRFs involved the analysis of data from samples extracted from deposited filler metal and taking the ratios with respect to the average strength of the 800H base metal reported earlier [3].

The procedures used to determine the average and minimum rupture strength values for the ASME III-NH have not been standardized. In some instances reports and open literature publications provide information on this topic, but, for the effort reported here, a procedure similar to that adopted by ASME Section II was followed. This was based on the use of the Larson-Miller temperature-time parametric correlation method that assumed a stress-dependent activation energy. Thus:

$$(1/t_R) = A \exp[-f_l(S)/RT] \quad (1)$$

Where t_R is the rupture life, A is a constant, $f_l(S)$ is a function of stress, R is the universal gas constant, and T is absolute temperature. Taking the log to base ten and rearranging produces the familiar Larson Miller parameter (LMP):

$$LMP = T (C + \log t_R) = f_l(S)/2.303R \quad (2)$$

Where C is $\log A$ and identified as the Larson-Miller parametric constant.

Typically, a stress function $f(S)$ is formulated as a polynomial in log stress:

$$f(S) = f_l(S)/2.303R = a_0 + a_1 \log S + a_2 (\log S)^2 + a_3 (\log S)^3 + \dots \quad (3)$$

where a_i is a series of constants that depend on the number of terms in the polynomial. Using a least squares fitting method in which $\log t_R$ is the dependent variable and T and $\log S$ are independent variables, the optimum values for C and a_i are determined. Although not explicitly required by Appendix 1 of ASME Section II-D, the consultants may employ a “lot-centered” procedure developed by Sjodahl that calculates a lot constant (C_h) for each lot along with the Larson-Miller constant, C , which represents the average lot constant (C_{ave}) for the lots [29]. However, only C_{ave} is used to determine the S_{Rave} . To determine S_{Rave} , eq. (2) needs to be solved for S at 100,000 hours. Although the lot constants, variants within a lot, variants between lots, and SEE of the $\log t_R$ can be

produced in the analytical procedure, it is important to recognize that the ASME II-D does not explicitly provide such information. Both the global and lot-centered fitting procedures were used for alloy A and alloy 82. Only the global procedure was used for other candidates.

Qualitative Evaluation of the Strength of Weld Metal and Weldments Relative to 800H:

Figures 13 through 18 compare stress-rupture data for weld metal and weldments with the trend for alloy 800H on the basis of the Larson Miller parameter. Here, the alloy 800H parametric curve is given by the parametric constant, C, 15.12487 and the following coefficients for the stress function, $f(S)$, of equation (3):

$$a_0 = 29648.78$$

$$a_1 = -7334.877$$

$$a_2 = 1903.854$$

$$a_3 = -619.4775.$$

The comparisons for alloy A (ENiCrFe-2) are shown in Figure 13 for weld metal and Figure 14 for weldments. As may be seen, the data are few but define a trend for weld metal and weldments. For low values of the Larson Miller parameter (LMP) welds and weldments appear to be stronger than base metal and SRF should be 1.0. At 750°C (1382°F), the pointers in the figures indicate that the SRF at 100,000 h should be less than 1.0. In ASME III-NH, Table I-14 C-1 provides a value of 0.66 for 100,000 h at 750°C (1382°F), which appears to be close to an estimate based on the data plotted in Figure 14. At high values of the LMP, the SRFs could be as low as 0.5. There are no data for the LMP value near 600,000 h at 900°C (1650°F).

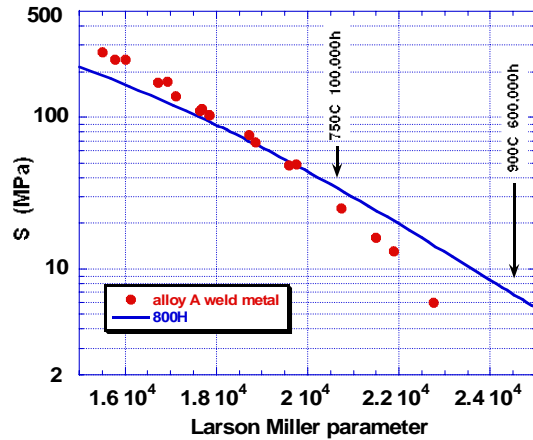


Fig. 13. Comparison of alloy A weld strength with alloy 800H base metal

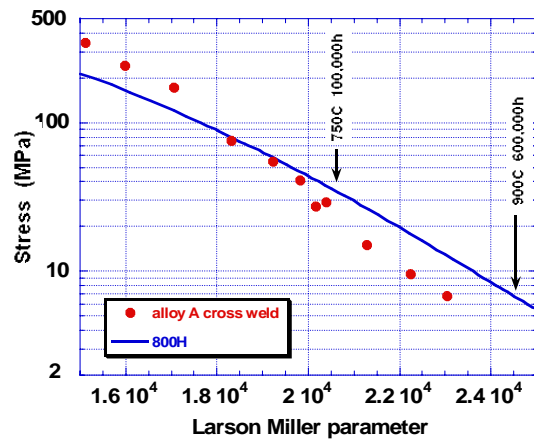


Fig. 14. Comparison of alloy A weldment strength with alloy 800H base metal

Comparisons for alloy 182 (ENiCrFe-3) deposited metal and weldments with alloy 800H are shown in Figure 15. Quite low strengths were observed over the entire range of test conditions. The 21/33Nb filler metal, however, appeared to be stronger than alloy 800H

at low temperatures and maintained good strength at high temperatures. As shown in Figure 16, good strength persisted to a LMP value of at least 23,000. This parametric value would correspond to 300,000 h at 850°C (1652°F) and suggests that further assessment of this filler metal would be beneficial.

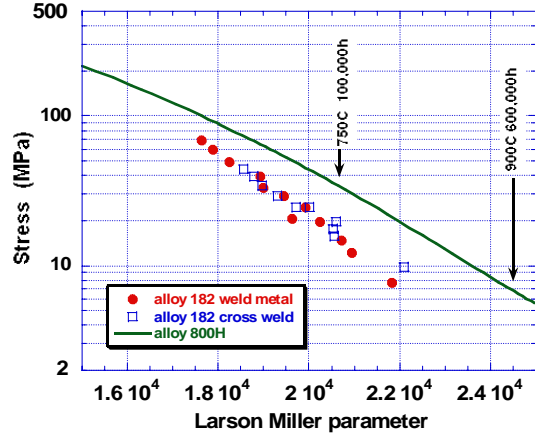


Fig. 15. Comparison of alloy 182 weld and weldment strength with alloy 800H base metal

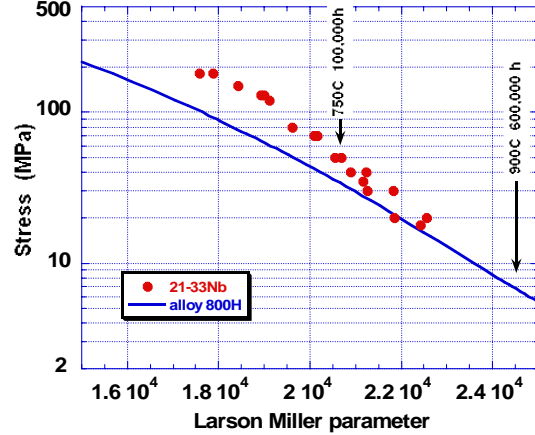


Fig. 16. Comparison of alloy 21/33Nb weld strength with alloy 800H base metal

Most of the evaluation of filler metals and weldments for alloy 800H focused on the bare wire material-alloy 82 (ERNiCr-Fe-3). A comparison of the strength of this deposited material with alloy 800H is shown in Figure 17 while weldment strengths are compared in Figure 18. Clearly, the data base is larger for this filler metal but the dearth of data at large values of the LMP is also evident. As with the other filler metals, the strength was greater than alloy 800H at low temperatures and LMP values. The alloy 82 strength crossed the LMP parametric curve for alloy 800H around the LMP value of 20,000.

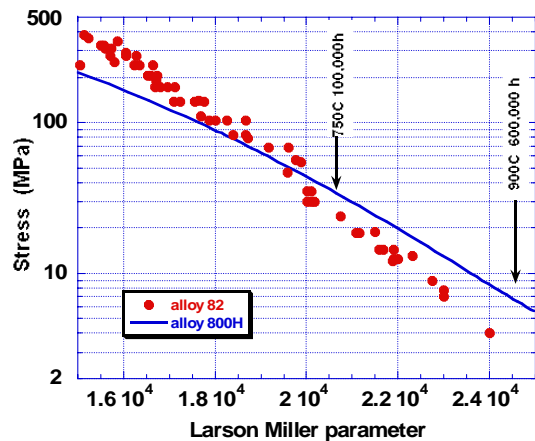


Fig. 17. Comparison of alloy 82 weld strength with alloy 800H base metal

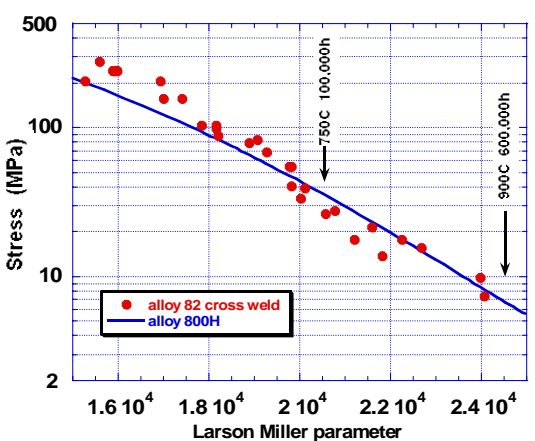


Fig. 18. Comparison of alloy 82 weldment strength with alloy 800H base metal

Calculation of Stress Reduction Factors:

It is clear in Figures 13 to 18 that the stress function $f(S)$ for the weld metal and weldments differed from that for the alloy 800H base metal. An “optimized” calculation of the LMP was needed to estimate the weld metal and weldment strengths. Equations (2) and (3) above were selected and a third-order polynomial was used in the $f(S)$ formulation. Only two of the filler metals were evaluated in this respect: alloy A (ENiCrFe-2) and alloy 82 (ERNiCrFe-3). Data for temperatures of 732°C (1350°F) and higher were selected. Alloy 82 was evaluated as two groups: all-weld metal and weld metal plus weldment. For each group two analyses were performed: Global and Lot-Centered. The SRFs at 100,000 h were calculated for each of the group and the value at 750°C (1382°F) was compared to the SRC tabulated in ASME III-NH. Table 4 lists the results of these calculations. Details of the parametric fits are provided in Appendix 2. Figure 19 provides a visual display of the results. Here, it may be seen that the Global parametric analyses produced lower SRFs at 100,000 h than the Lot-Centered analyses. The combined weld and cross-weld group produced the lowest SRFs at 750 and 800°C (1382 and 1472°F). The lowest value at 750°C (1382°F) was 0.72 which was greater than the tabulated value of 0.66 in ASME III-NH for alloy 82 to alloy 800H weldments.

Table 4. Calculated 10^5 h rupture strengths and SRFs for alloy 82 welds and weldments

| Temp (°C) | Base Metal | Global Analysis | | Lot-Centered Analysis | |
|--------------|------------|-----------------|-------------|-----------------------|-------------|
| | | S_R (MPa) | S_R (MPa) | SRF | S_R (MPa) |
| 750 | 34.9 | 25.1 | 0.72 | 29.4 | 0.84 |
| 800 | 23.3 | 14.1 | 0.61 | 17.7 | 0.76 |
| 850 | 15.3 | 8.45 | 0.55 | 10.5 | 0.69 |
| 900 | 9.97 | 5.5 | 0.55 | 6.1 | 0.61 |

Alloy A presented a problem. First, very few data were available at 732°C (1382°F) and above. Secondly, the optimized parametric function produced a stress function, $f(S)$, that could not be extrapolated to long times at the higher temperatures. Whereas the alloy 82 LMP constant C was fairly close to that for alloy 800H, the constant for alloy A was almost 19. The LMP analysis produced a significantly higher strength when the stress curve was extrapolated to 100,000 h at 750°C (1382°F). The resulting SRFs were greater than expected as illustrated in Figure 20. Some of the rupture data for weld metal and weldments are compared to curves based on the parametric fits in Figures 21 and 22.

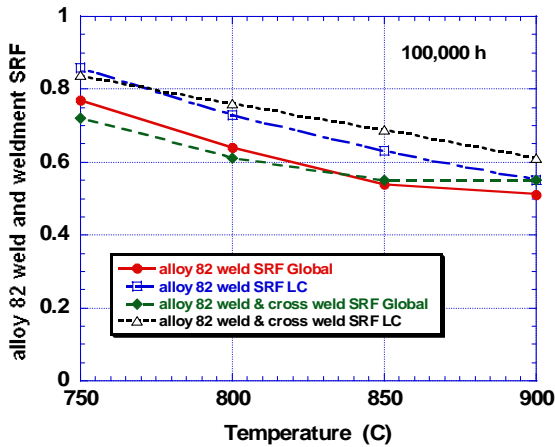


Fig. 19. Calculated Stress Rupture Factors for alloy 82 weld metal and weldments for 100,000 h

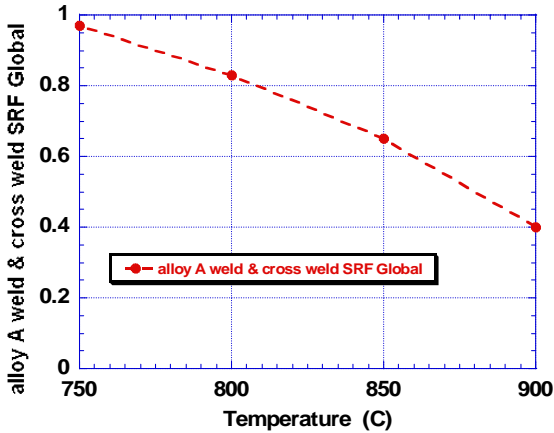


Fig. 20. Calculated Stress Rupture Factors for alloy A weldments for 100,000 h

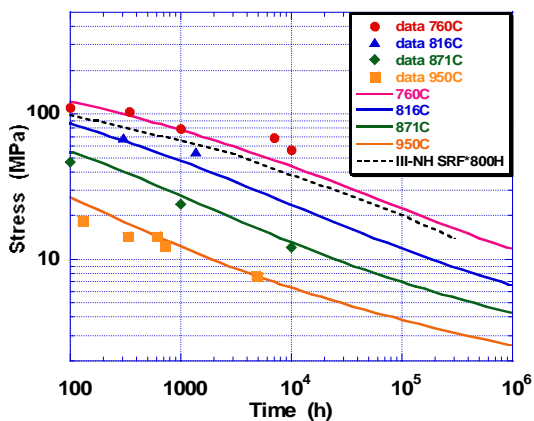


Fig. 21. Comparison of rupture data for alloy 82 weldments with calculated curves based on the LMP. Included is a curve for 760C based on the SRFs currently listed in ASME III-NH.

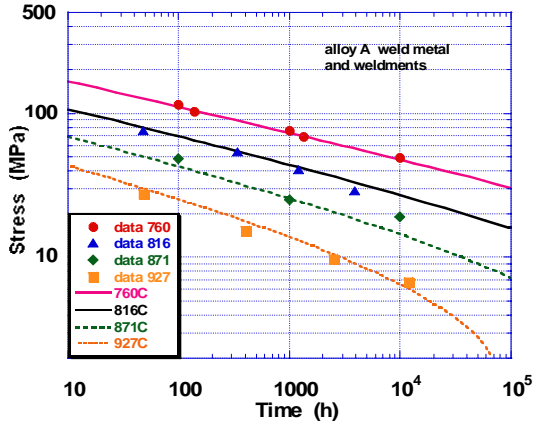


Fig. 22. Comparison of rupture data for alloy A weldments with calculated curves based on the LMP.

The calculated curves in Figures 21 and 22 exhibit either upward or downward curvature at long times and low stresses and these trends reflect the characteristics of the third order polynomial, $f(S)$ used to optimize the parametric constants. The curves should not be considered to be representative of long-time, low-stress behavior. The “cut-off” for estimating the SRFs is a matter of judgment but it is reasonable not to permit estimates for stresses lower than the lowest stress at which data were available or for times that exceed the longest rupture datum by an order of magnitude. For stresses, this position requires that values less than 6 MPa cannot be used to estimate the SRFs, while stresses for rupture lives in excess of 100,000 hours cannot be used to estimate SRFs. Examples of the calculated SRFs are tabulated in Appendix 3.

DISCUSSION

This report focused on the two filler metals currently approved for ASME III-NH, namely alloy A (ENiCrFe-2) and alloy 82 (ERNiCr-3). The database and experience with these two fillers is quite extensive at lower temperatures and there is no need to change the SRF values that are provided in ASME III-NH. It is interesting that efforts are underway to incorporate “weld strength reduction factors” (WSRFs) in ASME Section I, B31.1, and B31.3 for long-seam welded piping. Alloy 800H is included, and values without the identification of a specific filler metal are expected to be provided to 815°C (1500°F). It is anticipated that the WSRFs will be lower than the SRFs in ASME III-NH for 100,000 h but could be similar to those in ASME III-NH for longer time service. It is clear that the ASME III-NH approved filler metals produce low SRFs at temperatures above 750°C (1382°F), but it may be necessary to validate these values should the work on WSRFs be expanded to overlap the intent of the SRFs in ASME III-NH. The alloy 800H strength is quite low at the high temperatures, and further reduction of allowable stress intensities in ASME III-NH to accommodate the SRFs could make the use of alloy 800H impractical. Alternate base metal materials should be considered for long-time service at the higher temperatures. A better matched filler metal, such as 21/33Nb, or an overmatched filler metal, such as alloy 117 (617), could mitigate the problem and their usage should be examined. Recommendations for testing filler metals and weldments is provided in Appendix 4. Appendix 5 of this report suggests that one can expect issues to arise for undermatched and overmatched filler metals.

Although not part of this effort, the issue that needs to be addressed is how one uses the SRFs when the S_{mt} and S_t values in ASME III-NH at temperatures above 750°C (1382°F) are not controlled by the rupture strength. Minimum stress-to-rupture data are provided in ASME III-NH but it has not been established that the SRFs for weldments are the same for minimum strengths as for average strengths.

SUMMARY AND RECOMMENDATIONS

Filler metals for joining alloy 800H were reviewed and references bearing on the tensile and stress-rupture behavior of deposited weld metal and weldments were summarized. Data were collected for several coated and bare-wire electrodes.

Yield data for several weld and weldment materials were compared to the Y-1 and S_{y1} versus temperature trends for alloy 800H. Similarly, ultimate tensile strength data were compared to the U and S_U versus temperature trend for alloy 800H. Weld metal and weldments always exceeded the strength of the alloy 800H base metal.

The stress-rupture strengths of several weld and weldment materials were compared to the rupture strength of alloy 800H for the temperature range 750 to 1000°C (1382 to 1832°F) on the basis of the Larson Miller parametric curve using a common parametric constant characteristic of alloy 800H. Weld metals and weldments were stronger than

alloy 800H at low temperatures and high stresses but appeared to be weaker at high temperatures. Alloy 21/33Nb was an exception and the deposited filler metal was stronger or equivalent to alloy 800H over the range of temperatures and stresses where data were available.

An attempt was made to estimate the Stress Rupture Factors (SRFs) for weldments made with alloy A (ENiCrFe-2) and alloy 82 (ERNiCrFe-3). The lack of long-time, high-temperature data made it difficult to produce reliable results. Analysis was undertaken using the Larson Miller parametric procedure. Both global (batch) and lot-centered methods were applied. For alloy 82, estimates of SRFs were reasonably close to those provided in ASME III-NH Table I-10 C-2 for 760°C (1400°F). Values for alloy A were higher than expected and well above the SRFs provided in ASME III-NH Table I-10 C-1.

If a need for SRFs in the temperature range 750 to 900°C (1382 to 1650°F) was established, further testing of weld deposits and weldments was recommended. Testing of deposits from 21/33Nb coated electrodes and alloy 82 (ERNiCFe-3) bare wire electrodes was recommended. Testing to at least 10,000 h at temperatures of 900°C (1650°F) was recommended.

ACKNOWLEDGEMENTS

This undertaking was partially supported ASME-DOE Project on Generation IV Nuclear Reactor Materials, ASME Standards Technology, LLC and by UT-Battelle, LLC under Subcontract 4000045435. The authors acknowledge the patience and support of James Ramirez, ASME, and support and encouragement of W. R. Corwin and W. Ren of UT-Battelle, LLC.

REFERENCES

1. T. E. McGreevy and R. I. Jetter, "DOE-ASME Generation IV Materials Tasks," *Proceedings of PVP2006-ICPVT-11*, July 23-27, 2006, Vancouver, BC, Canada.
2. R. W. Swindeman, M. J. Swindeman, B. W. Roberts, B. E. Thurgood, and D. L. Marriott, *A Report on the Review of Databases, Data Analysis Procedure, and Verification of Minimum Yield and Ultimate Strengths for Alloy 800H in ASME Section III, Subsection NH*, draft report submitted to ASME Standards Technology, LLC, (March 2007).
3. R. W. Swindeman, M. J. Swindeman, B. W. Roberts, B. E. Thurgood, and D. L. Marriott, *Creep-Rupture Data Sources, Data Analysis Procedures, and Estimation of Strength for Alloy 800H at 750°C and Above, Part 1: Stress-Rupture*, draft report submitted to ASME Standards Technology, LLC, (March 2007).
4. R. W. Swindeman, M. J. Swindeman, B. W. Roberts, B. E. Thurgood, and D. L. Marriott, *Creep-Rupture Data Sources, Data Analysis Procedures, and Estimation of Strength for Alloy 800H at 750°C and Above, Part 2: Stress-Rupture Creep*, draft report submitted to ASME Standards Technology, LLC, (April 2007).
5. Regeln des Kemtechnischen Ausschusses (KTA-Regeln) KTA 3221.1: Metallische HTR-Komponenten, KTA-Sitzung am 15.06.1993.
6. *The Elevated-Temperature Properties of Weld-Deposited Metal and Weldments*, ASTM STP No. 226. American Society for Testing and Materials, Philadelphia, PA
7. J. W. York and R. L. Flury, *Assessment of Candidate Weld Metals for Joining Alloy 800*, WNET-119, Westinghouse Electric Corporation Tampa Division, Tampa FL (February, 1976).
8. R. L. Klueh and J. F. King, *Elevated Tensile Properties of ERNiCr-3 Weld Metal*, ORNL-5354, Oak Ridge National Laboratory, Oak Ridge, TN (December 1977)
9. J. F. King and R. W. Reed, Jr., *Weldability of Alloy 800*, ORNL/TM-6276, Oak Ridge National Laboratory, Oak Ridge, TN (April 1978).
10. R. L. Klueh and J. F. King, *Creep and Creep-Rupture Behavior of ERNiCr-3 Weld Metal*, ORNL-5404, Oak Ridge National Laboratory, Oak Ridge, TN (June 1978).
11. R. L. Klueh and J. F. King, *Mechanical Properties of ERNiCr-3 Weld Metal Deposited by Gas Tungsten-Arc Process with Hot-Wire Filler Additions*, ORNL-5491, Oak Ridge National Laboratory, Oak Ridge, TN (March 1979).

12. W. K. Sartory, *Inelastic Ratchetting Analysis of the 2 1/4Cr-1 Mo Steel to Type 316 Stainless Steel Dissimilar Metal Weldment Region of Specimen TTT-3*, ORNL-5512 Oak Ridge National Laboratory, Oak Ridge, TN (March 1979).
13. W. K. Sartory, *Revised Analysis of the Transition Joint Life Test*, ORNL/TM-9211, Oak Ridge National Laboratory, Oak Ridge, TN (July 1984)
14. M. K. Booker and J. P. Strizak, *Evaluation of Time-Dependent Fatigue Behavior of ERNiCr-3 Weld Metal by Strain-Range Partitioning*, ORNL/TM-7697, Oak Ridge National Laboratory, Oak Ridge, TN (May 1981).
15. R. L. Klueh and J. F. King, *Thermal Aging Behavior of ERNiCr-3 Alloy (Weld and Base Metal)*, ORNL-5783, Oak Ridge National Laboratory, Oak Ridge, TN (August 1981).
16. *Properties of Heat and Corrosion Resisting High Alloy Steel Tubes- Tempaloy 800H*, Nippon Kokan Technical Report Overseas No. 35, Nippon Kokan, Chiyoda-ku, Japan (1982)
17. G. Stannett and A. Wickens, "Alloy 800 Tube Welds- Assessment Report," *Project 2021; Creep of Steel*, ERA Technology Ltd., (December 1982)
18. R. L. Klueh and J. F. King, Elevated-Temperature Tensile and Creep-Rupture Behavior of Alloy 800H/ERNiCr-3 Weld Metal/2 1/4Cr-1Mo Steel Dissimilar-Metal Weldments, ORNL-5899, Oak Ridge National Laboratory, Oak Ridge, TN (November 1982).
19. H. E. McCoy and J. F. King, *Creep and Tensile Properties of Alloy 800H-Hastelloy X Weldments*, ORNL/TM-8728 (August 1983).
20. J. R. Lindgren, B. E. Thurgood, R. H. Ryder, and C-C Li, "Mechanical Properties of Welds in Commercial Alloys for High-Temperature Gas-Cooled Reactor Components," *Nuclear Technology*, Vol. 66, No. 1, July 1984, pp. 207-213.
21. T. H. Bassford and J. C. Hosier, "Production and Welding Technology of Some High-Temperature Nickel Alloys in Relation to Their Properties," *Nuclear Technology*, Vol. 66, No. 1, July 1984, pp. 35-43.
22. F. Schubert, U. Bruch, R. Cook, H. Diehl, P. J. Ennis, W. Jakobeit, H. J. Penkalla, E. te Heesen, and G. Ullrich, "Creep Rupture Behavior of Candidate Materials for Nuclear Process Heat Applications," *Nuclear Technology*, Vol. 66, No. 1, July 1984, pp. 227-239.
23. J. F. King and H. E. McCoy, *Weldability and Mechanical Property Characterization of Weld Clad Alloy 800H Tubesheet Forging*, ORNL/TM-9108, Oak Ridge National Laboratory, Oak Ridge, TN (September 1984).

24. *INCOLOY alloys 800 and 800HT*, Inco Alloys International, Huntington, WV, 1986.
25. T. H. Bassford, *Mechanical Properties on Incoloy alloy 800H Weldments Welded with Inconel 117 Welding Electrode*, Inco Alloys International, Huntington, WV, (February 1986).
26. *Survey and Guidelines for High Strength Superheater Materials- Alloy 800H*, EPRI Program RP1403-14 Task 13, November, 1987.
27. H. E. McCoy, *Interim Report on Mechanical Properties Data Analysis of Low Carbon Alloy 800 in Support of ASME Code Case N-47 Code Stress Allowables (INCO and ERA Interim Data Sets)*, unpublished report, Oak Ridge National Laboratory, Oak Ridge, TN (April 1991).
28. H. E. McCoy, *Tensile and Creep Tests on a Single Heat of Alloy 800H*, ORNL/TM-12436, Oak Ridge National Laboratory, Oak Ridge, TN (September 1993).
29. L. Sjodhal, “A Comprehensive Method of Rupture Data Analysis With Simplified Models,” pp. 501-516 in *Characterization of Materials for Service at Elevated Temperatures*, MPC-7, American Society of Mechanical Engineers, New York, NY, 1978.

APPENDIX 1
COMPILATION OF DATA ON WELD METALS AND WELDMENTS

Table A1-1. Stress-rupture data for alloy A deposited weld metal

| Lot ID | Temperature (deg C) | Stress (MPa) | Life (h) |
|-----------|------------------------|-----------------|-------------|
| INCO | 760 | 114 | 100 |
| INCO | 760 | 76 | 1000 |
| INCO | 760 | 49 | 10000 |
| INCO | 871 | 48 | 100 |
| INCO | 871 | 25 | 1000 |
| INCO | 871 | 19 | 10000 |
| INCO | 982 | 16 | 100 |
| INCO | 982 | 6 | 1000 |
| HT7728HEM | 482 | 482 | 47 |
| HT7728HEM | 538 | 414 | 436 |
| HT7728HEM | 649 | 241 | 177 |
| HT7728HEM | 649 | 172 | 1675 |
| HT7728HEM | 649 | 103 | 16900 |
| HT7728HEM | 760 | 138 | 27 |
| HT7728HEM | 760 | 103 | 139 |
| HT7728HEM | 760 | 69 | 1330 |

Table A1-2. Stress-rupture data for alloy A deposited cross welds

| Lot ID | Temperature (deg C) | Stress (MPa) | Life (h) | Failure Location |
|-----------|------------------------|-----------------|-------------|---------------------|
| HT7728HEM | 482 | 551 | | Weld |
| HT7728HEM | 482 | 482 | | Weld |
| HT7728HEM | 482 | 414 | 11550 | Weld |
| HT7728HEM | 538 | 414 | 315 | Weld |
| HT7728HEM | 538 | 345 | 3266 | Weld |
| HT7728HEM | 649 | 241 | 163 | Weld |
| HT7728HEM | 649 | 172 | 2318 | Weld |
| BMI | 816 | 75.8 | 48 | |
| BMI | 816 | 54.5 | 340 | |
| BMI | 816 | 40.7 | 1200 | |
| BMI | 816 | 29.0 | 3900 | |
| BMI | 927 | 27.6 | 48 | |
| BMI | 927 | 15.2 | 400 | |
| BMI | 927 | 9.7 | 2500 | |
| BMI | 927 | 6.8 | 12000 | |

Table A1-3. Stress-rupture data for 21-33Nb weld metal

| LoT ID | Temp (deg C) | Stress (MPa) | Life (h) |
|--------|-----------------|-----------------|-------------|
| 33431 | 750 | 180 | 220.7 |
| 33431 | 750 | 130 | 2807.7 |
| 33431 | 750 | 80 | 11333.0 |
| 33431 | 850 | 70 | 661.9 |
| 33431 | 850 | 50 | 1961.9 |
| 33431 | 850 | 40 | 6058.8 |
| 19424 | 950 | 30 | 536.0 |
| 19424 | 950 | 20 | 2078.7 |
| 19424 | 750 | 180 | 117.5 |
| 19424 | 750 | 150 | 761.1 |
| 19424 | 750 | 130 | 2398.4 |
| 19424 | 750 | 120 | 3516.3 |
| 19424 | 850 | 70 | 597.4 |
| 19424 | 850 | 50 | 1472.4 |
| 19424 | 850 | 40 | 2956.3 |
| 19424 | 850 | 35 | 5357.5 |
| 19424 | 950 | 30 | 183.3 |
| 19424 | 950 | 20 | 546.1 |
| 19424 | 950 | 18 | 1597.1 |

Table A1-4. Stress- rupture data for alloy 182 deposited weld metal

| Lot ID | Temp (deg C) | Stress (MPa) | Life (h) |
|--------|-----------------|-----------------|-------------|
| Shino | 816 | 68.6 | 11.5 |
| Shino | 816 | 59.8 | 19.5 |
| Shino | 816 | 49.0 | 43 |
| Shino | 816 | 39.2 | 180 |
| Shino | 816 | 33.3 | 205 |
| Shino | 816 | 20.6 | 800 |
| Shino | 927 | 29.4 | 12 |
| Shino | 927 | 24.5 | 30 |
| Shino | 927 | 19.6 | 56 |
| Shino | 927 | 14.7 | 140 |
| Shino | 927 | 12.3 | 215 |
| Shino | 927 | 7.6 | 1150 |

Table A1-5. Stress-rupture data for alloy 182 cross weld

| Lot ID | Temp (deg C) | Stress (MPa) | Life (h) |
|--------|-----------------|-----------------|-------------|
| Shino | 816 | 44.1 | 82.0 |
| Shino | 816 | 39.2 | 135.0 |
| Shino | 816 | 34.3 | 200 |
| Shino | 816 | 29.4 | 400 |
| Shino | 816 | 24.5 | 1750 |
| Shino | 927 | 24.5 | 20 |
| Shino | 927 | 19.6 | 110 |
| Shino | 927 | 17.7 | 99 |
| Shino | 927 | 15.7 | 100 |
| Shino | 927 | 9.8 | 1920 |

Table A1-6. Stress-rupture data for alloy 82 deposited weld metal

| Lot ID | Temp (deg C) | Stress (MPa) | Life (h) |
|--------|-----------------|-----------------|-------------|
| INCO | 538 | 400.0 | 100.0 |
| INCO | 538 | 359.0 | 1000.0 |
| INCO | 538 | 324.0 | 10000 |
| INCO | 649 | 252.0 | 100 |
| INCO | 649 | 190.0 | 1000 |
| INCO | 649 | 141.0 | 10000 |
| INCO | 760 | 110.0 | 100 |
| INCO | 760 | 79.0 | 1000 |
| INCO | 760 | 57.0 | 10000 |
| INCO | 871 | 47.0 | 100 |
| INCO | 871 | 24.0 | 1000 |
| INCO | 871 | 12.0 | 10000 |
| INCO | 982 | 19 | 100.0 |
| INCO | 982 | 9 | 1000.0 |
| INCO | 982 | 4 | 10000.0 |
| TM5404 | 454 | 517.1 | 3.2 |
| TM5404 | 454 | 510.2 | 142.3 |
| TM5404 | 454 | 496.4 | 715.1 |
| TM5404 | 454 | 496.4 | 1012.6 |
| TM5404 | 454 | 489.6 | 1075.4 |
| TM5404 | 510 | 482.7 | 10.9 |
| TM5404 | 510 | 455.1 | 39.4 |
| TM5404 | 510 | 448.2 | 357.1 |
| TM5404 | 510 | 434.4 | 1205.1 |
| TM5404 | 510 | 413.7 | 1645.4 |
| TM5404 | 510 | 393.0 | 3255 |
| TM5404 | 510 | 379.2 | 6770.4 |
| TM5404 | 566 | 434.4 | 29.5 |
| TM5404 | 566 | 413.7 | 112.8 |
| TM5404 | 566 | 396.5 | 448.2 |
| TM5404 | 566 | 379.2 | 841.1 |
| TM5404 | 566 | 365.4 | 1087.5 |
| TM5404 | 566 | 344.8 | 6003.3 |
| TM5404 | 621 | 379.2 | 21.2 |
| TM5404 | 621 | 310.3 | 295.1 |
| TM5404 | 621 | 293.0 | 653.1 |
| TM5404 | 621 | 275.8 | 1195.9 |
| TM5404 | 621 | 241.3 | 3109.4 |
| TM5404 | 677 | 275.8 | 26 |
| TM5404 | 677 | 241.3 | 89 |
| TM5404 | 677 | 206.9 | 215 |

Table A1-6 continued. Stress-rupture data for alloy 82 deposited weld metal

| Lot ID | Temp (deg C) | Stress (MPa) | Life (h) |
|----------|-----------------|-----------------|-------------|
| TM5404 | 677 | 172.4 | 778.5 |
| TM5404 | 677 | 137.9 | 3590 |
| TM5404 | 732 | 172.4 | 30.7 |
| TM5404 | 732 | 137.9 | 103.6 |
| TM5404 | 732 | 103.4 | 634.4 |
| TM5404 | 732 | 82.7 | 2792.8 |
| TM5491 | 454 | 496.4 | 1671.2 |
| TM5491 | 454 | 482.7 | 4228.8 |
| TM5491 | 454 | 455.1 | 8222.4 |
| TM5491 | 510 | 448.2 | 106.1 |
| TM5491 | 510 | 434.4 | 260 |
| TM5491 | 510 | 413.7 | 1049.7 |
| TM5491 | 510 | 396.5 | 6637.7 |
| TM5491 | 510 | 241.3 | 12746 |
| TM5491 | 566 | 379.2 | 129.8 |
| TM5491 | 566 | 365.4 | 247.1 |
| TM5491 | 566 | 344.8 | 432.3 |
| TM5491 | 566 | 327.5 | 2776.1 |
| TM5491 | 621 | 310.3 | 204.7 |
| TM5491 | 621 | 275.8 | 652.9 |
| TM5491 | 621 | 241.3 | 1401.2 |
| TM5491 | 677 | 206.9 | 183 |
| TM5491 | 677 | 172.4 | 546.7 |
| TM5491 | 677 | 172.4 | 366.8 |
| TM5491 | 677 | 137.9 | 2263.1 |
| TM5491 | 732 | 82.7 | 1526.6 |
| TM5491 | 732 | 103.4 | 459.1 |
| TM5491 | 732 | 137.9 | 77.2 |
| HEM7399 | 538 | 344.8 | |
| HEM7399 | 538 | 448.2 | 178 |
| HEM7399 | 593 | 206.9 | |
| HEM7399 | 593 | 275.8 | |
| HEM7399 | 649 | 137.9 | |
| HEM7399 | 649 | 206.9 | 1069.6 |
| HEM7399 | 704 | 103.4 | 9767 |
| HEM7399 | 704 | 137.9 | |
| HEM7399 | 760 | 69.0 | 6940 |
| HEM7399 | 760 | 103.4 | 347 |
| HEM7399 | 816 | 55.2 | 1364 |
| HEM7399 | 816 | 69.0 | 301 |
| Schubert | 850 | 35.0 | 500 |
| Schubert | 850 | 30.0 | 500 |
| Schubert | 850 | 30.0 | 600 |

Table A1-6 (continued). Stress-rupture data for alloy 82 deposited weld metal

| Lot ID | Temp (deg C) | Stress (MPa) | Life (h) |
|----------|-----------------|-----------------|-------------|
| Schubert | 850 | 35 | 600 |
| Schubert | 850 | 30 | 680 |
| Schubert | 950 | 18.5 | 130 |
| Schubert | 950 | 18.5 | 145 |
| Schubert | 950 | 14.5 | 330 |
| Schubert | 950 | 14.5 | 390 |
| Schubert | 950 | 14.5 | 600 |
| Schubert | 950 | 12.5 | 600 |
| Schubert | 950 | 12.5 | 720 |
| Schubert | 950 | 13 | 1300 |
| Schubert | 950 | 7.8 | 4800 |
| Schubert | 950 | 7 | 4800 |

Table A1-7. Stress-rupture data for alloy 82 cross welds

| Lot ID | Temp (deg C) | Stress (MPa) | Life (h) |
|------------|-----------------|-----------------|-------------|
| tm12438 | 811 | 275.8 | |
| tm12438 | 811 | 344.8 | 576 |
| tm12438 | 811 | 344.8 | 1332 |
| tm12438 | 866 | 275.8 | 760 |
| tm12438 | 922 | 137.9 | |
| tm12438 | 977 | 103.4 | 1399 |
| tm12438 | 977 | 103.4 | |
| tm12438 | 1033 | 69.0 | 3450 |
| tm12438 | 1033 | 103.4 | 288 |
| tm12438 | 1089 | 55.2 | 1159 |
| tm12438 | 1089 | 55.2 | 1082 |
| tm9108 | 922 | 206.9 | 1695 |
| tm9108 | 922 | 206.9 | 27.6 |
| tm9108 | 922 | 241.3 | 141 |
| tm9108 | 922 | 241.3 | 126 |
| tm9108 | 922 | 241.3 | 139 |
| tm9108 | 922 | 241.3 | 163 |
| tm9108 | 922 | 241.3 | 139 |
| tm9108ann | 922 | 241.3 | 157 |
| tm9108ann | 922 | 241.3 | 126 |
| tm8728 | 755 | 413.7 | 15373 |
| tm8728 | 755 | 482.7 | 1964 |
| tm8728 | 755 | 413.7 | 9578 |
| epri 82-15 | 1173 | 40.2 | 58 |
| epri 82-15 | 1173 | 33.3 | 90 |
| epri 82-15 | 1173 | 26.5 | 260 |
| epri 82-15 | 1173 | 17.7 | 900 |
| epri 82-15 | 1173 | 13.7 | 3000 |
| epri 82-13 | 973 | 156.9 | 220 |
| epri 82-13 | 973 | 156.9 | 580 |
| epri 82-13 | 973 | 98.1 | 3500 |
| epri 82-13 | 973 | 78.5 | 19000 |
| epri 82-13 | 1073 | 88.3 | 68 |
| epri 82-13 | 1073 | 83.4 | 440 |
| epri 82-13 | 1073 | 39.2 | 4200 |
| epri 82-13 | 1173 | 27.5 | 380 |
| epri 82-13 | 1173 | 21.6 | 1900 |
| epri 82-13 | 1173 | 17.7 | 7000 |
| epri 82-13 | 1273 | 15.7 | 490 |
| epri 82-13 | 1273 | 9.8 | 5200 |
| epri 82-13 | 1273 | 7.4 | 6000 |

APPENDIX 2

COEFICIENTS FOR THE LARSON MILLER FIT TO WELD METAL AND WELDMENT STRESS-RUPTURE DATA

| Item | Type Analysis | C | a0 | a1 | a2 | a3 | SEE |
|----------------------------------|---------------------|-----------------|------------------|------------------|------------------|------------------|--------------|
| Alloy 82 weld | Global | 14.49396 | 28782.89 | -12051.55 | 6372.657 | -1583.916 | |
| Alloy 82 weld | Lot-Centered | 15.64275 | 27907.73 | -6003.623 | 1787.85 | -566.021 | |
| Alloy 82 cross & weld | Global | 12.87579 | 27049.82 | -11949.62 | 6149.193 | -1486.356 | |
| Alloy 82 cross & weld | Lot-Centered | 14.27747 | 26069.8 | -4898.113 | 906.7137 | -351.8029 | |
| Alloy A weld & weld | Global | 18.87048 | 28410.55 | 991.5408 | -3051.934 | 454.2031 | 0.17 |
| Alloy A cross & weld | Lot-Centered | 19.02555 | 28342.266 | 1619.864 | -3494.767 | 544.7559 | |
| Alloy A cross weld | Global | 18.79754 | 33930.656 | -10931.24 | 4728.9531 | -1156.372 | 0.049 |
| Alloy A cross weld | Lot-centered | 18.58448 | 33781.492 | 11203.34 | 4974.8596 | -1222.845 | |
| Alloy 800H Base metal | Global | 15.12487 | 29648.78 | -7334.877 | 1903.854 | -619.4775 | 0.29 |

$$\log t_R = f(S)/T_K - C$$

$$f(S) = a_0 + a_1 \log S + a_2 (\log S)^2 + a_3 (\log S)^3$$

t_R in hours, T_K in Kelvins, S in MPa

APPENDIX 3

EXAMPLES OF CALCULATED STRESS FACTORS FOR ALLOY 82 WELDMENTS

| Item | Temp (deg C) | 10 h | 100 h | 1000 h | 10,000 h | 100,000 h | 600,000 h |
|-----------------------|--------------|-------------|-------------|-------------|-------------|-------------|-------------|
| Base metal | 750 | 142 | 104 | 74 | 51.4 | 34.9 | 24.4 |
| Weldment | | 188 | 131 | 83.8 | 48.3 | 25.1 | 15 |
| SRF (alloy 82) | | 1 | 1 | 1 | 0.94 | 0.72 | 0.61 |
| Base metal | 800 | 111 | 18.2 | 53.8 | 35.9 | 23.3 | 16.5 |
| Weldment | | 148 | 95.4 | 55.1 | 28.5 | 14.1 | 5.75 |
| SRF (alloy 82) | | 1 | 1 | 1 | 0.79 | 0.61 | 0.53 |
| Base metal | 850 | 85.7 | 58 | 38.1 | 24.5 | 15.3 | 10.6 |
| Weldment | | 112 | 66 | 34 | 16.3 | 8.45 | |
| SRF (alloy 82) | | 1 | 1 | 0.89 | 0.66 | 0.55 | |
| Base metal | 900 | 65 | 42.2 | 26.3 | 16.4 | 9.97 | 6.75 |
| Weldment | | 81.5 | 43.3 | 20.1 | 9.8 | | |
| SRF (alloy 82) | | 1 | 1 | 0.76 | 0.6 | | |
| ASME III-NH | 750 | 1 | 1 | 0.94 | 0.82 | 0.67 | |

Note: Data are insufficient to extend SRF values to 600,000 h at 850°C and 900°C

APPENDIX 4

RECOMMENDED CREEP-RUPTURE EXPERIMENTAL PROGRAM TO ADDRESS STRESS RUPTURE FACTORS FOR WELDMENTS IN ALLOY 800H FOR SERVICE ABOVE 750°C

To develop reliable stress-rupture factors for use above 750°C in ASME III construction of Class 1 components, a substantial experimental testing program will be necessary. The program should include the following elements:

- Selection of base metal for weldments
- Selection of filler metals and welding processes
- Specifications for testing coupons and testing methods
- Design of weldment specimens and testing methods
- Selection of testing temperatures and times
- Selection of analysis methods.

It is recommended that the base material be taken from archival material Jessup Steel Heat No. 37459 currently in storage at the Oak Ridge National Laboratory. See ORNL/TM-12436 [A4-1]. This material was purchased for use on the Modular High-Temperature Gas-Cooled Reactor Program and meets the necessary specifications required by ASME III-NH. When welded, the 12.7-mm (1/2-in) thick plates will be adequate for weld metal coupons, cross-weld coupons, and “full-thickness” weldments with transverse and longitudinal weld orientations.

Three filler metals for shielded metal arc (SMA) welding should be included: alloy A (ENiCrFe-2), alloy 117 (ENiCrCoMo-1), and 21/33Nb [A4-2]. Two fillers for gas tungsten arc (GTA), gas metal arc (GMA), or submerged arc (SA) welding should be included: alloy 82 (ERNiCr-3) and alloy 617 (ERNiCrCoMo-1). The introduction of the bare wire 21/33Nb wire should be optional and based on the experience with the material in the petrochemical and refining industries.

Testing coupons including base metal, weld metal, and cross welds should be round bars manufactured from the weld plates with a minimum test section diameter of 6.3-mm (1/4-in.) for short-time tests and 9.5-mm (3/8-in) for long-time tests. Testing methods shall conform to ASTM E 139.

Full thickness weldment specimens should be of two types: weld transverse to the loading axis and weld parallel to the loading axis. Typically, the length-to-width of the weldments should permit the relaxation of discontinuity stresses and produce a region of unaffected base metal.

Previous research on weldments in alloy 800H was limited to temperatures below 750°C. The program recommended here should cover the temperature range of 750 to 1000°C.

Alloy 82 testing (ERNiCr-3):

The testing plan for alloy 82 deposited weld metal or cross weld specimens should be designed to supplement existing data. Two data sets that may be considered are those published by McCoy [A4-1] and Schubert et al. [A4-3]. An example minimum test matrix is recommended in Table A4-1. No testing below 900°C is included under the assumption that the existing database is adequate to establish SRFs at lower temperatures and the test data recommended will be used to estimate SRFs for long times by means of time-temperature parametric prediction methods.

Table A4-1. Test matrix for alloy 82 weldment evaluation

| Temp. (deg. C) | Stress (MPa) | Time (h) weld/base | Cross Weld | Weld Metal |
|-------------------|-----------------|-----------------------|---------------|---------------|
| 900 | 12 | 4000/50,000 | X | |
| 900 | 8 | 20000/300,000 | X | |
| 925 | 12 | 2000/10,000 | X | |
| 925 | 8 | 10000/100,000 | X | |
| 950 | 8 | 4000/50,000 | X | X |
| 950 | 5 | 15000/300,000 | X | |
| 975 | 8 | 2000/2000 | X | |
| 975 | 5 | 7000/12,000 | X | |
| 1000 | 5 | 3000/5000 | X | X |
| 1000 | 3 | 12000/500,000 | X | |

Of these, the low-stress, high-temperature tests are the most significant. However, McCoy observed that failures occurred in the base metal for all testing conditions to 816°C [A4-1]. If so at the higher temperatures, then the testing times will prove to be far too long to be practical and the test stresses will need to be adjusted upwards. Such a trend is in conflict with the observations that the SRFs are less than 1.0 at high temperature and long times.

Alloy A (ENiCrFe-2):

The test matrix for alloy A may be the same as for alloy 82 (Table A4-1).

Alloy 117 (ENiCrCoMo-1) & alloy 617 (ERNiCrCoMo-1):

The testing plan for alloy 117 and 617 specimens should be directed toward the understanding of the effect of the mismatch in strength on the high-temperature performance of weldments. The creep-behavior of the high-alloy weld metals (alloys 117 and 617) needs to be estimated from test data (a few cross-weld tests would be of benefit to establish the failures will occur in the base metal removed from the fusion line when restraint is minimal). It should be recognized that the performance of alloy 117 and alloy 617 at 750°C and above will be investigated as part of the DOE project work on Gen IV

materials at the National Laboratories [A4-4], so only a minimal test matrix is needed. The temperatures, stress values, and estimated times in the table below are based on short-time test data produced on alloy 117 weld metal by INCO (Special Metals Inc.).

Table A4-2. Test matrix for alloy 117 or alloy 617 weld metal evaluation

| Temp. (deg. C) | Stress (MPa) | Time (h) weld | Weld Metal |
|-------------------|-----------------|------------------|---------------|
| 900 | 60 | 1000 | X |
| 900 | 30 | 10000 | X |
| 950 | 30 | 1000 | X |
| 950 | 18 | 10000 | X |
| 1000 | 11 | 1000 | X |
| 1000 | 7 | 10000 | X |

Alloy 21/33Nb:

The matching weld metal, alloy 21/33Nb, is used extensively for high-temperatures service. Test data are scarce, some has been reported by Metrode [A4-2] and Schubert et al.[A4-3]. Again, if this material is to be evaluated for service above 750°C, some creep data would be helpful in the analysis of tests on weldments. Alloy 800H stresses and temperatures provide a basis for developing a test matrix, and a minimal testing program on deposited filler metal is suggested below in Table A4-3.

Table A4-3. Test matrix for alloy 21/33Nb weld metal evaluation

| Temp. (deg. C) | Stress (MPa) | Time (h) weld | Weld Metal |
|-------------------|-----------------|------------------|---------------|
| 900 | 30 | 1000 | X |
| 900 | 16 | 10000 | X |
| 950 | 20 | 1000 | X |
| 950 | 12 | 10000 | X |
| 1000 | 12 | 1000 | X |
| 1000 | 7 | 10000 | X |

Weldment testing:

The “full-thickness” weldment tests should be performed on plate-type specimens with a nominal cross-section of 100-mm (4-in.) width and 12.5-mm (1/2-in. thickness). The “reduced section” length should be at least 300-mm (12-in.) for transverse welds and 300-mm (12-in.) length for longitudinal welds. These dimensions assume that the weld crown width is 25-mm (1-in.). A narrower weld would permit a smaller specimen cross section and reduced section length.

Two weldment tests should be performed on each orientation and each filler metal. A recommended test matrix is shown below in Table A4-4. Two temperatures are recommended: 800°C and 900°C. It is assumed that sufficient data exist at 800°C to undertake analysis of the weldment test [A4-1]. If this is not the case, additional testing at 800°C may be required. Three filler metals are recommended: alloy 82, alloy 117, and 21/33Nb. Weldments of alloy 82 should be weaker than alloy 800H at both temperatures. Weldments of alloy 117 should be stronger than alloy 800H at both temperatures. Weldments of 21/33Nb may be stronger at 800°C and equivalent at 900°C.

Table A4-4. Test matrix for alloy 800H weldments

| Filler metal | Weld Orientation | Temp. (deg. C) | Stress (MPa) | Time (h) weld |
|---------------|------------------|----------------|--------------|---------------|
| alloy 82 | transverse | 800 | 50 | 10000 |
| alloy 82 | transverse | 900 | 15 | 10000 |
| alloy 82 | longitudinal | 800 | 50 | 10000 |
| alloy 82 | longitudinal | 900 | 15 | 10000 |
| alloy 117 | transverse | 800 | 50 | 10000 |
| alloy 117 | transverse | 900 | 15 | 10000 |
| alloy 117 | longitudinal | 800 | 50 | 10000 |
| alloy 117 | longitudinal | 900 | 15 | 10000 |
| alloy 21/33Nb | transverse | 800 | 50 | 10000 |
| alloy 21/33Nb | transverse | 900 | 15 | 10000 |
| alloy 21/33Nb | longitudinal | 800 | 50 | 10000 |
| alloy 21/33Nb | longitudinal | 900 | 15 | 10000 |

Analysis methods:

The analysis methods for evaluating the creep and stress-rupture response of weldments at high-temperature are well-developed and were used extensively in the determination of stress-rupture factors for the materials incorporated in ASME III-NH [A4-5 to A4-8]. Appendix 5 provides an analysis of value for the round-bar samples recommended in Table A4-1 above. Also the use of a special notched bar sample is suggested.

References:

A4-1. H. E. McCoy, *Tensile and Creep Tests on a Single Heat of Alloy 800H*, ORNL/TM-12436, Oak Ridge National Laboratory, Oak Ridge, TN (September 1993).

A4-2. Thermet 800Nb, Data Sheet 09-06A, *Technical Handbook*, Metrode Products Limited, Surrey, KT, UK (not dated)

A4-3. F. Schubert, U. Bruch, R. Cook, H. Diehl, P. J. Ennis, W. Jakobeit, H. J. Penkalla, E. te Heesen, and G. Ullrich, "Creep Rupture Behavior of Candidate Materials for Nuclear Process Heat Applications," *Nuclear Technology*, Vol. 66, No. 1, July 1984, pp. 227-239.

A4-4. W. Ren and R. W. Swindeman, "Preliminary Consideration of Alloy 617 and 230 for Generation IV Nuclear Reactor Applications," paper PVP 2007-26091 presented at the 2007 Pressure Vessel and Piping Conference, July 23-28, San Antonio, TX, 2007.

A4-5. J. M. Corum, "Evaluation of Weldment Creep and Fatigue Strength-Reduction Factors for Elevated Temperature Design," pp.9 to 17 in *Structural Design for Elevated Temperature Environments- Creep, Ratchet, Fatigue, and Fracture*, ASME PVP Vol. 163, American Society of Mechanical Engineers, New York, NY, 1989.

A4-6. M. J. Manjoine, *Creep-Rupture Tests of Type 304 Stainless Steel Weldments with Central Axial Welds of Type 308 Stainless Steel at 593°C*, WARD-HT-94000-3, Westinghouse Advanced Reactors Division, Pittsburgh, PA, September, 1979.

A4-7. W. J. McAfee, R. L. Battiste, and R. W. Swindeman, *Elevated Temperature (593°C) Tests and Analysis of Type 304/308-CRE Stainless Steel Plate Weldments*, ORNL/TM-9064, Oak Ridge National Laboratory, Oak Ridge, TN, May, 1984.

A4-8. J. M. Corum and W. K. Sartory, "Assessment of Current High-Temperature Design Methodology Based on Structural Failure Tests," pp. 160 to 168 in *Journal of Pressure Vessel Technology*, Vol. 109, May, 1987.

APPENDIX 5 – PARAMETRIC STUDY OF WELDMENT BEHAVIOR

This study has been carried out as a preparatory step toward predicting weldment creep life from the basic properties of the parent and weld metal. The objective was to explore the effects of different parent and weld metal creep properties on weldment rupture life,

Test data indicates that, regardless of which of the parent or weld metal is the weaker, weldment strength is invariably less than the weaker of the two components. In the most common situation, when weld metal is stronger than the parent metal, the weldment is still weaker even than the parent plate.

There are two possible contributory causes for this finding. Firstly, it may be that the welding process generates an interface layer which is weaker than either of the two metals being joined. The second is that the complex stress state developed by inhomogeneous properties causes premature failure in the weaker component.

If the problem lies in the formation of complex low strength layers in the fusion zone, then it will be necessary to develop some equally complex test methods to evaluate local strength variations.

The development of complex stress states is easier to evaluate, since this is largely a question of stress analysis. With a view to examining this possible factor, if necessary for the purposes of eliminating it if that be the case, some typical weld geometries have been analyzed under creep conditions. These geometries are illustrated in Figure A5-1, and include a round bar, often used for weldment testing programs, tubes in axial tension or pressure, and a plane strain configuration. The basic weld geometry for the bar is shown in Figure A5-2 and Figure A5-3 which includes a blow-up of the weld/parent interface. This geometry represents a V-prep weld in a 6.3-mm (0.25-in.) thick specimen. Allowance has been made in the model to account for variations of fusion line properties, but no such variations have been considered as yet. This study has been limited to a single variation, which is a difference in creep properties between the parent metal and the weld.

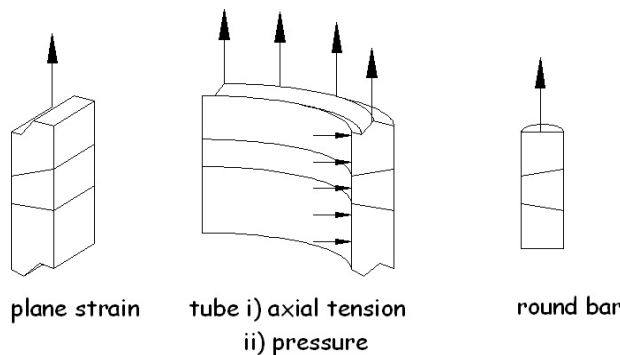


Figure A5-1. Example geometries of weldments with 20° interface angle

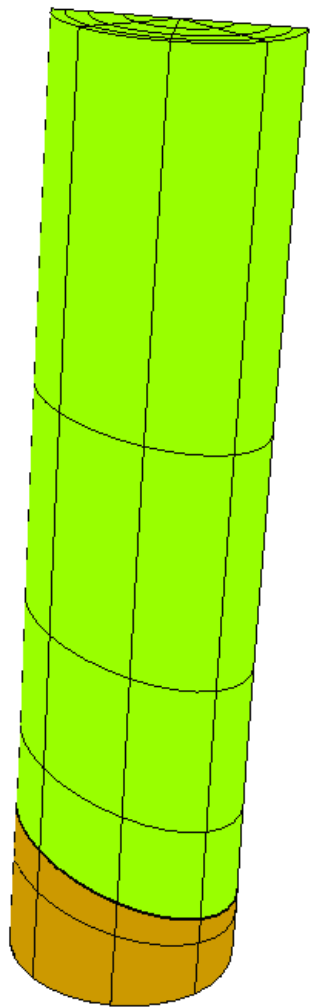


Figure A5-2 – General View of Weld FE Model

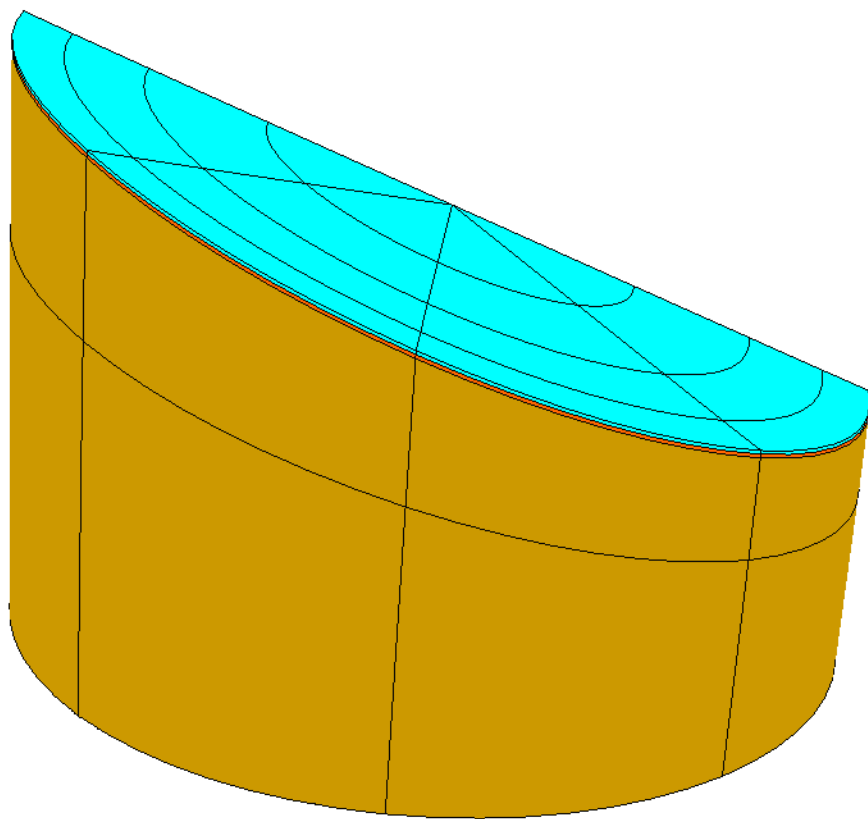


Figure A5-3 – Detail of Weld Interface

It is difficult to find equivalent data on parent plate and weld material for the purpose of generating the types of material model required in finite element analysis and, since this is intended as a trend analysis only, use has been made of the fact that creep strength in weld components appears to be proportional to indentation hardness and this, in turn suggests a typical strength ratio of approximately 1.5 between the plate and the weld. Furthermore, this ratio can apply in both directions, with the parent plate being either 1.5 times weaker or 1.5 times stronger than the weld.

This study has therefore used a single material, Alloy 800H, at a temperature of 850°C (1562 °F) where its nominal design allowable would be approximately 10 MPa (1.45 ksi), based on the minimum of 1% in 100,000 hours or 2/3 or the 100,000 hour rupture strength.

Creep properties for the above condition were extracted from the MPC Omega model published in API 579, Part 10, using a simplified Bailey/Norton power law with a best fit exponent “n”, calculated at the nominal stress of 10MPa (1.45 ksi). Three material models were used in the study, a nominal model, one with a an equivalent strength of 1.5 times the nominal, and a third with 2/3 of the nominal strength. Given that “n” for this material is approximately 7.35, the ratios of creep rates in the strongest/nominal, and nominal/weak at the same stress level are both approximately 18:1

The weldment configurations shown in Figure A5-1 have been run under 4 different boundary conditions. These are,

1. Plane strain
2. Axisymmetric circ. weld in 50-mm (2-in.) diameter tubing under axial load
3. As 2. above but under internal pressure with closed ends
4. Round cross weld specimen

In all cases loading was adjusted to produce the same equivalent (Mises) stress of 10 MPa (1.45 ksi).

Failure in a weldment is complicated due to the stress state. It has been assumed that failure is defined by an effective S_{eff} which is a function of the stress state. A version of Huddleston's multiaxial rupture criterion, as employed in API 579, was used to calculate S_{eff} in this study, i.e.

$$\begin{aligned} S_{eff} &= S_{mises} \exp[0.24(J_1/S_s - 1)] & (5-1) \\ J_1 &= (S_{11} + S_{22} + S_{33}) = 3S_h \\ S_s &= (S_{11}^2 + S_{22}^2 + S_{33}^2)^{0.5} \end{aligned}$$

This criterion only governs the onset of creep rupture failure. In practice, in an inhomogeneous stress field, damage starts at the highest stresses location, and propagates until the material loses load carrying capacity. This can only be evaluated accurately with a continuum damage model such as Kachanov, Dyson, or Omega. To avoid the complications of user subroutines introduced by a more detailed analysis, it has been assumed that the onset of creep rupture damage is equivalent to initiation of a creep crack. A simplified C* analysis then established that crack growth following creep rupture damage occurring at one location, would be rapid, and that onset of creep damage

is therefore a reasonable approximation to specimen life – *in this application*. It is recognized that this may not be a generally correct assumption, but is reasonable in this instance because there are no severe stress concentrations or gradients involved.

Failure in this study is therefore defined as the time to rupture, as predicted by simple tensile creep rupture versus time curves, using the effective stress calculated as a function of the multiaxial stress state using Equation (A5-1) above.

A typical result is shown in Figures A5-4 and A5-5, for the round-bar cross-weld specimen. Note that, although this model appears relatively crude, it consists of high order 20-node brick elements and the region of high stress needs to be sufficiently extensive to produce significant creep damage. Therefore a geometrically crude model is adequate in this case.

Figure A5-4 shows the distribution of the Mises stress on the interface. On the other hand, the hydrostatic stress, S_h , (Figure A5-4) which has a value of only 3.3 MPa (0.48 ksi) remote from the weld, increases to 10 MPa (1.45 ksi) locally, and is greater than 7 MPa (1 ksi) over a large proportion of the weld interface. According to the Huddleston multiaxial criterion, this would result in an S_{eff} of about 11.6 MPa (1.68 ksi), or an increase of 15% over the nominal uniaxial value. Translated into weld SRF's this predicts a value of SRF = 0.87.

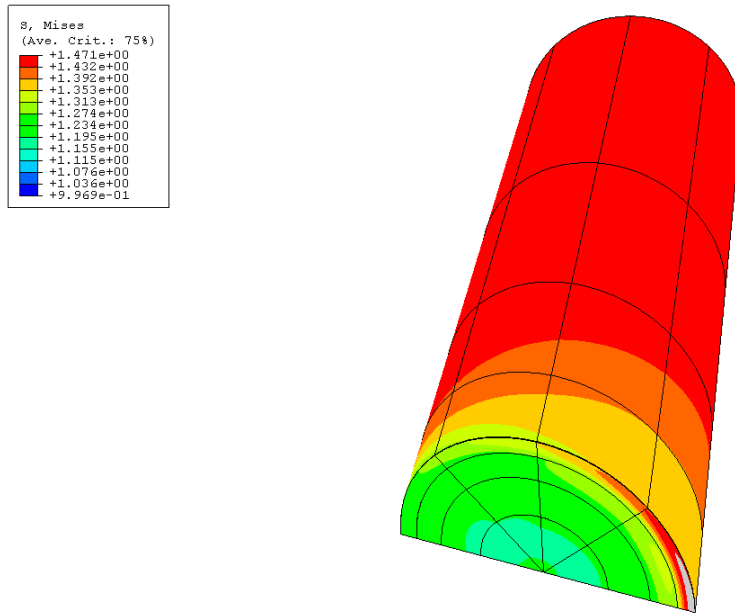


Figure A5-3 – Mises Stress Distribution on Weld Interface under full developed Creep Conditions

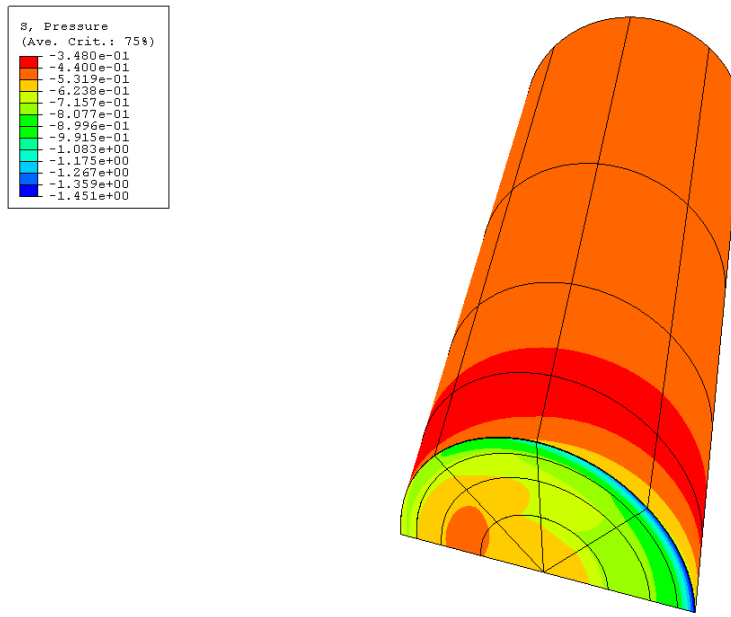


Figure 5-4 – Hydrostatic Stress Distribution on Weld Interface under full developed Creep Conditions

Additional analyses were performed on the geometries shown in Figure A5-1, but with different assumptions regarding the material behavior. Here, the exponent of the Bailey/Norton power law was reduced to 5 and the relative creep rates of the weld metal to based metal was assumed to 0.1 (stronger weld) and 10 (weaker weld). Again, the Mises stress was taken to be a nominal 10 MPa (~1.45 ksi). The results, which include the SRFs for ten conditions, are shown in Table A5-1.

Table A5-1. Effect of weldment geometry on the calculated strength reduction factor

| | Material relative strength | | Nominal Mises Stress (A) (ksi) | Huddleston Effective Stress (B) (ksi) | Strength Reduction Factor SRF (A/B) |
|----------------------|----------------------------|------------|--------------------------------|---------------------------------------|-------------------------------------|
| | Parent | Weld metal | | | |
| Tensile Bar | nominal | strong x10 | 1.447 | 1.45 | 1.000 |
| | strong x10 | nominal | " | 2.39 | 0.605 |
| Tube-in-tension | nominal | strong x10 | " | 2.08 | 0.695 |
| | strong x10 | nominal | " | 2.45 | 0.589 |
| Tube-under-pressure | nominal | strong x10 | " | 1.99 | 0.727 |
| | strong x10 | nominal | " | 2.02 | 0.717 |
| Plane Strain tension | nominal | strong x10 | " | 2.13 | 0.679 |
| | strong x10 | nominal | " | 2.33 | 0.621 |
| Round bar tension | nominal | strong x10 | " | 2.48 | 0.582 |

Conclusions:

1. A creep strength disparity between parent metal and weld metal reduces creep rupture strength by producing a metallurgical SCF at the interface together with elevated hydrostatic stress
2. This effect, alone, is sufficient to develop significant weld SRF's for a typical difference in creep strength of the two constituents.
3. The SRF depends on the weld geometry but is generally on the order of 0.6 to 0.7, regardless of which constituent is the weaker
4. Additional reduction in weldment strength may result from weak or brittle zones forming along the weld interface. This problem has not been fully investigated yet for lack of reliable material data on interface material

Recommendation:

There is a need for a test on weldments to identify the effects of multiaxiality and, if possible, the specific properties on the weld/parent metal interface.

A candidate specimen that could serve both purposes is the so-called “yo-yo” specimen, a deeply notched, but blunt root notch specimen which generates a high level of hydrostatic stress over a large proportion of the neck area. This is a good geometry to test both parent and weld metals separately and, by placing the notch root carefully at the weld/parent metal interface, distinctive behavior of the interface could be deduced by comparison with similar tests on the homogeneous materials.